KINETICS OF THE REACTIONS OF TRIARYLMETHYL-CARBONIUM IONS IN AQUEOUS SOLUTIONS

A Thesis

Presented for the Degree of

MASTER OF SCIENCE

In The Faculty of Science of the

University of St.Andrews

by

Zbigniew Mieczyslaw Zochowski

DECLARATION

I declare that this thesis is my own composition, that the work of which it is a record has been carried out by me, and that it has not been submitted in any previous application for a Higher Degree.

This thesis describes results of research carried out at the Department of Chemistry, United College of St. Salvator and St. Leonard, University of St. Andrews, under the supervision of Professor P.A.H. Wyatt.

CERTIFICATE

I hereby certify that Zbigniew M. Zochowski has spent the prescribed number of terms of research work under my supervision, has fulfilled the conditions of Ordinance General No. 51 and Resolution of the University Court 1974 No. 2, and is qualified to submit the accompanying thesis in application for the degree of Master of Science.

P.A.H. Wyatt
Director of Research

ACKNOWLEDGMENTS

I would like to thank Professor P.A.H. Wyatt for his help and encouragement during the course of this research.

My thanks are also due to Dr. J.N. Ride for his help with the computational problems encountered initially in this research, Dr. A.R. Butler for the timely loan of his stopped-flow apparatus, and my friends and colleagues in the Department of Chemistry.

I am indebted to the University of St. Andrews for the opportunity and to the Head of the Chemistry Department for the facilities to pursue this research.

CONTENTS

SUMMARY

The results of this work show that the reaction of tris-p-methoxyphenyl-methyl cation with water is subject to general base catalysis. Values of reaction rate constants have been found for $(C_2H_5)_3N$, $(CH_3)_3N$, and 1,4-diazabicyclo 2,2,2 - octane, (Dabco), and H_2O. The catalytic effect of OH^- has been shown and, while a value for k_{OH} has not been deduced, evidence has been produced which suggests the value is much larger than the current literature data.

The deduced catalytic constants have been shown to obey the Brønsted relationship over a large range of the variables.

A related compound, containing one oxygen bridge, the 3,6-dimethoxy, 9-phenyl,xanthen-9-ol was synthesised and its pK (S_o), quantum yields of fluorescence and the quenching effects of anions upon the fluorescence intensity of R^+ form were determined.

The pK (S_o) and pK (S_1) of the related intermediate compound, 3,6-dimethoxyxanthone were determined by absorption and fluorescence spectroscopy respectively.

Since the stopped-flow apparatus was unable to cope with reactions of half-lives greater than 5-15 ms, a pressure jump instrument was built, and was tested on the example of $CoCl_2$ in iso-propanol/water solution.

PART I

INTRODUCTION

From 1923, the new Brønsted theory of acids and bases was developed and this led in the 1930's to Hammett's[1] quantitative evaluation of the basic properties of compounds, capable of being protonated by strong acids. As a quantity suitable for the comparison of the ability of strongly acid solutions to donate protons to weak bases, Hammett and Deyrup[1] introduced a logarithmic term, analogous to pH and called it the acidity function H_o.

Experimentally, the method consists of adding to an acid solution a small amount of the base B, which has suitable indicator properties, and measuring spectrophotometrically the extent to which it is converted into the protonated form BH^+.

The protolytic equilibrium involving B can be written $BH^+ + H_2O \rightleftharpoons B + H_3O^+$ and this is commonly abbreviated to $BH^+ \rightleftharpoons B + H^+$. This has a true thermodynamic equilibrium constant

$$K_a = \frac{a_B \, a_{H^+}}{a_{BH^+}} = \frac{[B][H^+]}{[BH^+]} \times \frac{f_B \, f_{H^+}}{f_{BH^+}} \qquad \text{I. 1.}$$

where the "a" terms are activities, the "f" terms activity coefficients and $[\ ]$ represents concentrations. Taking logarithms gives an alternative representation of the above equation

$$-\log_{10} K_a = pK_a = -\log_{10} \frac{a_B \, a_{H^+}}{a_{BH^+}} \qquad \text{I. 2.}$$

$$= \log \frac{[BH^+]}{[B]} + \log \frac{f_{BH^+}}{f_B a_{H^+}} \qquad \text{I. 3.}$$

The problem with any formulations I. 1, I. 2, or I. 3 is the evaluation of the various terms employed. This becomes particularly difficult when experimental conditions depart substantially from dilute aqueous solutions. If the latter conditions exist, then the f_{BH^+} and f_B could tend to unity at infinite dilution and we could convert equation I. 3 into

$$pK_a = \log \frac{[BH^+]}{[B]} - \log_{10} a_{H^+} = \log \frac{[BH^+]}{[B]} + pH \qquad \text{I. 4.}$$

Only certain indicator bases will protonate sufficiently to give reasonable values for the ratio $[BH^+] / [B]$ in these ideal conditions. Such a case is p-nitroaniline and for it a value of pK_a follows if $[BH^+] / [B]$ is measured at known pH values.

In so far as less ideal acidic systems were concerned, Hammett suggested that equation I. 3 could be useful. He defined

$$H_o = - \log \frac{f_B \, a_{H^+}}{f_{BH^+}} = \log \frac{f_{BH^+}}{f_B \, a_{H^+}} \qquad \text{I. 5}$$

which permits equation I. 3 to be re-written as

$$pK_a = \log \frac{[BH^+]}{[B]} + H_o \qquad \text{I. 6}$$

This gives a form of equation analogous to I. 4 with H_o, the acidity function replacing pH. Just as pH, in an ideal aqueous solution indicates that medium's proton donating capacity, so H_o can be considered to determine a value for this property for the medium under consideration.

Equation I. 6 is useful in two ways. If a suitable acid BH^+

permits its pK_a to be found by use of equation I.4 in ideal dilute solution, and if it gives measurable ratios $[BH^+]/[B]$ in some other medium, x, then equation I.6 can be applied. Knowing pK_a the H_o value can be deduced for that medium. Inspection of I.5 shows that the H_o definition involves properties of the conjugate acid-base pair used to evaluate H_o experimentally. Hammett's original postulate was that for 2 bases, B_1 and B_2, the ratio

$$\left(\frac{f_{B_1}\, H^+}{f_{B_1}}\right)\left(\frac{f_{B_2}}{f_{B_2H^+}}\right)$$

was approximately unity, if the "f" values depended on medium environment and were reasonably independent of the nature of B. He produced experimental work to support this and his work suggested that an acidity scale for media could be established, based on the degree of protonation of suitable indicators.

The second use of equation I.6 is to take the determined value of H_o for a certain medium and the ratio $[BH^+]/[B]$ for a new indicator in that medium. Clearly this permits pK_a for the new BH^+ to be found.

Hammett used a series of weak indicator bases in sulphuric acid / water mixtures and measured the variation of $[BH^+]/[B]$ indicator ratio with increasing acidity. Using indicators which protonated at different acidities and by defining the slope of the graph of $\log_{10}[BH^+]/[B]$ against H_o as unity, a complete acidity scale was evaluated up to 100% H_2SO_4. The acidity scale was anchored in the pH range by the most basic compound, p-nitroaniline. An account of a stepwise procedure for a determination of the pK_a values of weak bases, having measurable ionisation ratios at acid concentrations greater than 1 mol dm^{-3}, is given in a review by Paul and Long[2].

Over 40 years of experience in the application of Hammett's ideas to several hundred bases of different types and in numerous solvent systems shows that it forms a very useful framework, but the initial hope that a single acidity scale might cope with all classes of bases has not been realised. Hammett's original H_o scale has therefore come to be assigned to the primary amines, examples of which form the majority of the original indicators. Even for bases of structure obviously related to that of primary amines, such as tertiary amines, the differences are sufficient for the generation of their own acidity function[3], H_o'''.

Several other acidity functions have subsequently been constructed using amides[4], azulenes[5], indoles[6], and benzophenones[7].

It is now clear that there is nothing absolute about the original H_o acidity function itself, but all bases, whether they conform to it or not, can nevertheless be characterised in an empirical way in terms of the strength of acid required for their half-protonation. The use of aqueous mineral acids provides a wide range of acidities, which extend the pH scale and can be used for placing the majority of bases on scales referred back to infinite dilution in water.

An additional acidity function, H_R (also symbolised by J_o or C_o) has been established for aryl carbinols[8], which behave as secondary bases in the equilibrium

$$R^+ + H_2O \rightleftharpoons ROH + H^+ \qquad \text{I. 7.}$$

where H_R was defined as:

$$H_R = pK_{R^+} + \log \frac{[ROH]}{[R^+]} \qquad \text{I. 8}$$

$$\text{where } H_R = -\log \left[(a_{H^+}/a_{H_2O}) \times (f_{ROH}/f_{R^+}) \right] \qquad \text{I. 9}$$

It is also convenient sometimes to use the related quantity h_R,

defined as

$$h_R = \frac{a_{H^+} f_{ROH}}{a_{H_2O} f_{R^+}} , \qquad \text{also } h_o = \frac{a_{H^+} f_B}{f_{BH^+}}$$

Reagan[9] proposed a new Hammett-type acidity function H_C, as more appropriate than $H_{R'}$ ($H_{R'} = H_R - \log a_{H_2O}$) to the protonation of carbon bases (aromatic polyethers, substituted azulenes, and 1,1-diarylethylenes) in aqueous H_2SO_4 and $HClO_4$.

The validity of the acidity function idea was extended into aqueous organic acids and H_o has been evaluated for fluoroacetic[10] and trichloroacetic[11] acids, and both H_R and H_o for formic acid[12].

The H_o scales have been established in aqueous solutions of 2-butoxymethanol[13], ethylene glycol[14], and dioxan[15].

An H_R scale has been established in dioxan[16,17]. All these functions (H_A, H_1, J_o, C_o, H^+, $H_{R'}$, H_C, H_R) show noticeable deviations from the original H_o scale, which has itself been improved by Jorgensen and Hartter[18] for solutions above 60% H_2SO_4 and by Bascombe and Bell[11] for media containing less than 10% H_2SO_4.

The differences between the H_R and H_o functions are considerable, especially at higher acid concentrations where the H_R changes nearly twice as rapidly with increasing acidity as H_o,(Fig. I. 1) Two factors which might contribute to this striking difference are the presence of water activity in the H_R function and a difference between the activity coefficient behaviour of carbonium ions and the ammonium ions derived from Hammett's bases.

Simultaneously, Bell and Bascombe[19] and Wyatt[20] have calculated the H_o function for acid solutions from the relationship of stoichiometric acidity, the activity of water, and hydration of the proton. Wyatt showed that the H_o is a common function of the water activity

Fig. I.1

Variation of acidity functions with the strength of sulphuric acid.

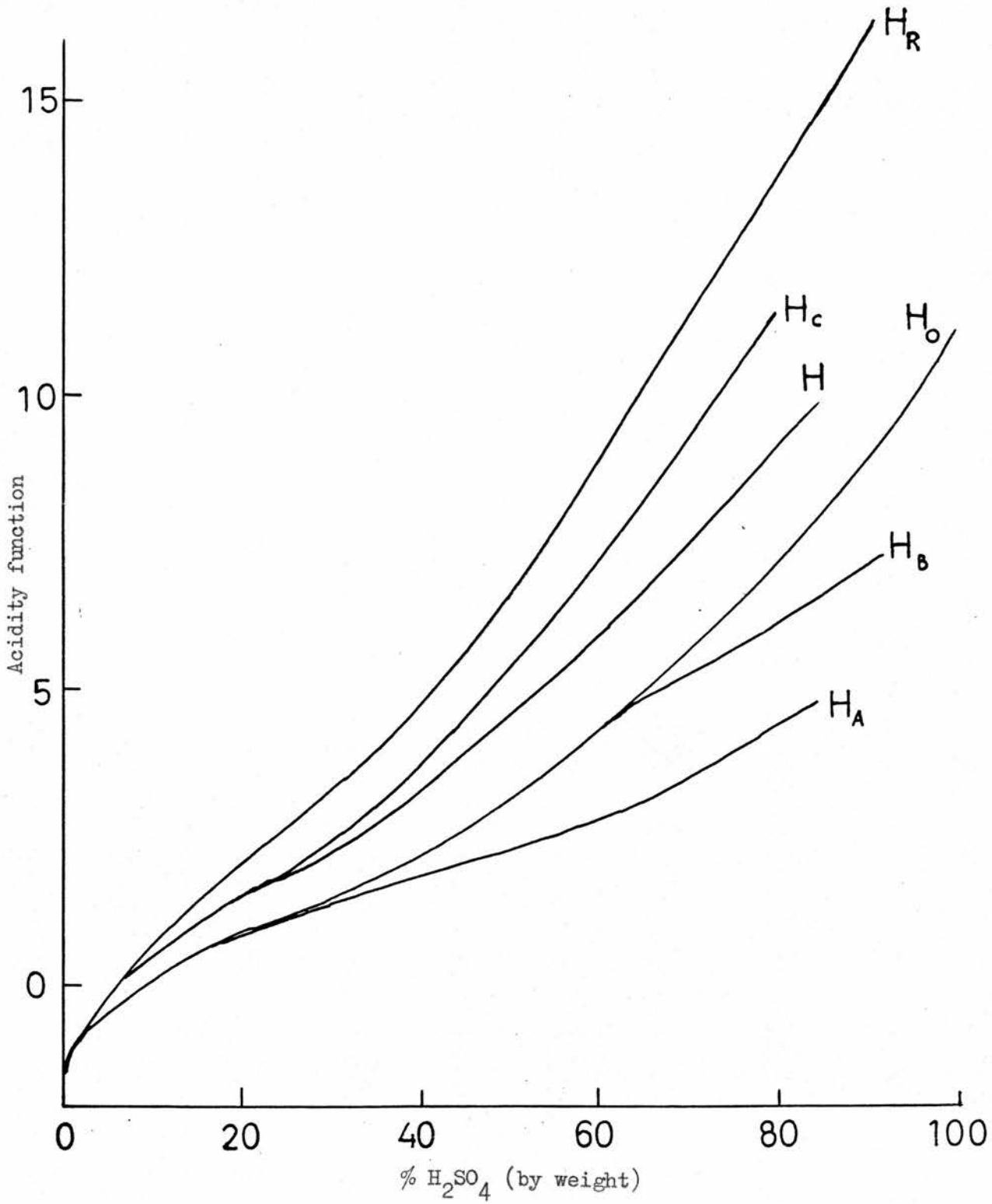

for H_2SO_4, $HClO_4$, HCl, and HNO_3. The dependence of the H_o function in H_2SO_4 solutions between 20% - 60% was explained satisfactorily by the assumption of statistical addition of 4 H_2O to the H_3O^+ ion, thus coping with the successive hydration of the proton in a simple way.

Bascombe and Bell, on the other hand, only considered the hydrated species $H_9O_4^+$ and their theory was therefore bound to break down in stronger acids where there is not enough water to support tetrahydration.

According to Wyatt, H_3O^+ associates with progressively smaller numbers of H_2O molecules and as a consequence the protonic species becomes more acidic.

Högfeldt[21] confirmed Wyatt's theory for the H_o scale, but concluded that the H_R acidity scale is not a common function of a_{H_2O} for all strong acids. He suggested that other competing reactions, similar to the protonation equilibria of triphenylmethane dyes, might interfere.

Meanwhile Yates,[22] using the present H_o data for H_2SO_4 and redetermined H_o data for $HClO_4$, showed that Wyatt's relationship is obeyed, the remarkably rapid increase in the $HClO_4$ acidity being mirrored precisely by the corresponding decrease in the a_{H_2O} of this acid compared with H_2SO_4, Fig. I. 2.

Re-examination[23] of the a_{H_2O} dependence of the H_R function for H_2SO_4, $HClO_4$, and HNO_3 showed very similar, but clearly separate curves for each acid. Plots of H_A versus a_{H_2O} for H_2SO_4 and HCl acids also showed two separate curves, diverging by some 1.7 units.

Fig. I.2

Plot of H_o against a_{H_2O} for $HClO_4$(△) and H_2SO_4(0).

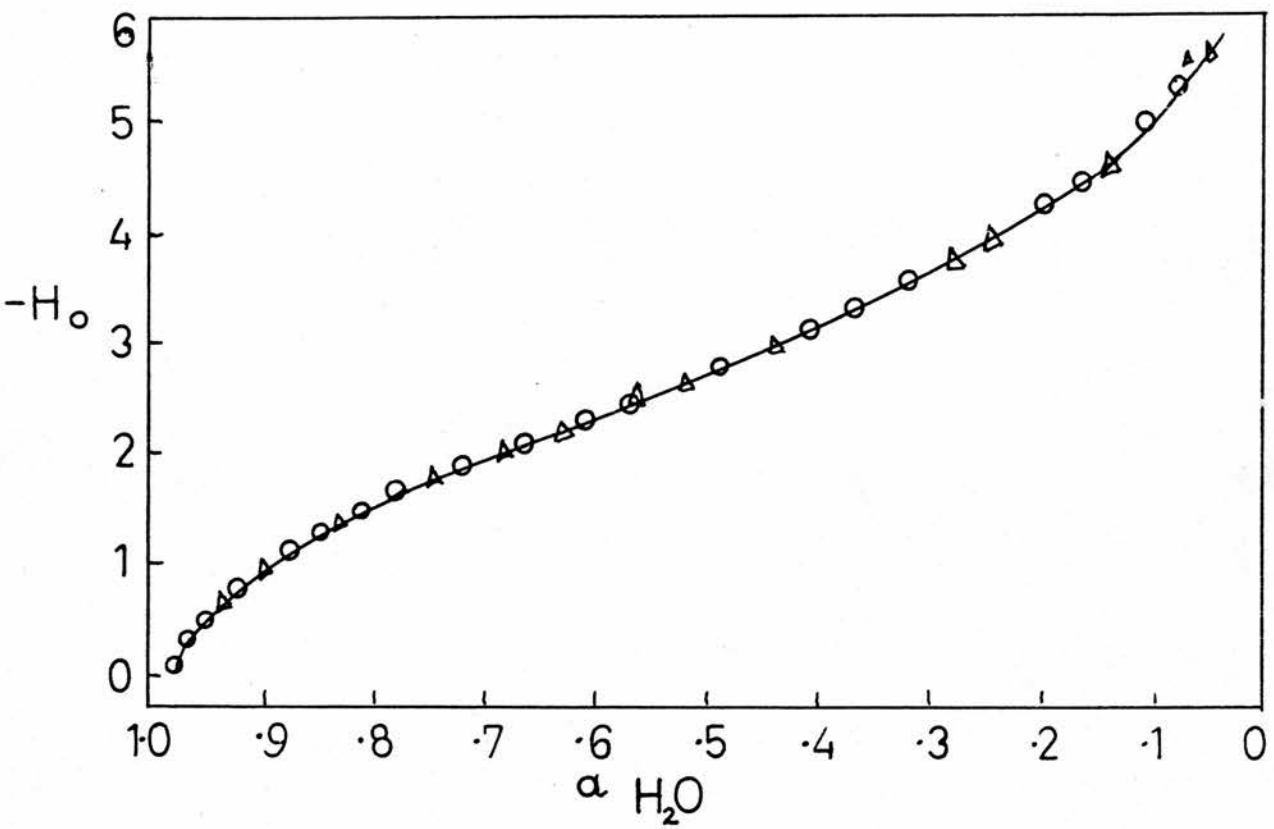

Thus, although acidity functions in general are strongly dependent on a_{H_2O}, the unique character of the H_o - a_{H_2O} relationship for different acids may, according to Yates, be purely fortuitous[23].

Other factors put forward to explain the departures of H_R from the original H_o acidity function scale include:

(a) the extent of hydration of the indicators themselves;[24]

(b) the stability of triarylmethyl carbonium ions (Malachite Green, Crystal Violet) in aqueous solutions and their relatively slow reaction with anionic and other nucleophiles;[25]

(c) stabilisation of the R_3C^+ by large ions relative to p-nitroanilinium ion;[26]

(d) indirectly, by some evidence of the negative salt effects by chlorides and perchlorates on the reaction of tri-p-anisylmethyl carbonium ion;[27]

(e) decreased rate of formation of R_3C^+ by dioxan in aqueous solutions and the accelerating of attack of water upon it;[17]

(f) the structure enforced association between R_3C^+ and ClO_4^- ions[28] (prevents correlation between $H_R - a_{H_2O}$ for strong acids).

(g) consideration has also been given to the solvent in the related kinetic problems of Malachite Green with nucleophiles[29].

We can see that investigations in many solvents and by varied techniques are helping to form theories underlying acid - base reactions and the acidity functions. This work is being constantly revised and re-focussed from different viewpoints. To understand the acid - base equilibria and the different dependencies upon acid - base concentration ratios it could be helpful to have more detailed knowledge of the influence of medium changes on the rates of forward

and back reactions involved in the equilibrium.

For simple proton reactions, extensive information of this kind was already available from very fast reaction studies by a variety of relaxation methods, especially by Eigen[30] but up to 1966 no really systematic studies were carried out on the triphenylcarbinol system, in which the reaction rates are slower and fall within the range of stopped-flow technique. Wyatt and co-workers[17,28,31] began their investigations in this field by the study of the effects of salts and other additives upon the reaction rates with the specific purpose of elucidating the acid - base equilibria, but during the same period similar work involving this compound was carried out with a different end in view. Reactions of organic cations with nucleophiles were investigated by Ritchie[29], Bunton[32] and their co-workers. Much of their studies were done using the stopped-flow technique and triphenylmethyl dye cations.

Although much of the work discussed subsequently in this thesis is concerned with measurements of reaction rates by the stopped-flow technique, it was the original intention to attempt to extend the range of rate constants and so to be able to explore systems in solutions of higher acidity, where the rates are too fast to be detected by flow methods.

With this aim in view some preliminary work was centred on the pressure jump relaxation technique. The results of this lengthy study are summarised in the Appendix A. This project was not very successful, due to the relatively small changes of concentration of tris-p-methoxyphenylmethylcation produced by the accessible pressure changes. During the course of this work, some progress was nevertheless made by

the n.m.r. study of the ionisation kinetics of triphenylmethanols in the more acidic regions[33], and in the fluorescence study of 3,6-dimethoxy, 9-phenyl, xanthen-9-ol[34] in an attempt to follow still faster reactions. In the event, kinetic information on the excited acid-base reaction was not obtained for the latter compound, but it had other properties of interest for comparison with the normal R_3COH indicators lacking the bridging oxygen atom between the rings. The fluorescence work reported is therefore principally concerned with quenching reaction rates, but the "normal" behaviour of the ClO_4^- ion in this context led to a full study of the effects of salts upon the forward and reverse reactions in the ground state for this compound, along the lines of the investigation of Postle and Wyatt[28].

Spurred by literature[35] findings of general base catalysis for reaction of Malachite Green with tertiary bases, effects of these bases and of trimethylamine, on the tris-p-methoxyphenylmethanol system were examined. Evidence for general base catalysis in the reaction between this compound and water is presented.

PART II

KINETIC STUDIES ON SUBSTITUTED TRIPHENYLMETHANOL COMPOUNDS

The preparative work on the organic compounds for use in this research was determined by the factors outlined in the last paragraph of the Introduction.

1. Indicators

Scrupulous care was taken to maintain anhydrous conditions, including oven drying of glassware and distillation of starting materials.

(a) Tris-p-methoxyphenylmethanol was prepared by the method of Smith et al[36] from diethyl carbonate and p-anisylmagnesium bromide in benzene - ether mixture and repeatedly gave crude product as a brown-red oil. Different attempts to crystallise it failed and it was eventually converted into tris-p-anisylmethylchloride hydrochloride[37], by dissolving in benzene and treating the solution with acetyl chloride. The product was obtained as dark-red needles. It was washed with dry benzene and dried for 24 h over potassium hydroxide, yielding tris-p-methoxyphenylchloride as pale-orange crystals m.p. 154-155°C.

Microanalysis gave 71.56% C, 5.69% H;

calculated 71.54% C, 5.66% H.

Molecular weight of 368.86 for $C_{22}H_{21}O_3Cl$ was confirmed by the presence of M^+ at 368 in the mass spectra of the compound.

The brown-red oil from the original preparation was analysed by spectrometric methods and appeared to consist mainly of the desired alcohol. The oil (53g) was dissolved in the minimum amount of ethanol and picric acid (53g), previously dried between two sheets of filter

paper, and dissolved in ethanol, was added to the hot solution of red oil in ethanol. Instant, copious precipitation of picrate occurred. The precipitate was washed with ethanol, re-dissolved in 1 M sodium hydroxide and was extracted with benzene. After removal of solvent a bright-red oil was obtained. The spectroscopic examination by U.V. and the microanalysis confirmed it to be pure $(C_6H_4OCH_3)_3$ COH.

The oil was dissolved in the minimum amount of benzene and a 10-fold excess of petroleum (b.p. 60-80°C) and was allowed to stand for 24 h. Yellow-orange crystals, m.p. 82-83°C were obtained, literature[38] m.p. 83.5-84°C.

Microanalysis for $C_{22}H_{22}O_4$ gave 75.00%C, 6.25% H;
calculated 75.42%C, 6.29% H.

(b) Tris-(4-methylphenyl) methanol. This compound was prepared by the method of Newman and Deno[39] from diethyl carbonate and 4-methylphenylmagnesium bromide. The crude product was recrystallised from petroleum b.p. 60-80°C and gave colourless crystals m.p. 92-93°C, literature m.p. 93.4 - 94°C.

Microanalysis gave 87.10% C, 7.24% H;
calculated 87.14% C, 7.29% H.

(c) 4-Methoxy-triphenylmethanol was prepared from ethyl anisate and phenylmagnesium bromide by the method of Bayer and Villiger[40] in 24% yield m.p. 56-58°C, Literature[40] m.p. 58-61°C.

(d) 4-t-Butyltriphenylchloromethane was prepared by the method of Marvel et al.[41] Pale yellow crystals m.p. 133-134°C, (lit. m.p. 133-134°C) were obtained.

(e) 9-Phenyl xanthydrol was prepared, by the modification of two literature preparations[42, 43], from xanthone (19.6g) dissolved in hot benzene (80ml) and phenylmagnesium bromide in ether.

The latter reagent was prepared from bromobenzene (15.7g) and Mg turnings (2.4g). The mixture was refluxed for 1 h, then half of the benzene was removed by distillation. The remaining Grignard compound was decomposed with c.HCl and extracted with benzene, till the lightly-orange coloured extract was colourless. The phenylxanthonium salt precipitated on neutralisation with $NaHCO_3$ was filtered, washed twice with water, and dried in a desiccator over silica gel. When recrystallised from ethanol - petroleum ether (b.p. 60-80°C), crystals, m.p. 159-160°C were obtained in 92% yield.

Microanalysis for $C_{19}H_{14}O_2$ gave 83.26% C, 5.19% H;
calculated 83.29% C, 5.14% H.

(f) 3,6-Dimethoxy xanthone. This compound was prepared by different routes, due to the paucity of experimental data[44] and initial lack of starting materials for its synthesis.

Route I WARNING!! Standard Carius tubes proved liable to explode in this reaction when heated above 220°C. For work above this temperature the use of thicker Pyrex glass and longer tubes is recommended.

The mixture of 2,2'- dihydroxy-4,4'- dimethoxybenzophenone (1g) and water (50 ml), in a sealed Pyrex glass tube (3 mm wall X 23 mm diam. X 400 mm long), was heated in a Carius oven at 210-215°C for 4 h. The tube was cooled, opened, and the product was filtered. The residue was dissolved in the minimum quantity of EtOH, treated with charcoal, filtered, and allowed to crystallise. Silky, brown-yellow needles m.p. 187-188°C in 32% yield were obtained.

Microanalysis for $C_{15}H_{12}O_4$ gave 69.83% C, 4.81% H;
calculated 70.30% C, 4.70% H.

Route II

From 2:2', 4:4'-tetrahydroxybenzophenone (2g) and demineralised water (11 ml), heated in Carius tube at 200-220°C for 2-2.5 h. The resulting 3,6-dihydroxy xanthone, obtained in clusters of long needles, was washed with water, cleaned with charcoal and crystallised from pyridine.

It did not melt below 300°C, literature[44,45] gives decomposition 330°C.

Microanalysis for $C_{13}H_8O_4$ gave 68.21% C, 3.55% H;
calculated 68.40% C, 3.50% H.

The yield was 98-100%.

The 3,6-dihydroxyxanthone obtained in this way was methylated in mild[46] and more rigorous[47] conditions to improve the overall yield.

The first method, using 3,6-dihydroxyxanthone (0.114g) in acetone (10 ml), anhydrous potassium hydrogen carbonate (0.5g), and methyl sulphate (0.5 ml) gave the desired product m.p. 187-188°C in 40% yield.

The second method, using 3,6-dihydroxyxanthone (4g) and methyl sulphate (15 ml) in 5M NaOH (30.5 ml), gave white-brown crystals, which when recrystallised from acetone had m.p. 186-187°C and were obtained in 52% yield.

Progress of methylation was followed by T.L.C., using Al_2O_3 and toluene : ether in 19 : 1 ratio[48], as stationary and mobile phases respectively.

The 3,6-dimethoxyxanthone obtained by the two routes was combined, recrystallised from methanol and identified by : the mixed m.p., 190°C, mass spectrum, M^+ at 256, n.m.r. and i.r. spectra.

Microanalysis for $C_{15}H_{12}O_4$ gave 69.92% C, 4.63% H;
calculated 70.30% C, 4.70% H.

Literature m.p. for this compound ranged from 184°C[49], through 187°C[47] to 186°C[44].

(g) 3,6-Dimethoxy, 9-phenyl, xanthen-9-ol. The Grignard compound prepared from Mg(0.3g) in ether (4ml) and phenylbromide(1.9g) was added, with vigorous stirring to a flask containing 3,6-dimethoxyxanthone (2g in dry benzene (10ml), under an atmosphere of oxygen-free nitrogen. The ketone was dissolved after 6 h of stirring. The magnesium complex was decomposed with a cold, saturated solution of NH_4Cl. The organic phase was washed with water, dried over $MgSO_4$ and concentrated by use of a Büchi evaporator to half of its original volume. Hexane (5ml) was added while the solution was still hot. After cooling for 24 h, hard orange crystals m.p. 138.5 - 140°C were collected in 80% yield. These, when recrystallised from an ether-hexane mixture had m.p. 139 - 140°C.

Microanalysis for $C_{21}H_{18}O_4$ gave 75.24% C, 5.66% H;
calculated 75.43% C, 5.43% H.

The mass spectrum showed M^+ at 334, consistent with the supposed molecular formula.

The attempted preparation of the trimethoxy analogue by coupling of p-anisylmagnesium bromide with 3,6-dimethoxyxanthone ended unaccountably in failure.

2. Materials used and their purification

Analytical grade reagents used without further purification were:-

Hydrochloric acid 35%
Sulphuric acid 98%
Perchloric acid 60%
Acetic acid, glacial

The following salts were all analytical grade and were dried before use either in oven or in desiccator over silica gel:-

Potassium bromide
Potassium chloride
Potassium iodide
Potassium nitrate

Potassium sulphate
Sodium acetate
Sodium carbonate
Sodium dihydrogen orthophosphate
Sodium hydroxide
Sodium perchlorate
Ammonium chloride
Calcium chloride
Magnesium perchlorate

Diazabicyclo - [2.2.2.] octane was dried over $CaCl_2$, then over Na and was sublimed in vacuo, m.p. 157 - 159°C, literature[50] m.p. 158 - 160°C.

Triethylamine was distilled at S.T.P., collecting fraction b.p. 89 - 90°C.

Trimethylamine, a very old sample (I.C.I. 1951) was converted to hydrochloride $(CH_3)_3N$ HCl m.p. 278 - 281°C and regenerated by treating the hydrochloride with aqueous 50% NaOH (Beilstein quotes m.p. 277°C). Eventually, Fisons 25% aqueous solution was used. It was diluted to approx. 1 M and titrated, using Bromothymol blue indicator, with 1 M acid, prepared from B.D.H. conc. volumetric solution ampoule. Check for purity, gave $(CH_3)_3$ N HCl m.p. 283 - 284°C.

Solvents were either analytical or spectroscopic grade. Those used for preparation of organic compounds were distilled before use and dried. For example diethyl ether and benzene over Na; tetrahydrofuran over calcium hydride, after distillation from Na.

Melting points were determined on the Kofler hot-stage microscope.

3. Stopped-Flow Kinetic Measurements

(a) General description of instrument

The disappearance of the coloured R_3C^+ ion was followed spectrophotometrically on the stopped-flow instrument built in Sheffield. It was based on the design of Gibson[50a] and its construction, specifications, and test of performance are described in detail elsewhere[51]. The instrument was suitable for work with strong acids since the materials used for its construction were Kel - F, Teflon, and borosilicate-filled Teflon. These special materials were not readily available and replacement of worn-out parts of the instrument was frequently protracted.

Several modifications were made to this apparatus during the course of present work, concerning the recording and display of kinetic traces and the light source. The rather lengthy method of photographing the trace from the oscilloscope, developing the film, enlarging and transferring of the trace on to the graph paper, was speeded up using the Southern Instruments u.v. recorder (M 1330A). A signal of up to 10 ma from the photomultiplier was fed into an operational amplifier, current to voltage converter, equipped with off-setting facilities, and hence to the sensitive galvanometer of the u.v. recorder. A spot of intense u.v. light is reflected from the galvanometer on to photosensitive recording paper and the traces become visible as soon as the completed record is exposed to daylight. The image is permanent for up to six months, longer if stored in darkness.

A new 6-12 V, 3 A, d.c., stable power supply unit was constructed to power the light source of the Beckman quartz spectrophotometer. The latter was used solely as a monochromator. After thermostatting, the solutions were driven under even pressure through the mixers, past the

observation tube, and into the stop syringe. Variations of optical density of the stationary fluid were recorded. The "spent" solution was then expelled from the stop syringe and the apparatus was re-set for another run. The effluent from stopped-flow apparatus was expelled via a flow-through cell, which contained a pH combination microelectrode, so that the pH of the solution was continually monitored. A Radiometer 26 pH Meter was used for measurements of pH to within $\pm$ 2%.

The temperature of water, circulating around the flow syringes, mixers and observation tube, was thermostatted to within $\pm$0.05 - 0.10°C.

Fig. II 1 General view of the stopped-flow apparatus.

Fig. II 2 The flow-through cell with a pH microelectrode.

(b) Description of a typical experiment

For a typical experiment on a stopped-flow apparatus, the two solutions were prepared and de-gassed by equilibration at about 35°C. Each of the storage syringes was washed with air-free distilled water, followed by three washes with the appropriate solution. Finally the whole apparatus was flushed with the air-free water and solutions. The de-gassing and careful washing procedure is emphasised, since the presence of air bubbles causes irregular trace-lines, which in turn lead to larger errors in calculated values of rate constants.

Before each kinetic run the zero transmission line was printed and as the result of an experiment a record of the pattern in Fig. II 3 was obtained.

Fig. II. 1

General view of the stopped-flow apparatus

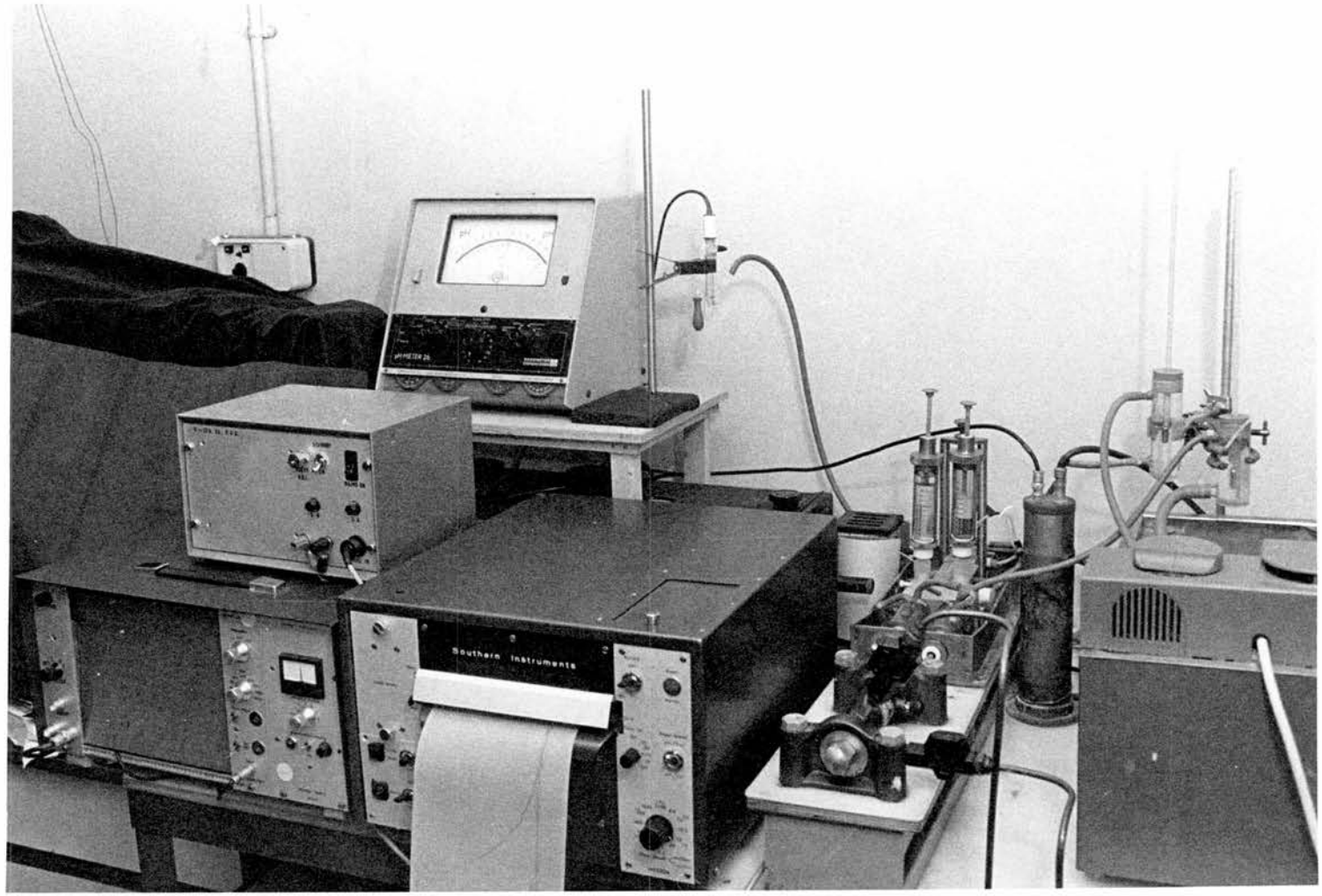

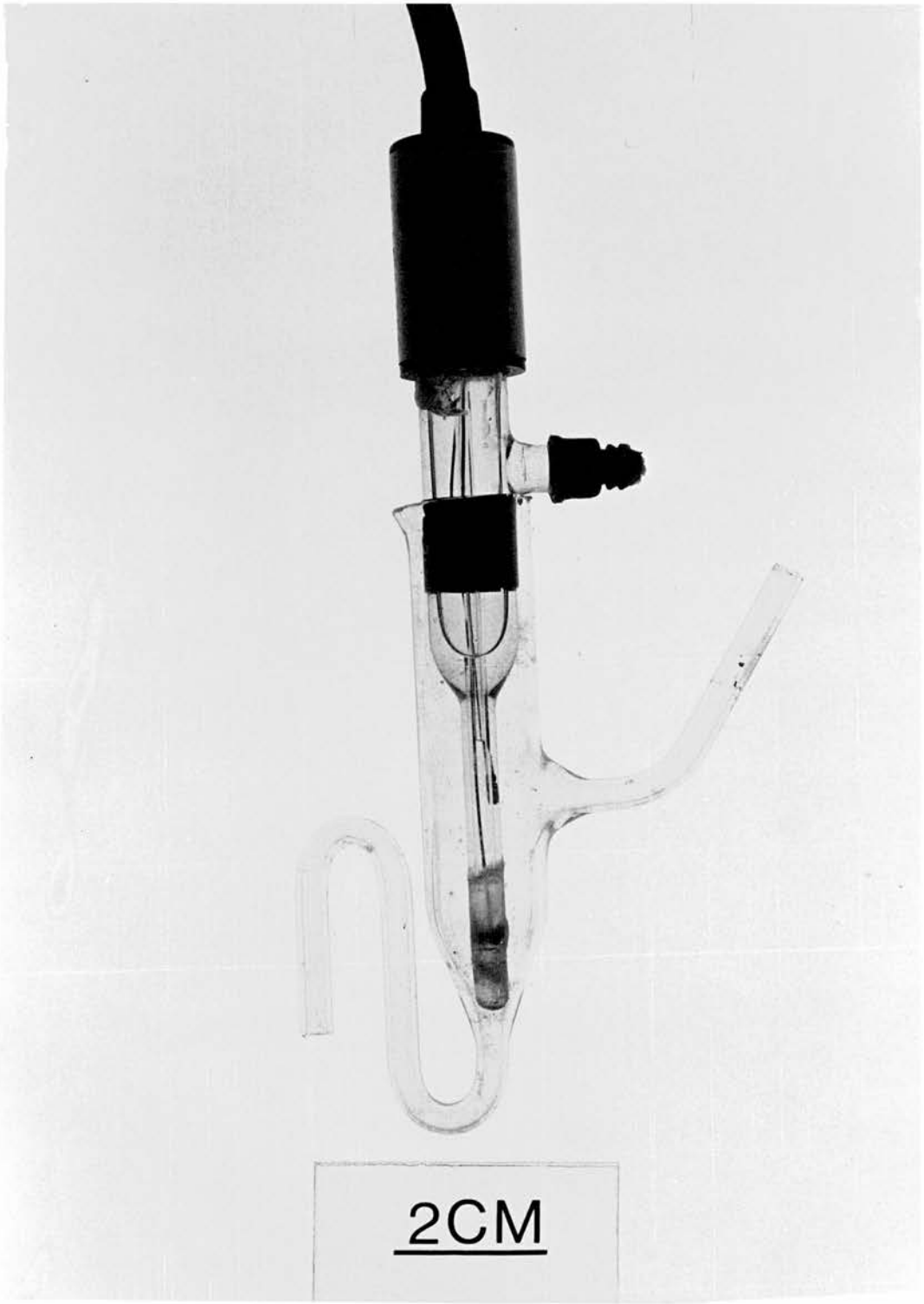

Fig. II.2

The flow-through cell with a pH microelectrode

Fig. II 3 Record of an experiment

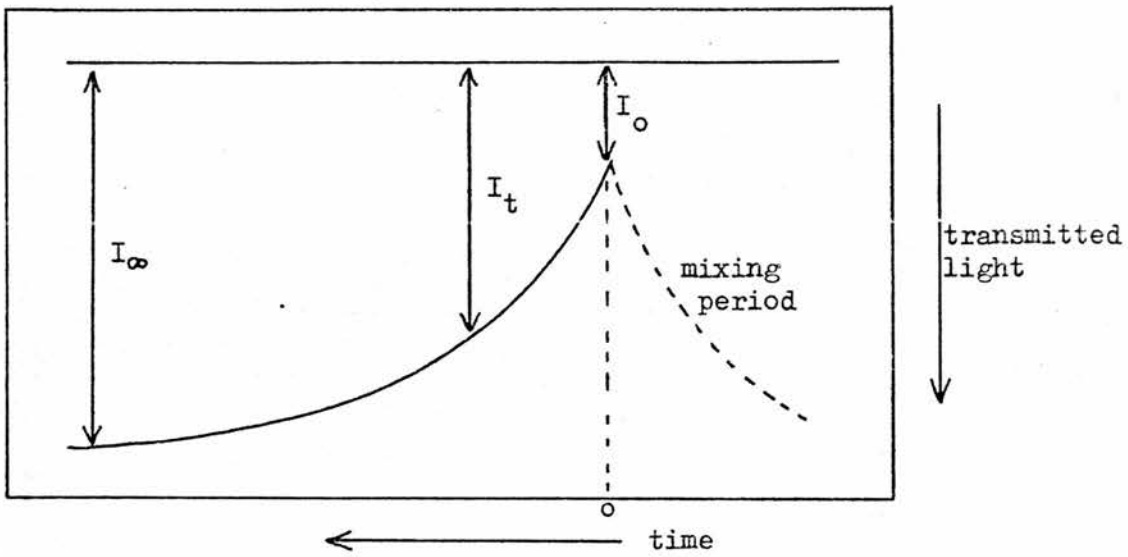

Usually, 2-3 kinetic traces from the same experiment were finally recorded and used for calculation of the rate constant, although up to 8 traces were observed for each solution to check the reproducibility.

(c) Analysis of data

In Fig. II 3 the quantity I measures the light at 100% transmission, i.e. zero reactant concentration. The optical density D_t at any time t, is given by log (I_∞ / I_t) and this is proportional to the concentration of absorbing reactant at time t. The first order rate equation $kt = \ln (a/a-x)$ can therefore be evaluated as $kt = 2.303 \log (D_o / D_t)$. In the first instance the pseudo first order constants were evaluated by the usual graphical method of plotting the logarithmic term against time and taking the slope.

To obtain a more precise idea of the error involved in these calculations, the data were transferred to computer cards and the first order rate constants from light transmission were computed using a LSQPT (version of the) programme. Those are the "standard error" of k values, quoted in the result tables.

When the Canterbury stopped-flow instrument (loaned from Dr. A.R. Butler, this department) was used, the kinetic traces displayed on the oscilloscope were recorded by a Polaroid camera.

When a weak absorption was being measured the use of a sensitivity adequate for producing a suitable trace of the reaction curve could result in the zero line of Fig. II 3 being off scale. When this occurred a suitable correction was applied based on the gain control settings.

Weak absorption conditions also made it possible to introduce a standard mathematical simplification for D_t.

Thus if we define D_t in terms of logarithm to base 10 in

$$D_t = \log_{10}\left(\frac{I_\infty}{I_t}\right) \quad \text{, we can write}$$

$$D_t = \frac{1}{2.303} \ln\left(\frac{I_\infty}{I_t}\right) = \frac{1}{2.303} \ln\left[1 + \left(\frac{I_\infty - I_t}{I_t}\right)\right]$$

By the usual approximation formula ln (1 + x) is approximately equal to x, when x is less than 0.1.

Thus $D_t \approx \left(\frac{I_\infty - I_t}{I_t}\right)$ under these conditions.

Since I_∞ and I_t were directly available from the reaction trace this was a convenient simplification.

Using an x-y reader, the co-ordinates on the photographic record were transferred to punched paper tape in terms of voltages on the digital voltmeter of the Solartron/Facit 4070 equipment[52]. The paper tape output was calculated by the I BM 360 computer, using the DATEML programme, which was designed to give natural lifetime and the first

order decay constant for emission decay curves of weak transients. The values of k_{obs} calculated by computer were compared with those obtained graphically, and were in good agreement. For example, for the experiment 24.4.73:

	computer k_{obs}	graphical k_{obs}
photograph 2a	$18.5 \pm 2.3\ s^{-1}$	$18.0\ s^{-1}$
photograph 3a	$16.6 \pm 2.0\ s^{-1}$	$16.7\ s^{-1}$

For slower reactions, the method of Kezdy and Swinbourne[53] was employed to determine first-order rate constants (k). Considering a first order reaction of which the optical density readings are $D_o, D_1 \ldots\ldots\ldots\ldots D_n \ldots\ldots\ldots\ldots 0$

at times $0\ ,\ t_1 \ldots\ldots\ldots\ldots t_n \ldots\ldots\ldots\ldots t_\infty$

Since $D_n = \epsilon d . C_n$ and $C_n = C_o \exp(-kt_n)$,

we can write the reaction rate law as:

$$D_n = D_o \exp(-kt_n)$$

$$D_{n'} = D_o \exp(-kt_{n'}) \quad \text{where } t_{n'} = (t_n + \Delta t)$$

By division $$\frac{D_n}{D_{n'}} = \exp k(t_{n'} - t_n) = \exp k\Delta t$$

or $$D_n = \left[\exp(k\Delta t) \right] D_{n'}$$

So a plot of D_n against $D_{n'}$ gives a line of slope = exp ($k\Delta t$), from which k can be deduced as being $\left[\frac{\ln(\text{slope})}{\Delta t}\right]$.

In order to obtain reliable estimates of k the data should be recorded over a period of time greater than the half-life of reaction, and preferably at t > two half-lives, and Δt should be of the order of $0.5t_{\frac{1}{2}}$ to $t_{\frac{1}{2}}$. It should also be noted that the method is relatively insensitive to deviations from the strict first-order law. In the work recorded here, Δt was chosen to be 0.7 x the half-life. The method is fast since it uses easily constructed plots of the optical densities.

(d) Preparation of buffer solutions

It had been hoped to prepare buffer solutions in situ, in the mixing chamber of the stopped-flow apparatus, by the addition of an excess of acid indicator from a syringe and partially neutralising it with a base solution from a second syringe. But, since the molarities of acid and alkali were as high as 0.8 M and 1.6 M respectively, the heat of neutralisation gave temperature rises of between 1.7 and 3.0°C, and this method was abandoned.

Instead, the following procedure was adopted. The "S_1" syringe contained indicator tris-(4-methoxyphenyl) methanol in 0.1 M acid (HCl or $HClO_4$). The "S_2" syringe contained a suitable buffer solution, made from calculated volumes of weak base (dabco, Et_3N, or Me_3N) and acid (HCl or $HClO_4$) together with an appropriate amount of NaOH to neutralise the acid used to produce the R_3C^+ indicator ion, and sufficient NaCl or $NaClO_4$ to maintain constant ionic strength of the solution.

The quantities required were calculated as follows. It is convenient to consider the stoichiometry of the buffer mixture in syringe "S_2" without initial allowance for the NaOH added to neutralise the acid from S_1 syringe, on mixing. With this understanding, for a buffer ratio of $[BH^+] / [B] = 1/1$, if $[B]$ the free base concentration in syringe "S_2", is to be xM and $[BH^+]$, the conjugate acid concentration, is xM (both without reference to the extra NaOH present) then initial $[B]$ in the stock solution for S_2 has to be 2xM and if $[NaOH]$, the concentration in "S_2" necessary ultimately to neutralise acid in syringe "S_1", is 0.1 M after mixing equal volumes of the "S_1" and "S_2" syringe content in the cell, an inventory of ionic contributions to the ionic strength in the final mixture is therefore:-

	+ ve ions	- ve ions	
BH^+	x/2		
Cl^- or ClO_4^-		x/2	from the stoichiometric acid addition to make the 1/1 buffer mixture from the conjugate base in syringe "S_2".
NaCl	y/2	y/2	
NaOH	0.1/2	0.1/2	
	(0.1+x+y)/2	(0.1+x+y)/2	

then, since $I = \frac{1}{2}\sum_i C_i Z_i^2$,

we have, if the desired $I = 0.2$,

$$I = 0.2 = \tfrac{1}{2}\left[(0.1 + x + y)/2\ (1)^2 + (0.1+ x + y)/2(-1)^2\right]$$

$$0.4 = 0.1 + x + y$$

$$x + y = 0.3$$

Therefore, to prepare 50ml of the solution for syringe "S_2", using e.g. 1 M NaOH, 0.5M Et_3N, 1M HCl, and 1M NaCl solutions,

amount of 1M NaOH required is $\underline{5\ ml}$;

amount of Et_3N required is $2x$ moles l^{-1}

$$= \frac{2x}{20} \text{ moles/50 ml.}$$

$$= \frac{1000 \times 2x}{20 \times 0.5} \text{ ml of 0.5 M } Et_3N/50ml$$

$$= \underline{200\ x} \text{ ml of 0.5 M } Et_3N/50 \text{ ml.}$$

The amount of HCl required is $\underline{50x}$ ml of 1 M,

and the amount of NaCl required is $\frac{(0.3-x)}{20}$ moles/50 ml

$$= \frac{(0.3-x)1000}{20} \text{ ml of 1 M NaCl/50 ml}$$

$$= \underline{15 - 50x} \text{ ml of 1M NaCl/50 ml}$$

Thus the total volume $= \left[5 + 200x + 50x + 15-50x \right]$ ml $= 20(10x +1)$ ml.

If $20(10x + 1)$ is equated to 50 ml, we get $x = 0.15$, and this will correspond to the highest concentration of Et_3N when using the various concentrations of solutions (NaOH,HCl, NaCl) given above. In fact, concentrations greater than $x = 0.15$ were not attainable, due to the limited solubility of the base in water.

Since 200x ml of 0.5 M Et_3N/50 ml is required, we deduce 30 ml of 0.5 M Et_3N/50 ml for this case. Other values of x yield the values calculated below:-

TABLE II 1.

Triethylamine buffer

buffer ratio $BH^+/B = 1$

x	ml of solution			
	1 M NaOH	0.5 M Et_3N	1 M HCl	1 M NaCl
0.150	5	30	7.50	7.50
0.125	5	25	6.25	8.75
0.100	5	20	5.00	10.00
0.075	5	15	3.75	11.25
0.050	5	10	2.50	12.50
0.025	5	5	1.25	13.75

Similar calculations were used subsequently to prepare buffers of dabco, Me_3N, and Et_3N in different ratios, and when the preparation of these buffers is mentioned, the above procedure was followed.

4. Base Catalysis

(a) General introduction

There are two types of base catalysis observed experimentally. In the first type catalysis is only by hydroxide ion and the rate is determined solely by the pH and is independent of the buffer concentration. This is specific base catalysis and this type of reaction involves either hydroxide ion directly, or a reactant, or a conjugate base of one of the reactants, formed in an amount proportional to the hydroxide ion concentration in a fast equilibrium step before

the rate-determining step.

In the second type of reaction there is an increase in rate with increasing buffer concentration at a constant pH and constant ionic strength and this type shows a larger increase when the buffer contains larger amounts of basic component.

Since the hydroxide ion concentration does not change with increasing buffer concentration, at a fixed buffer ratio the buffer itself, or the basic component of the buffer catalyses the reaction. This is general base catalysis and occurs where bases other than hydroxide ion can accelerate the reaction.

Graphically these two types of reaction can be represented by Figs. A and B.

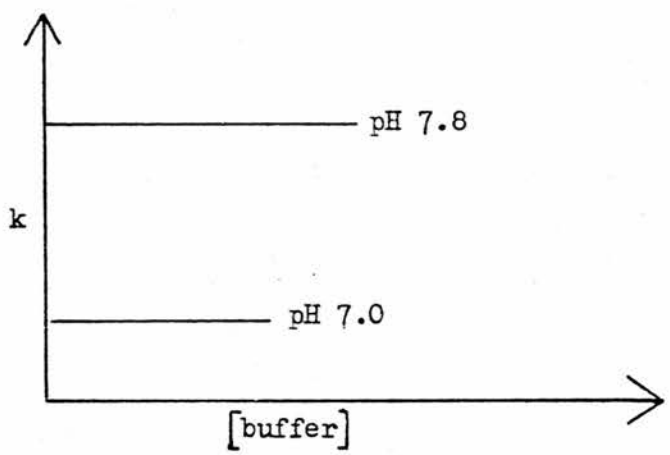

Fig. A.

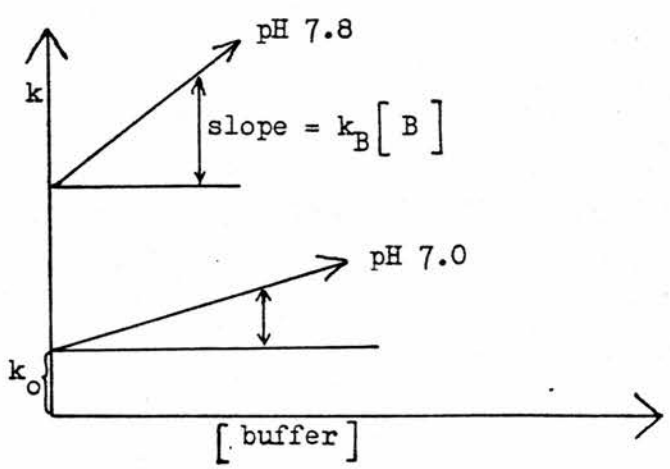

Fig. B.

The intercepts of the lines in Fig. B, at $\left[\text{base}\right] = 0$, represent the OH^- and solvent catalysed parts of the reaction, k_o, i.e. the first two terms in the notation below, and the slope of the plot against $\left[\text{base}\right]$ gives the observed rate constant of the base catalysed reaction, k_B. If we assume general base catalysis to begin with i.e. the proton donation not important, the complete rate law can be written as

$$\text{rate} = \left\{ k_{H_2O}(H_2O) + k_{OH^-}(OH^-) + k_B(B) \right\} \left[\text{Organic compound} \right]$$

Solvent can act as proton acceptor or donor and has to be included.

$$\text{now } k_{obs} = k_{H_2O}(H_2O) + k_{OH^-}(OH^-) + k_B(B)$$

$$\therefore \text{rate} = k_{obs} \left[\text{Organic compound} \right]$$

Ritchie[29] noticed that OH^- in water and methoxide ion in CH_3OH react faster than CN^- in the respective solvents. These unexpectedly high rates of reactions of OH^- and CH_3O^- ions can be rationalised by a possibility of a reaction path where a proton transfer across solvent molecules can achieve the same transformation as that accomplished by the removal of solvent molecules in other cases. This implies the existence of general base catalysis for the reaction of a cation with solvent, contrary to the general belief that this reaction, $R_3C^+ + H_2O \rightleftharpoons R_3COH + H^+$ is not subject to such catalysis.[27,32] In view of the inconclusiveness of the existing data, Ritchie[35] investigated the reaction of Malachite Green with water and showed direct dependence of the rate of this reaction on buffer concentration with 1,4-diazabicyclo $\left[2.2.2\right]$ -octane (Dabco) and triethylamine as buffers. Although the reaction of Malachite Green is much slower than the reaction

of tris-p-methoxyphenylmethanol, results, similar to those reported by Ritchie[35] were obtained in the present work with Dabco, triethylamine and trimethylamine.

(b) Results and discussion

In all the experiments given below, the initial concentration of tris-p-methoxyphenylmethanol was 3.68×10^{-5} mol dm^{-3} in 0.1 mol dm^{-3} acid in all cases. The ionic strength was maintained at 0.2 mol dm^{-3} by the addition of NaCl or $NaClO_4$ and buffers were prepared as described previously on page 21. The pH of the reaction solution was measured at the end of each kinetic run. The values of k_{obs} are mean values of several rate determinations (subscripted to k_{obs} in Tables II 3 and II 4), agreeing to within $\pm$ 6%.

Data for the reaction of tris-p-methoxyphenylmethyl cation in aqueous solutions buffered with the 3 bases are presented in tables 2 - 4.

TABLE II 2.

Reaction of tris-p-methoxyphenylmethyl cation in aqueous solutions buffered with Dabco

[Dabco]/mol dm^{-3}	pH	k_{obs}/s^{-1}	standard error/s^{-1}
0.200	9.09	25.7	1.0
0.150	9.16	21.3	0.3
0.100	9.15	18.3	0.6
0.050	9.09	15.5	0.4
0.025	9.09	13.8	0.2
0.017[5]	9.10	13.6	0.3
buffer ratio = 2/1, acid HCl			
0.150	8.99	19.7	0.63
0.125	8.74	17.5	0.50
0.100	9.00	16.4	0.67
0.075	8.93	15.9	0.60
0.050	8.61	15.0	0.40
0.025	8.95	12.9	0.33
buffer ratio = 1/1, acid HCl			
0.150	8.91	17.7	0.5
0.125	9.06	17.4	0.4
0.100	8.70	16.4	0.5
0.075	9.00	14.8	0.6
0.050	8.75	13.8	0.5
0.025	8.72	13.0	0.25
buffer ratio = 1/1, acid $HClO_4$			

TABLE II 3.

Reaction of tris-p-methoxyphenylmethyl cation in aqueous solutions buffered with trimethylamine

$[(CH_3)_3N]$/mol dm^{-3}	pH	k_{obs}/s^{-1}	standard error/s^{-1}
0.025	9.60	19.30_{10}	0.63
0.050	9.65	23.61_{8}	0.31
0.075	9.65	28.60_{11}	0.05
0.100	9.65	31.32_{11}	0.62
0.125	9.58	38.30_{14}	0.91
0.150	9.60	40.40_{9}	1.20
buffer ratio = 1/1, acid HCl			
0.025	10.31	21.17_{4}	0.53
0.050	10.31	24.60_{6}	1.40
0.100	10.10	36.70_{8}	1.40
0.150	10.31	39.90_{4}	1.50
0.200	10.32	56.00_{10}	2.20
buffer ratio = 1/2, acid HCl			

TABLE II 4.

Reaction of tris-p-methoxyphenylmethyl cation in aqueous solutions buffered with triethylamine.

$[(C_2H_5)_3N]$ /mol dm^{-3}	pH	k_{obs}/s^{-1}	standard error/s^{-1}
0.075	10.50	28.20_7	0.42
0.063	10.45	25.70_4	0.54
0.050	10.45	23.20_4	0.89
0.037	10.50	21.90_4	0.89
0.025	10.45	19.50_4	0.48
0.013	10.50	18.40_6	0.77
buffer ratio = 1/1, acid HCl			
0.050	10.20	25.70_6	1.3
0.038	10.31	22.20_4	0.43
0.025	10.25	20.95_4	0.88
0.013	10.30	20.39_4	0.60
0.006	10.30	18.04_6	0.59
buffer ratio = 2/1, acid HCl			

The direct experimental data contained in Tables 2 - 4 was used to construct graphs Fig. II 4 and II 5, from which slopes and intercepts were calculated for each of the three bases and these are summarised in Table 5 below.

TABLE II 5.

Values of slopes and intercepts for Dabco, $(CH_3)_3N$, and $(C_2H_5)_3N$		
base	slope (k_B)	intercept
Dabco	63 $dm^3\ mol^{-1}s^{-1}$	12.2 s^{-1}
$(CH_3)_3N$	202 $dm^3\ mol^{-1}s^{-1}$	13.6 s^{-1}
$(C_2H_5)_3N$	162 $dm^3\ mol^{-1}s^{-1}$	16.0 s^{-1}

Free base concentrations in Tables 2 - 4 were calculated from the nominal buffer ratios (1/1, 1/2, 2/1) and the k_B values in Table 5 were obtained from a plot of k_{obs} against $k_B[B]$. Estimates of the $[OH^-]$ will obviously affect the interpretation of the intercept value, since it equals $\{k_{H_2O}(H_2O) + k_{OH^-}(OH^-)\}$. If the $[OH^-]$ was not the value aimed at when setting up a particular experiment, (e.g. due to variations caused by leaking syringes at the time of flow, or seepage of reactants from the stop syringe etc.) it becomes important to use the measured pH achieved since there will also be an effect on the calculated free $[B]$.

For example, if the measured pH is accepted for $(Et_3)N$ in Table 4, then the pH of the nominal buffer 1/1 is 10.47, i.e. some 0.4 pH unit

Fig. II 4

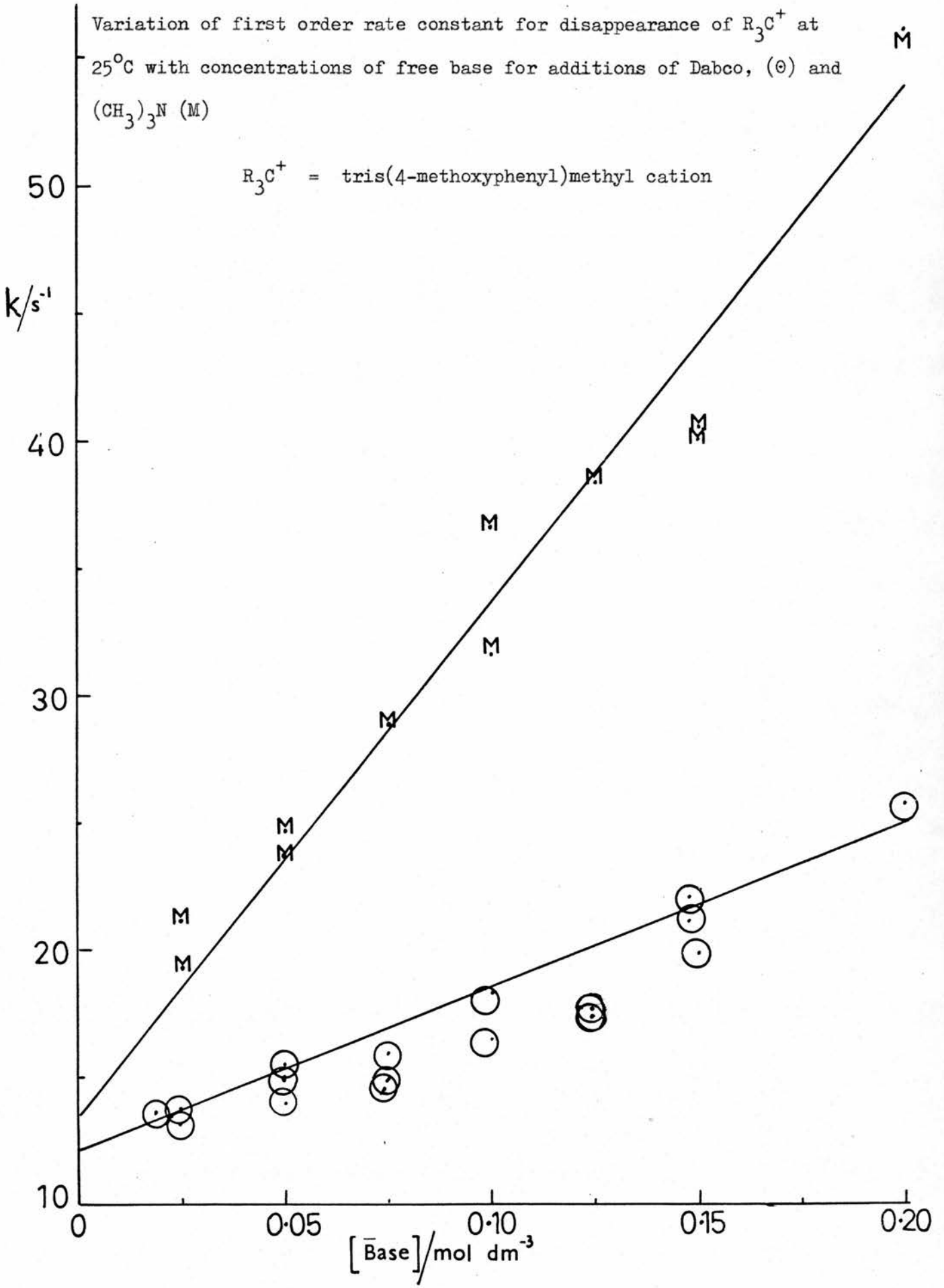
Variation of first order rate constant for disappearance of R_3C^+ at 25°C with concentrations of free base for additions of Dabco, (Θ) and $(CH_3)_3N$ (M)
R_3C^+ = tris(4-methoxyphenyl)methyl cation
k/s⁻¹
50
40
30
20
10
0
0·05
0·10
0·15
0·20
[Base]/mol dm⁻³
M

Fig. II 5

Variation of first order rate constant for disappearance of R_3C^+ at 25°C with concentration of free base for addition of $(C_2H_5)_3N$.

R_3C^+ = tris (4-methoxyphenyl)methyl cation.

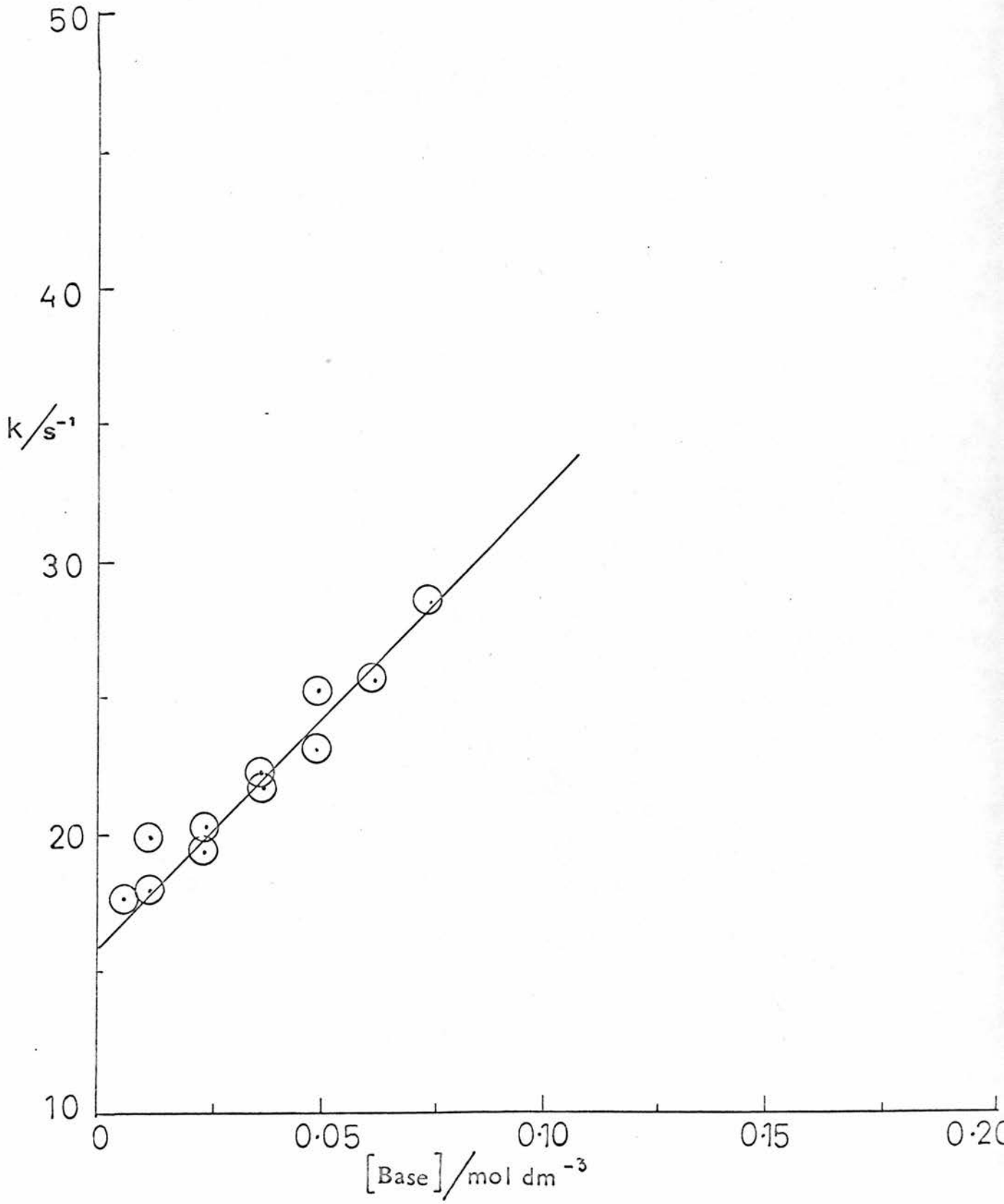

less than pK_a of Et_3NH^+, 10.87[54] ; hence $[BH^+]/[B] \simeq 2.5$, but $[B] + [BH^+] = x$ here, therefore $[B] = x/3.5$ and not $x/2$, and should be multiplied by a factor of 0.57, $[(x/3.5)/(x/2)]$.

Values of $[B]$ recalculated thus are shown in Tables 6 and 7.

TABLE II 6.

Variation of first-order rate constants for disappearance of R_3C^+ at 25°C with concentration of free base adjusted for pH of effluent.

$[Et_3N]$ /mol dm^{-3}	k_{obs}/s^{-1}	average pH
0.043	28.2	10.47
0.036	25.7	
0.029	23.2	
0.021	21.9	
0.014	19.5	
0.007	18.4	
0.038	25.70	10.27
0.028	22.20	
0.019	20.95	
0.009	20.39	
0.004	18.04	

TABLE II 7.

Variation of first-order rate constants for disappearance of R_3C^+ at 25°C with concentration of free base adjusted for pH of effluent.

$[(Me)_3N]$/mol dm^{-3}	k_{obs}/s^{-1}	average pH
0.111	40.4	9.62
0.093	38.3	
0.074	31.3	
0.056	28.6	
0.037	22.8	
0.019	19.3	
0.180	56.00	10.15
0.135	39.90	
0.090	36.70	
0.045	24.60	
0.023	21.17	

pK_a for Me_3NH^+ was taken as 9.80[55].

In the case of experiments with Dabco as a buffer these adjustments were unnecessary since the average pH of effluent was 8.86, i.e. almost the same as the pK_a value for protonated Dabco of 8.82[56].

We can now discuss the data which we have produced in this work and outlined above. The first point which has been clearly shown is that there is a definite catalytic action by each of three bases used in the buffer mixtures. This is directly opposite to the conclusions of Postle and Wyatt[28] and Bunton and Huang[32] in their investigation of the same reaction. While some of their work was done with buffer mixtures not used in this research Postle and Wyatt did a substantial amount with triethylamine buffer mixtures, which ought to be directly comparable with this work. Unfortunately the design of their experiments was different. In this research the pH was kept constant while the buffer concentration was varied. In their Table 2 most of the data were with triethylamine buffers 0.1 M Et_3N at different pH values, which means different amounts of OH^- and free base at the same time. They stated that the increases in rate observed depended on pH increases and not on buffer concentrations. Their experiments do not seem to be sufficiently clear-cut to isolate effects due to $[OH^-]$ and $[Et_3N]$ variations. The pH values quoted are presumably measured values but there is no indication whether these were in agreement with those predicted from the buffer mixture compositions used. As found above there can be differences between predicted and measured values in these difficult mixing techniques and this causes quantitative errors in deduced constants.

The results of this work however parallel those of Ritchie using the Malachite Green cation with Dabco buffers[35] where general base catalysis was proved. In the same report Ritchie points out that a re-interpretation of data of a previous research on the same cation (Malachite Green) using triethylamine buffer systems was in agreement with catalysis by that base during reaction to form the alcohol. It is considered therefore that the results of this work are in qualitative

agreement with the work of Ritchie.

There is another aspect of the effect of pH which it was thought desirable to take into account in the graphing of the re-calculated concentrations. For each of the bases the experiments were done in sets covering a range of concentrations and at approximately a constant pH for each set. But the variation between sets could be important through its effects on total rate constant arising from hydroxyl ion being a catalyst. As indicated previously k_{obs} is composite and given by $k_{obs} = \left\{ k_{H_2O} \left[H_2O\right] + k_{OH^-} \left[OH^-\right] + k_B \left[B \right] \right\}$. Hence the graphs of k_{obs} against $\left[B \right]$ should be done at constant $\left[OH^-\right]$, i.e. constant pH. The intercepts of such graphs on the axis where $\left[B \right] = 0$ are interpreted as equal to $\left\{ k_{H_2O} \left[H_2O\right] + k_{OH^-} \left[OH^-\right] \right\}$.

In the case of $(CH_3)_3N$ buffer systems, examination of the two sets of data in Table II 3 shows that one has a mean pH of 9.62 and the other 10.27. This means an increase of $10^{0.65}$ in $\left[OH^-\right]$ in the latter case, i.e. by almost a factor of 4.5. If OH^- catalysis occurs to an appreciable extent in the pH range - and there is literature evidence, which is discussed below, that this is the case - then the two sets of data should lie on parallel lines with different intercepts on the vertical axis. As shown in Fig. II 6 this appears to be the case when lines are drawn for each set. This procedure has been followed for the other bases. In the case of Dabco the higher pH set at 9.11 does show faster rates than the lower sets at 8.85 and 8.87 but the slopes are not as parallel as might be desired. In the case of $(C_2H_5)_3N$ buffer systems the sets only differ by 0.2 pH and although the layout of the points justified treating each set separately the higher rate was given by the

Fig. II 6

Variation of first-order rate constants for disappearance of R_3C^+ at 25°C with concns. of $(CH_3)_3N$ and Dabco adjusted for pH of effluent.

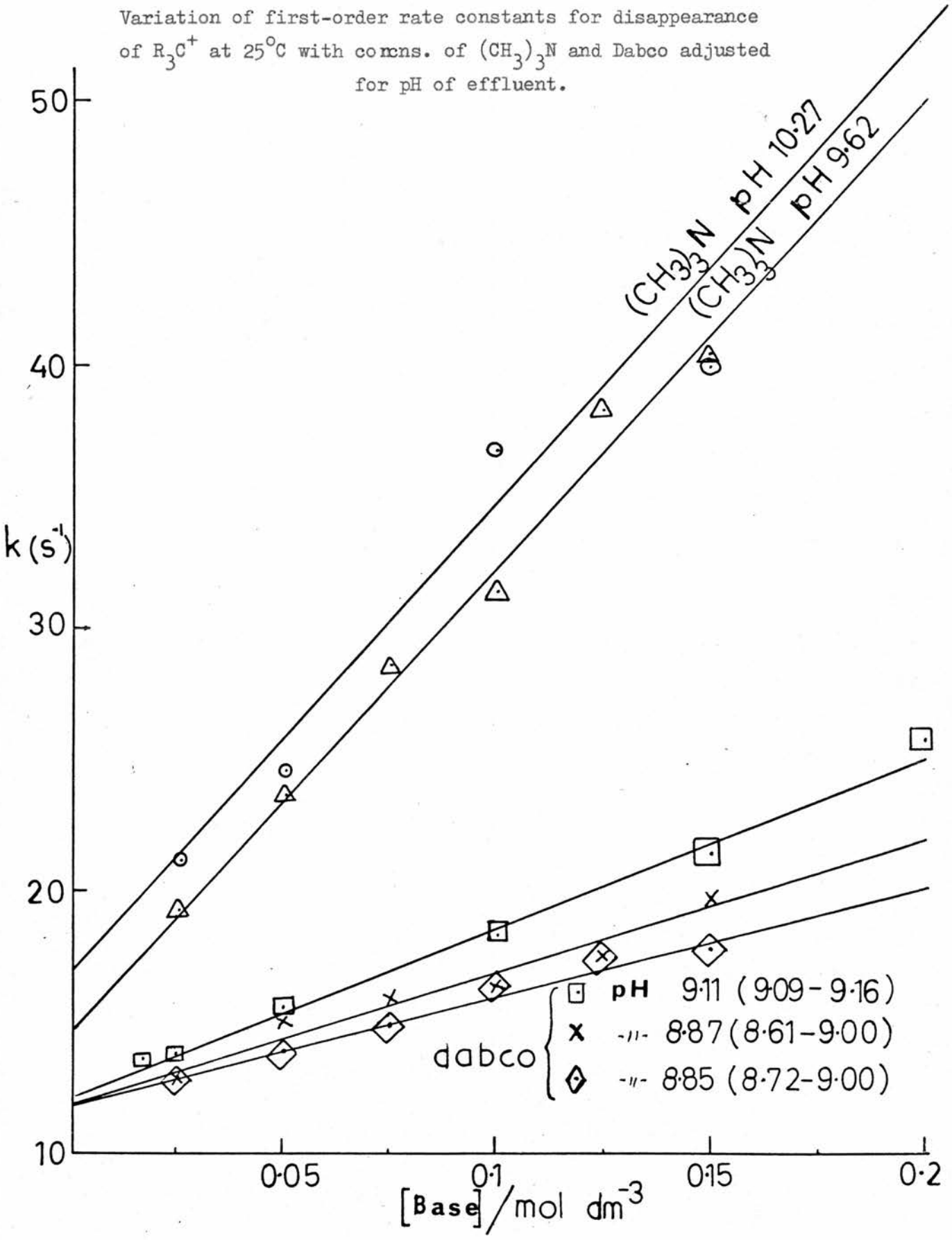

set with the lower measured pH. If the mixture proportions are considered this set should have had the higher pH. This difficulty apart it seems reasonable to draw two lines to represent the data in Fig. II 7.

The significant results of Figs. II 6 and II 7 can be summarised in Table II 8.

TABLE II 8.

Base	Slopes, $k_B/dm^3\ mol^{-1}s^{-1}$	Intercepts/s^{-1}	mean pH
Dabco	65.00	12.1	9.11
	50.50	11.9	8.87
	40.15		8.85
$(CH_3)_3N$	174	16.9	10.27
	176	14.7	9.62
$(C_2H_5)_3N$	157	17.6	10.27
	157	15.9	10.47

On the quantitative aspect of Table II 8 there are unfortunately no numerical comparisons for k_B available from literature. The order of catalytic efficiencies of the bases is not precisely that of their strength as bases since triethylamine would have been expected to be superior to trimethylamine. A more detailed discussion of catalytic efficiency and base strength is given later when examining the applicability of the Brønsted relationship.

Fig. II 7

Variation of first-order rate constants for disappearance of R_3C^+ at 25°C with $\left[(C_2H_5)_3N\right]$ adjusted for pH of effluent.

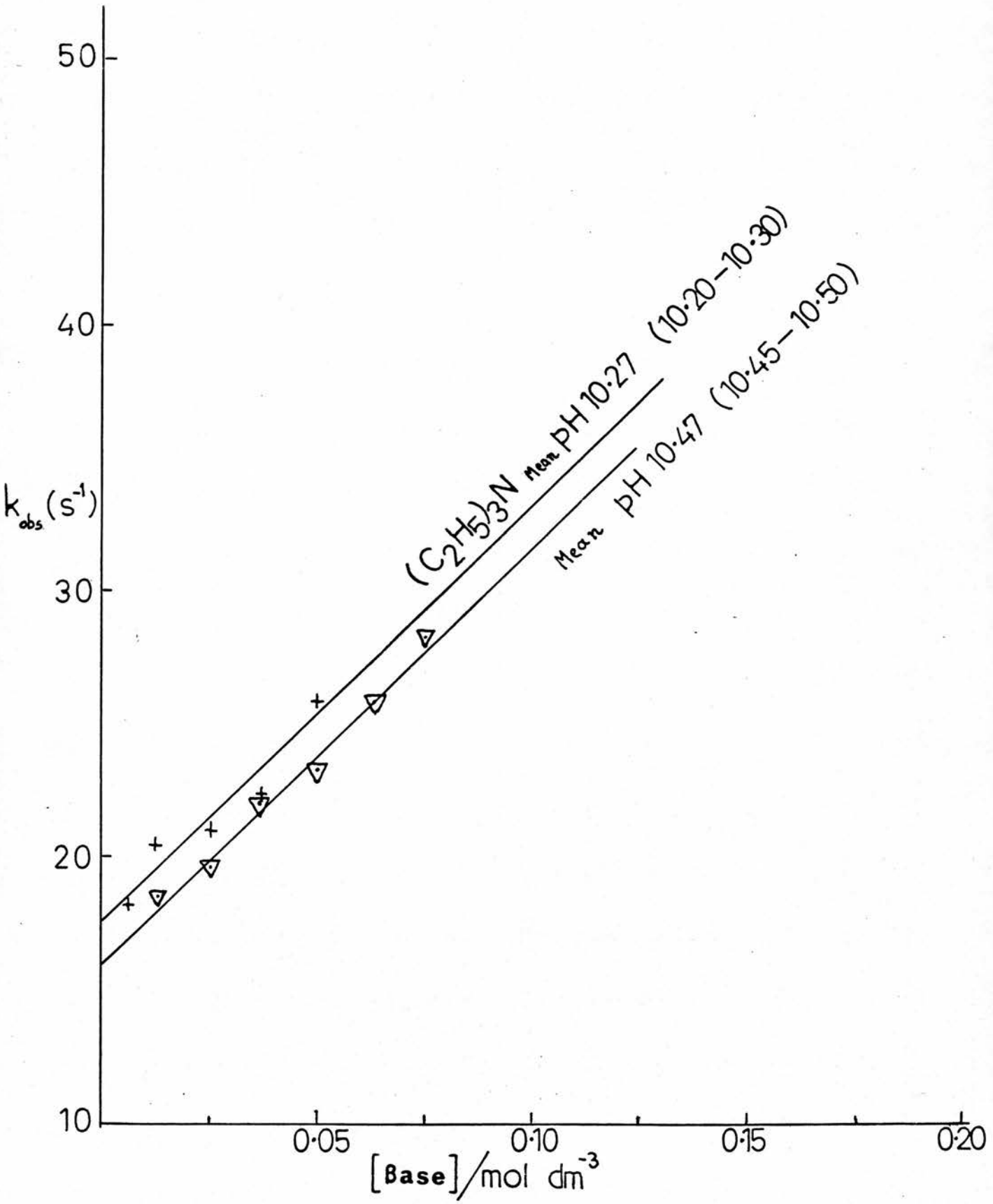

The part played by the hydroxyl ion in this reaction has been studied by Bunton and Huang[32] who followed the rate of disappearance of the carbonium ion in the presence of 0.25×10^{-2} to 3.5×10^{-2} M concentrations of OH^-. Their graph looks convincing and they deduced $k_{OH^-} = 8200\ dm^3\ mol^{-1}\ s^{-1}$. These concentrations are about one hundred times those of the most alkaline buffer mixtures of this work. It is clear however that at pH 10 the contribution to k_{obs} due to the term $k_{OH^-}(OH^-)$ is $0.82\ s^{-1}$ and this term is a significant part of the intercept's value. In theory the range of pH and intercept values in Table II 8, together with the relationship Intercept $= \left\{ k_{H_2O}(H_2O) + k_{OH^-}(OH^-) \right\}$ makes it possible to deduce k_{OH^-} and $k_{H_2O}(H_2O)$. However the difficulties of the mixing technique prevent the acquisition of the highly accurate rate data which would be required for this.

In the same research Bunton and Huang[32] assessed the $k_{H_2O}(H_2O)$ term in two ways. When studying the disappearance of the carbonium ion in 0.05 M HCl they measured a constant $k = k_f + k_b$ in $R^+ + H_2O \underset{k_b}{\overset{k_f}{\rightleftharpoons}} ROH + H^+$. After allowing for k_b by use of K_{eq} they deduced $k_{H_2O}(H_2O) = 11.4\ s^{-1}$. In a more direct way they used acetate ion to neutralise the H^+ and obtained $12\ s^{-1}$. In this research experiments were carried out also to measure $k_{H_2O}(H_2O)$ in near neutral conditions and the mean of 23 experiments gave $11.8 \pm 0.3\ s^{-1}$, in good agreement with Bunton and Huang. It must also be noted that the pH of the Dabco buffers was about 9 and that $k_{OH^-}(OH^-)$ on their values would be $0.082\ s^{-1}$ at pH 9. Even if their k_{OH^-} value of 8200 was not highly accurate it is clear that the intercept for the Dabco buffers of 11.9 to $12.1\ s^{-1}$ contains only a contribution of about 0.1 from the OH^- ion catalysis. Thus two methods in this work confirm $k_{H_2O}(H_2O)$ to

be about 12 s^{-1}.

The limitations of the intercept data as a source of k_{OH^-} can be shown by Fig. II 8. In this Fig. the intercepts, i.e. $\left\{k_{H_2O}(H_2O) + k_{OH^-}(OH^-)\right\}$ are plotted against the $\left[OH^-\right]$ deduced from the measured pH. On each point is placed an estimate of accuracy of deduction from the graphs of k_{obs} against $\left[B\right]$ in Figs. II 6 and II 7. A dotted line has been drawn to give Bunton's data of $\left\{12 + 8200\ (OH^-)\right\}$. It is clear that our data does not permit a deduction of k_{OH^-} but it does indicate quite strongly that it could be at least double Bunton's value. The uncertainty in the value of k_{OH^-} is considerable since Hill and Mueller[27] have suggested the value 4600 $dm^3\ mol^{-1}s^{-1}$ for this constant.

An examination can now be made of base catalytic efficiency in relation to base strength. The classical way of doing this is to look at the Brønsted relationship between log $k_{catalyst}$ and log K_{eq} where K_{eq} applies to the equilibrium of the bases with H^+. By combining the data of this work with data from Bunton and Huang we can range from H_2O to OH^-, with our organic bases as intermediate in character. Before constructing a graph, k_{H_2O}, which is a second order constant, has to be deduced from $k_{H_2O}(H_2O)$ by dividing 12 s^{-1} by 55.5, which is the moles of H_2O per dm^3, and so deriving

k_{H_2O} = 0.216 $dm^3\ mol^{-1}\ s^{-1}$. Also for comparability the equilibrium constant $\frac{(H^+)(OH^-)}{(H_2O)}$ has to be taken as $\frac{10^{-14}}{55.5}$. mol. dm^{-3}

With these adjustments Fig. II 9 is obtained giving a reasonable linearity with a Brønsted coefficient $\frac{\Delta \log k}{\Delta \log K}$ of 0.31. This can be considered a reasonable value and has been taken over a 10^5 range in catalyst efficiency.

Fig. II 8

Plot of intercepts (for $(C_2H_5)_3N$, ⊡ ; $(CH_3)_3N$, ⊙ ; dabco, x.) against the OH^- deduced from the measured pH.

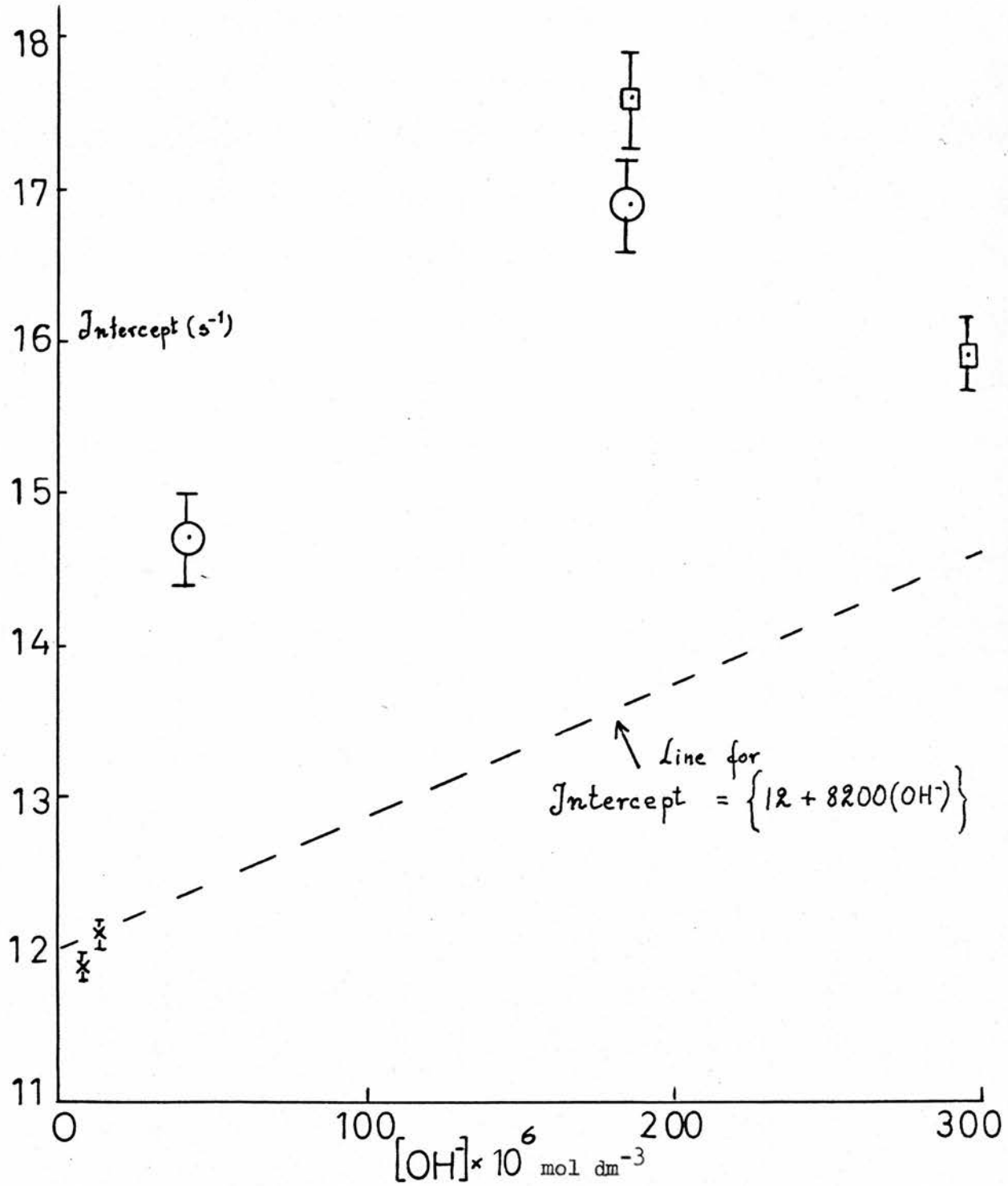

Fig. II 9

Brønsted plot of the catalysis constants for general base catalysis of tris-p-methoxyphenylmethyl cation.

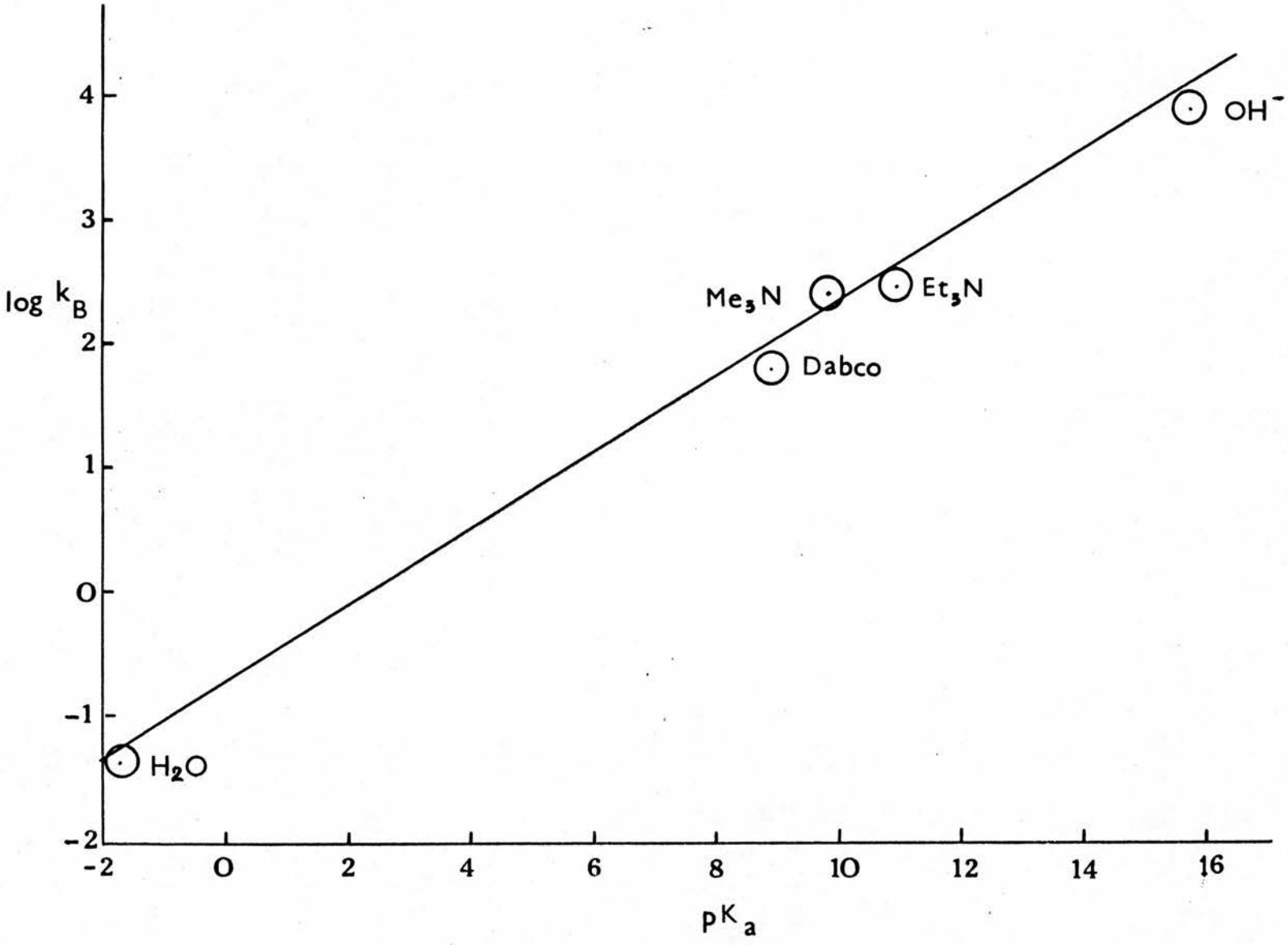

The fact that $(C_2H_5)_3N$ did not prove quite as efficient a catalyst as might be expected from its strength as a base may be due to steric effects.

Summary

The results of this work show that the reaction of tris-p-methoxyphenylmethyl cation with water is subject to general base catalysis. Values of reaction rate constants have been found for $(C_2H_5)_3N$, $(CH_3)_3N$, Dabco (1,4-diazabicyclo [2,2,2] -octane) and H_2O. The catalytic effect of OH^- has been shown and, while a value for k_{OH^-} has not been deduced, evidence has been produced which suggests the value is much larger than the current literature data.

The deduced catalytic constants have been shown to obey the Brønsted relationship over a large range of the variables.

PART III

Special study of the related fluorescent compound 3,6-dimethoxy, 9-phenyl, xanthen-9-ol, including excited state and ground state experiments.

1. Introduction

Absorption or emission of radiation by matter occurs in discrete quanta (photons) and obeys the relationship

$$\Delta E = h\nu = hc/\lambda , \qquad \text{Eqn. III 1.}$$

where ΔE is the energy absorbed or emitted at frequency ν and h is Planck's constant (6.6256×10^{-34} Js). The amount of energy absorbed or emitted is inversely proportional to the wavelength of the radiation. The molecule is raised from its ground state (S_o) of minimum energy, to an excited state (S_1) of higher energy. The application of quantum mechanical theory to electronic excitation processes has led to a set of selection rules, which classify transitions as allowed or forbidden.

Most filled molecular orbitals contain 2-spin-paired electrons, which results in each molecular orbital contributing no net spin to the entire molecular system. This is the electronic ground state of the molecule. The resulting spin S = zero, the multiplicity M = 2s + 1 of this state is one and this state is referred to as a singlet ground state, S_o. The excited electronic states with M = 1, although an

electron is promoted to a higher electronic level, are referred to as excited singlet states S_1, S_2, S_3 ... etc.

For every excited singlet state, there will be a state in which the spin of the promoted electron has been reversed. These states with S = 1 and multiplicity equal 3 are referred to as triplet states (T T_1, T_2, ... etc.).

When a photon with an appropriate energy is absorbed by a molecule, an electron is raised from the zero vibrational level of the singlet ground state to one of the several vibrational levels of an excited singlet state. This process occurs in $\approx 10^{-15}$s. A triplet state can then be formed from the excited singlet by intersystem crossing (see below).

Fig. III 1. Excitation and deactivation routes.

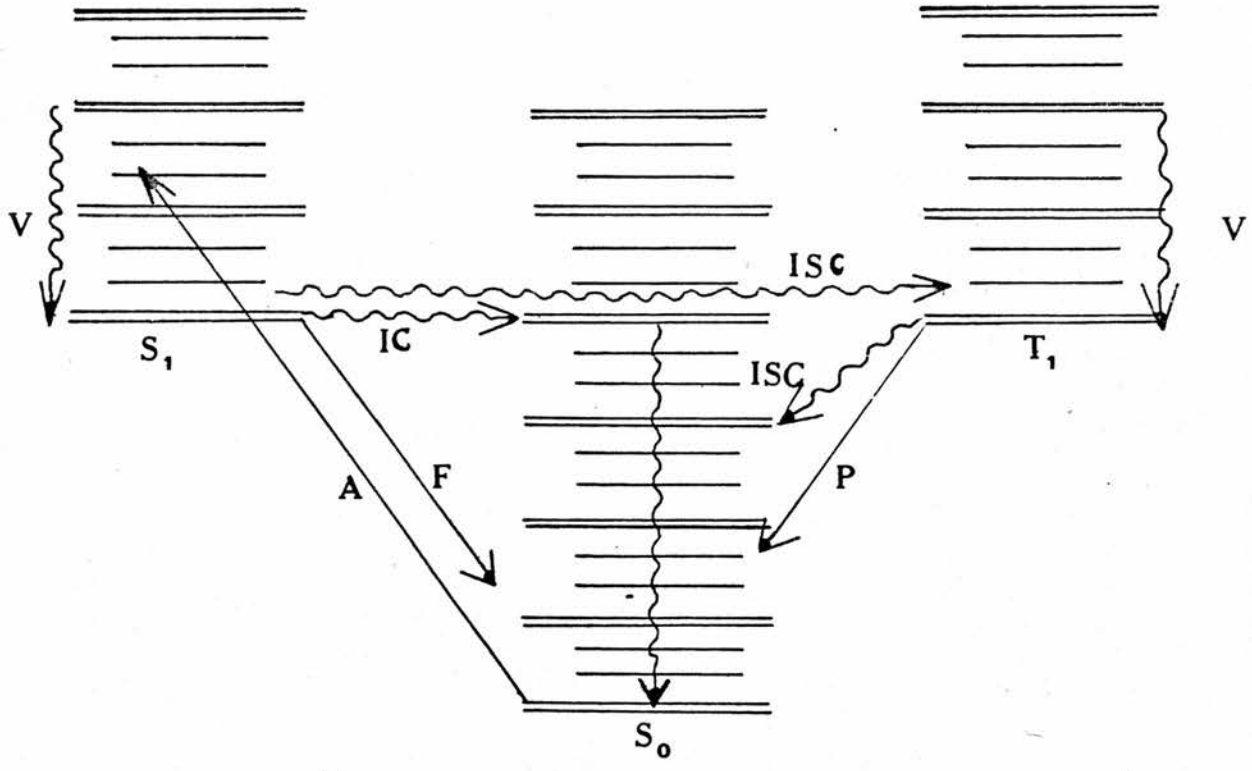

A, absorption 10^{-15}s

F, fluorescence 10^{-9} - 10^{-5}

P, phosphorescence 10^{-5} - 10^{-3}s

V, vibrational cascade

IC, internal conversion 10^{-10}s

ISC, intersystem crossing 10^{-6}s

Once formed, the excited singlet and triplet states will react chemically or lose their excitation energy by radiation or non-radiative processes (Fig. III 1). There are two types of radiative deactivation, fluorescence and phosphorescence.

Fluorescence is the emission of radiation accompanying the deactivation of an excited species to a lower state of the same multiplicity, for instance $S_1 \longrightarrow S_o$, or $T_2 \longrightarrow T_1$, and is a spin allowed process.

Phosphorescence is the emission of radiation accompanying the deactivation of an excited species to a lower state of different multiplicity, for instance $T_1 \longrightarrow S_o$, and is a spin forbidden process.

Excitation results in the occupation of excited states high in vibrational energy. This energy is rapidly lost (in $\sim 10^{-10}$s) by collisions, a process referred to as vibrational cascade, and radiative deactivation occurs usually from the lowest vibrational level of the excited state.

Therefore, less energy will be emitted than is absorbed and the emission spectrum will be shifted to longer wavelengths compared with the absorption spectrum.

The non-radiative processes are of two general types, internal conversion (IC) and intersystem crossing (ISC).
IC involves the transition from one state to another of the same multiplicity, without loss of energy, e.g. the $S_1 \longrightarrow S_o$ process in Fig. III 1. There, the ground state is initially formed at a high vibrational level and subsequently undergoes rapid vibrational cascade to its lowest energy level.

ISC is the conversion of one state to another, of different multiplicity, without loss of energy and usually provides the most favourable route to the triplet state. This process is most efficient when the singlet and triplet excited states have comparable energy and the triplet produced in this way will be high in vibrational energy and the vibrational cascade will rapidly follow. The ease and efficiency of ISC varies from compound to compound and the longer lived an excited singlet, the more likely it is to undergo ISC.Carbonyl compounds give a high triplet state population by this route.

Irradiation of a molecule normally results in the absorption of a single photon with subsequent competition between radiative and non-radiative processes, deactivation, and chemical reaction. Not every photon absorbed will bring about a chemical change and the efficiency of a photochemical process is very important.

The determination of quantum yields provides valuable information as to the nature of the chemical reaction.

2. Experimental techniques

(a) General techniques

Luminescence generally and fluorescence and phosphorescence measurements in particular are used as a basis for analytical methods. The methods are much more sensitive than absorption, because the light emitted from a sample may be compared to a "zero" background, rather than comparing the transmitted light to the incident light as is done in absorption spectroscopy. It is therefore easier to detect a small

signal above a "zero" signal than it is to measure the small difference in two large signals. This high sensitivity demands great care in avoiding sample contamination. Sample cells, solvents, and glassware must be scrupulously clean. The general techniques recommended by Parker[57] were followed. Ethanol (3 litres) was purified by distillation from aqueous potassium hydroxide (3g), followed by fractionating. The middle fraction, consisting of 50% ethanol was collected. Water was distilled from alkaline potassium permanganate using 40" fractionating column. n-Pentane and cyclohexane, both spectroscopic grade were used without further purification.

(b) Absorption spectroscopy

Either an SP 500, with temperature controlled facilities, or a 402 Perkin Elmer spectrophotometer was used to measure ground state pK values or the optical densities of solutions used in quantum yield determinations. Quartz cells were used throughout.

(c) Emission spectroscopy

A Perkin Elmer Hitachi MPF - 2A Fluorescence Spectrophotometer was used to obtain the emission spectra. The instrument had two monochromators: one for irradiation of the sample at 200 -700 nm (excitation monochromator), and the other for measuring the intensity of light emitted by the sample at 200 - 800 nm (emission monochromator). The 150 W xenon arc lamp was fitted as a source.

(d) Sampling techniques

All solutions used for fluorescence measurements were sufficiently dilute to avoid the inner filter effects[58], and their optical densities at the analytical wavelengths used were measured to ensure that ϵcl was less than 0.02. The method of right-angle illumination was employed to minimise stray light interference, or fluorescence from the cell; the cells used were of synthetic silica.

Quenching processes tend to affect the triplet molecules more than excited singlet species, due to the longer life-times of the triplet state. To eliminate the possibility of quenching by oxygen, solutions used in the flash photolysis experiments were vigorously de-gassed on a vacuum line, by the freeze-pump-thaw technique. Care was exercised on thawing of samples, to avoid cracking the flask during sudden expansion of liquid.

When de-gassed, the liquid sample was transferred still under vacuum, to the quartz cell. Extra care was required during this operation to avoid the "hammer effect" of the liquid and blowing out of the quartz windows. A few samples were lost in this way with consequent delays in repair of the damaged cells.

(e) Emission from solid solutions at low temperature

Phosphorescence emission spectra at 77 K were obtained using the phosphorescence accessory of the MPF - 2A spectrophotometer. The sample was contained in 1 - 2 mm diameter quartz tube which fitted into the Dewar flask containing liquid nitrogen. Solvents for this type of measurement should form clear glasses at low temperatures. Depending

Fig. III 2.

Degassing cell

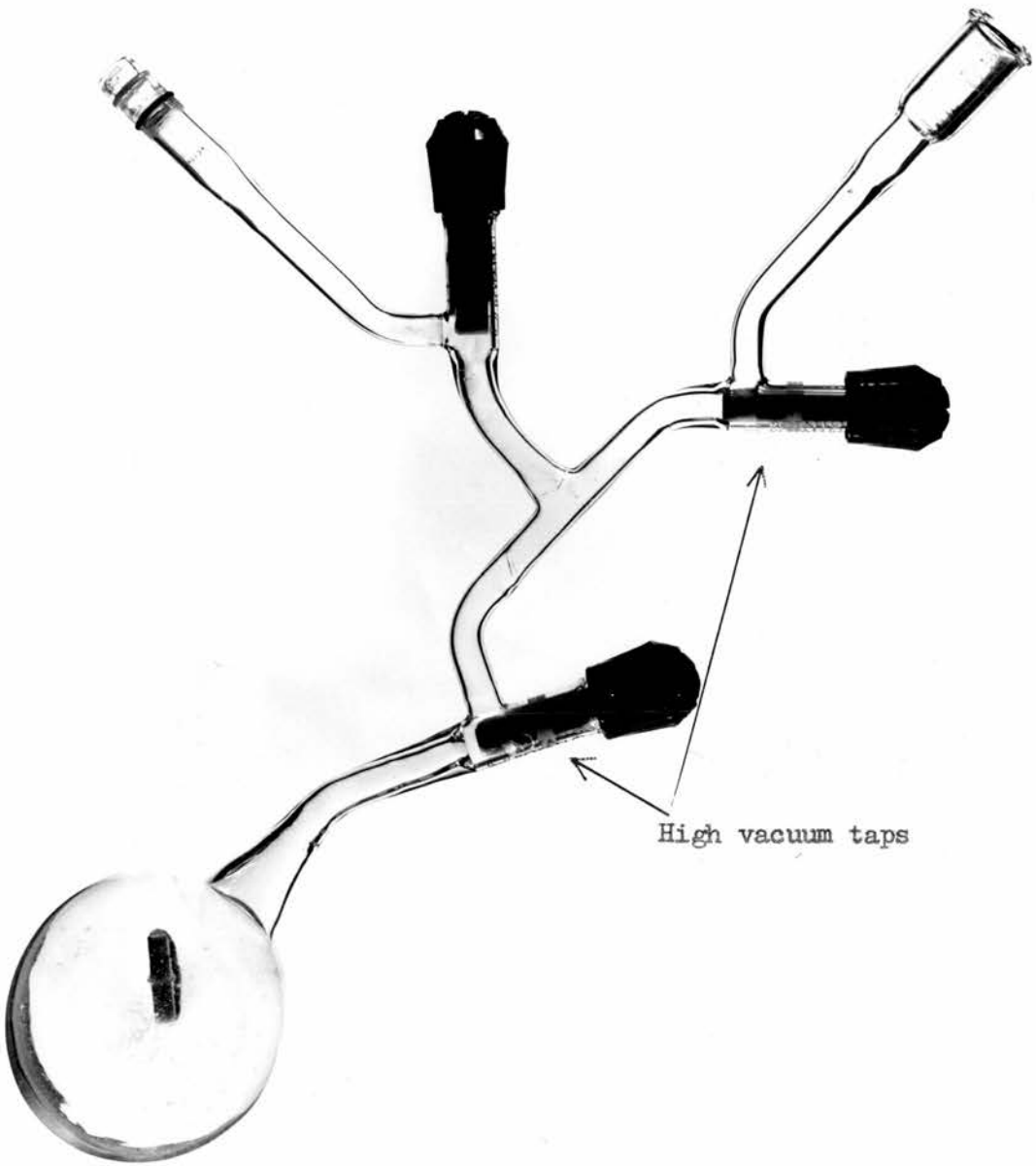

Fig. III 3

Flash photolysis cell

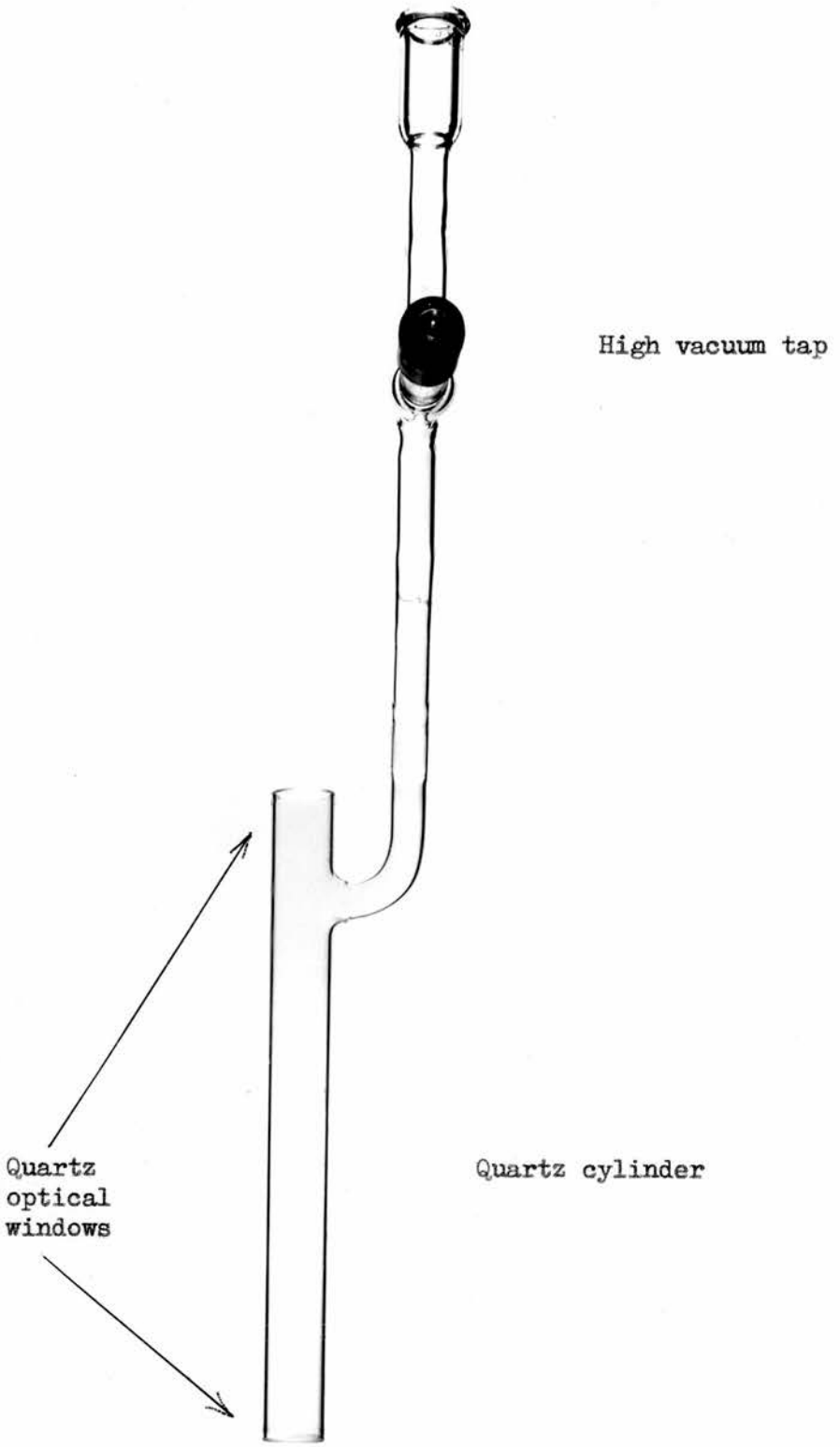

on the solubility of the compound used, suitable solvents in different proportions are tried to achieve the clearest glass[59]. Acidic solvents in particular, form cracked and opaque solids on freezing, thus increasing the difficulty of measurements. The amount of incidental light reflected from a sample depends on the extent of cracking. Although not perfectly clear of cracks, satisfactory frozen solutions were obtained using ethanol/ether/n-pentane/perchloric acid mixtures.

(f) Correction of emission spectra

Few spectrofluorimeters measure the true luminescence emission spectrum directly. The instrument used gave only an apparent emission curve. The observed photomultiplier output must be corrected for the photomultiplier sensitivity, the transmission of the emission and excitation monochromators, and light losses due to the varied output of the xenon light source.

The spectral sensitivity curve for our apparatus was obtained using six dilute fluorescent solutions, functioning as quantum counters, covering the 300 - 750 nm range. The absolute fluorescence spectra of these solutions have been determined previously. The apparent spectral sensitivities were obtained and compared with the absolute spectra, using a CALIB computer programme, which calculated the relative spectral sensitivity curve.

The spectral data were transferred into a computer - readable form using automatically punched paper tape[52]. The un-corrected detector voltage of the MPF - 2A was sampled and recorded at rates up to 4 samples per s, i.e. approximately every 0.1 nm, when the spectrofluorimeter was

scanned at 25 nm/60s.

The data from the paper tape were processed on the IBM 360/44 computer when a ZOSPEC (up-dated version of the SPEKA programme) was used.

This gave a line print-out of wavelength, wavenumber and the experimental and corrected spectral intensities in terms of detector voltage, normalised to 100 units of maximum intensity. The programme also allowed for the corrected emission or excitation spectra to be plotted with either the wavenumber or the wavelength linear scales.

(g) Determination of quantum yields of fluorescence

Quantum yields of emission from fluid solution were determined, under conditions where the inner filter effects are negligible. This was checked by diluting solutions in the same ratio for both the standard and the tested solutions.

The total emission of fluorescence is proportional to $I_o \epsilon c l Q_f$, where I_o is the intensity of incident light,

ϵ the molar extinction coefficient,

c the concentration,

and Q_f the quantum yield of the fluorescer.

The total rate of emission is also proportional to the integrated area under the corrected fluorescence spectrum. Therefore, if the fluorescence emission spectra of two solutions are measured on the same instrument and at the same intensity of exciting light, the ratio of the two observed fluorescence intensities is given by:

$$\frac{F_2}{F_1} = \frac{\text{area 2}}{\text{area 1}} = \frac{I_o \epsilon_2 c_2 l Q_2}{I_o \epsilon_1 c_1 l Q_1} = \frac{Q_2}{Q_1} \times \frac{(\text{optical density})_2}{(\text{optical density})_1} \quad \text{Eqn.III 2.}$$

If the absolute fluorescence efficiency (Q_1) of one of the components is known, the other can be calculated. For both solutions, the factor of the area of corrected spectrum over the un-corrected peak height was obtained separately and the fluorescence intensities at their respective peak heights were compared. The ratio of observed peak intensities multiplied by the ratio of the factors gives the value of F_2/F_1 for insertion in equation III 2.

A change of solvent, and therefore a change of the refractive index, alters the instrumental geometry, and a further correction factor must be applied when the two substances are dissolved in different solvents. The observed intensities are corrected by multiplying by the square of the refractive index of the solution.

3. Triplet state absorption spectroscopy

This method, of irradiating a sample by high intensity light flashes of short duration and studying the effects at various wavelengths and times, is termed flash photolysis.

(a) The flash photographic technique

The method[60] is suitable for the detection of short-lived species, using a spectrograph and photographic plate. It utilises a second discharge, the spectroscopic flash, to produce a photograph via the spectrograph, with the absorption of a sample shown at the time when the second flash was initiated. By varying the delay between the photolytic and spectroscopic flashes, absorption at a series of wavelengths at specific times after excitation of a sample can be studied.

(b) The flash-photoelectric technique

This method was used in search for any intermediate product, appearing after irradiation of a sample. A Hilger-Watts Scanning Unit E 720 was attached to the spectrograph. A continuous source was used to monitor the absorbance at a fixed wavelength. The light from the monitoring source fell on the IP 28 photomultiplier fitted in a place of a photographic plate. The photomultiplier output was fed into a Tektronix 545 B oscilloscope and the resulting trace was recorded if required.

The flash photolysis experiments were performed on a Northern Precision FP-1-pH instrument. The sample, contained in a 20 cm long, 2.5 cm diameter quartz cell was held in the vertical position for all experiments. Flash energy of about 500 J was achieved by triggering both capacitors previously charged to 10kV.

(c) Operation of flash photolysis apparatus to obtain data

The cell containing the de-gassed sample was placed in the holder and the cell-holder casing was closed. The spectrograph plate holder was loaded with Ilford HP3 photographic plate and the following general procedure was employed for each sample examined:

(1) spectroflash only, to obtain reference spectrum;
(2) photoflash alone, to obtain emission from the sample and scattered light;
(3) a double flash with a delay set between the flashes;
(4) spectroflash only, to determine the degree of decomposition of the sample in comparison with reference spectrum (1).

A wavelength scale of the spectrograph was recorded on the plate at the start of an experiment.

Any transient will be seen by comparison of experiment (3) with (1). Once a transient is found it is necessary to calibrate the spectrographic plate. This was achieved by using a series of neutral filters in front of the spectrograph slit and firing the spectroflash only. The position of the sample, and therefore, the spectroflash energy, was the same and a measure of the optical density of the transient was obtained.

The photographic plate was developed for 4 min. in Johnson FF contrast developer, was washed for 1 h and dried in air. These, seemingly trivial operations were kept constant, to avoid the introduction of unnecessary variations in the plate density prior to its measurement on the Vickers M 41 Microdensitometer.

Experience of the flash photolysis technique was gained by repeating the experiment used in the study of decay of triplet anthracene in n-hexane[61]. Several triplet spectra of anthracene were recorded and the correct performance of our instrument was thus verified.

4. Acid-base and photochemical properties of 3,6-dimethoxy, 9-phenyl, xanthen-9-ol

(a) Preliminary u.v. spectra

The spectra were obtained at 190 - 590 nm, using identical concentrations of the compound, 4×10^{-5}M in different solvents. The spectra in ethanol, acetonitrile, hexane and benzene were substantially the same, those in 1 M $HClO_4$ showing a strong absorption band at 438 nm. This band, due to the R^+ form, was diminished by approximately 75% when

exposed to daylight for 12 h.

Solutions containing 2 x 10^{-5} M concentrations of the compound were examined for stability and fluorescence appearance in perchloric, sulphuric and hydrochloric acids. Changes of optical density at 438 nm were measured immediately after mixing suitable amounts of compound in the respective solvents and after 1,2, and 4 h exposure in daylight and after standing for 4 h in darkness. The intensity of peak at 438 nm and fluorescence decreased markedly in both $HClO_4$ and H_2SO_4 in daylight, the unknown reaction being initially slightly faster in H_2SO_4. No corresponding decrease was observed in HCl. The optical densities at 438 nm in all three acids were unchanged after standing in darkness, which indicated that some form of photochemical reaction took place, summarised in Table III 1.

TABLE III 1.

Relative variations of R^+ peak height at 438 nm

Acid	immediately after mixing *	in daylight		in dark
		after 2 h	after 4 h	
$HClO_4$	100	38	6.5	100
H_2SO_4	100	9.5	6.5	100
HCl	100	100	100	100

Concentration of compound in all cases was 2 x 10^{-5} M, at pH3

* normalised to 100

Freshly prepared stock solutions and all solutions used for spectroscopic measurements were stored in blackened flasks. The transfer of these solutions to spectroscopic cells and the recording of spectra were completed within 6-10 min and control experiments showed that in those cases the extent of photochemical reaction was negligible.

The indications were that these photochemical reaction rates were measurable in $HClO_4$ and H_2SO_4 acids. The difficulties in further study might lie in the identification of reaction products. Deeper study of these phenomena, although not pursued at the time, should lead to better understanding of the processes occurring.

The absorption, fluorescence and phosphorescence spectra of the ROH and R^+ forms of the 3,6-dimethoxy,9-phenyl,xanthen-9-ol are shown in Fig. III 4. Concentrations of 2×10^{-5} mol dm^{-3} were used for the absorption and fluorescence measurements. The phosphorescence was determined at a concentration of 10^{-4} mol dm^{-3} in ethanol for ROH species, and in ethanol/ether/n-pentane/$HClO_4$ in the ratio 1/16/4/2[59] for the R^+ species.

The absorption maxima correspond to extinction coefficients of 460 $mol^{-1}m^2$ ($4.6 \times 10^3 dm^3\ mol^{-1}\ cm^{-2}$) for ROH at 277 nm and of 3.2×10^3 $mol^{-1}\ m^2$ ($3.2 \times 10^4\ dm^3\ mol^{-1}\ cm^{-2}$) for R^+ at 438 nm.

(b) Determination of pK values by spectrometry

The $pK(S_o)$ was determined by spectrometry, using the method of Albert and Sergeant[62] and the equation:

$$pK = pH \pm \log \frac{\epsilon_1 - \epsilon}{\epsilon - \epsilon_m} \quad . \qquad \text{Eqn. III 3.}$$

Fig. III 4

Absorption (abs), fluorescence (fl), and phosphorescence (ph) spectra of ROH and R^+ : abs. in neutral and 0.1 mol dm^{-3} $HClO_4$ aqueous solution respectively, fl. in similar ethanol solutions, and ph. in neutral and acid glasses.

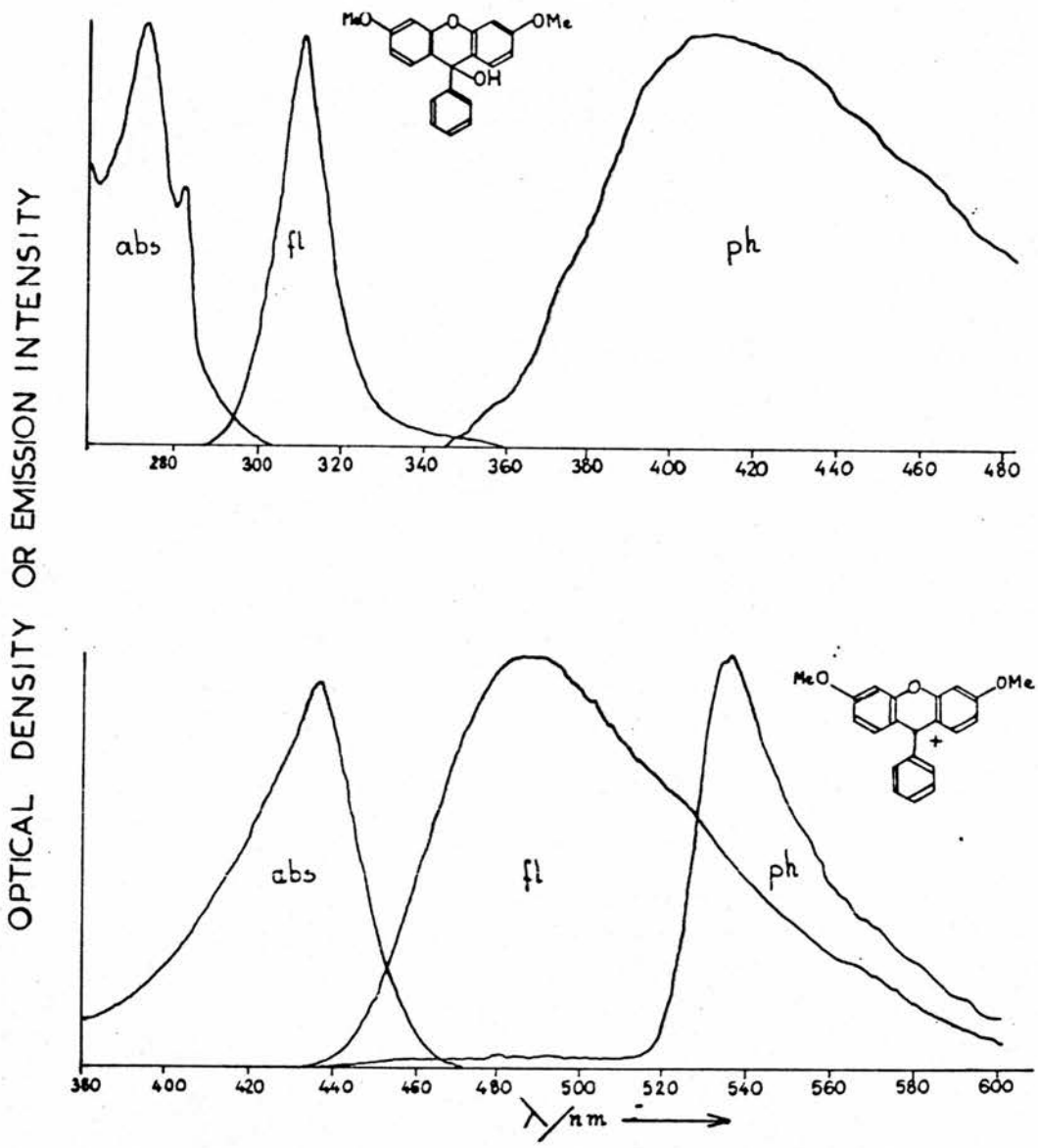

Where ϵ_1 is the extinction coefficient of the ion (d_{ion}) at the analytical wavelength,

ϵ_m is the extinction coefficient of the molecule (d_m) at the same wavelength, and

ϵ is the extinction coefficient of the mixture of ion and molecule (d) at the same wavelength.

ϵ changes with the pH, which must be varied to solve the equation at various degrees of ionization.

If the same concentrations and cells are used, the above equation may be written with optical densities d, instead the extinction coefficient ϵ. If d_{ion} is greater than d_m and the functional group being determined is basic,

$$pK = pH + \log \frac{d - d_m}{d_1 - d} \quad . \text{ Eqn. III 4.}$$

The method consists of determining the relative proportions of ion to molecule in the unknown when it is dissolved in a series of solutions of accurately known pH values.

These were determined on the "Radiometer pH 26" meter if the pH was > 2.

Strongly acidic solutions were prepared by diluting weighed amounts of 98% sulphuric or 60-70% perchloric acids which were previously standardised by dilution and titration with standard alkali. The pH values of solutions in acids were calculated from the acid concentration tables[63], based on data of Yates and Wai[22] and Ryabova et al[64].

Preliminary experiments in un-buffered solutions indicated a $pK(S_o)$ value of 5.7, which would have been quite well covered by citric acid/ sodium citrate buffers. However, unexplained buffer effects were

observed and it was thought more prudent to change to acetate buffers which did not affect the position of R^+ absorption at 438 nm. In a series of 0.02 mol dm^{-3} acetate buffers of pH between 4.37 and 7.00 a pK_{R^+} value of 5.44 $\pm$ 0.07 at 24.4°C was calculated.

Results of a pK_{R^+} determination in 0.02 mol dm^{-3} acetic buffer, where ionic strength of solution was maintained at 0.1 by the addition of NaCl are shown in Table III. 2.

TABLE III 2.

Calculation of $pK(S_o)$ values of 3,6-dimethoxy,9-phenyl,xanthen-9-ol from optical density measurements.

pH	Optical density at 438 nm			$\log \frac{d - d_m}{d_i - d}$	antilog of pK_{R^+}	pK_{R^+}
	d	$d-d_m$	d_i-d			
5.71	0.45	0.43	0.72	-0.2233	0.3067	5.4867
5.39	0.63	0.61	0.54	0.0512	0.2775	5.4432
5.22	0.69	0.67	0.48	0.1446	0.2331	5.3676
5.12	0.82	0.80	0.35	0.3590	0.2990	5.4757
5.00	0.86	0.84	0.31	0.4329	0.2657	5.4244
4.89	0.93	0.91	0.24	0.5798	0.2950	5.4698
4.82	0.96	0.94	0.22	0.6307	0.2817	5.4498
4.64	0.99	0.97	0.18	0.7314	0.2342	5.3696
1.20	1.17					
13.00	0.02					
	(d_i) optical density of the ion (1.17)					
	(d_m) optical density of the molecule (0.02)					
	(d) optical density of the mixture					

It appears that the bridging oxygen of the 3,6-dimethoxy,9-phenyl, xanthen-9-ol makes it much more basic than trianisyl methanol, (pK_{R^+} = 0.82)[65] which has one more methoxy group, but no oxygen bridge.

Presumably, the R^+ form is stabilised more by the delocalisation through the bridging oxygen, which in turn, disrupts the "natural propeller" shape by forcing two rings into coplanarity. A similar, and more marked, effect was observed in the case of sesquixanthydral (pK_{R^+} = 9.05),[66]

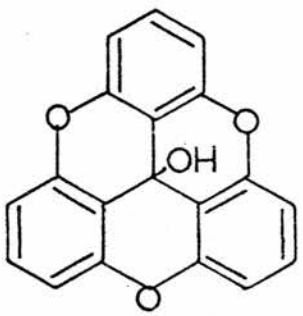

which has no methoxy groups at all, but has three bridging oxygens which confer on it completely coplanar configuration with little if any more strain than is present in the tetrahydral carbinol. The pK_{R^+} of triphenylmethanol, the nearest comparison compound, is -6.89.[67]

(c) Attempted determination of $pK(S_1)$ by fluorescence spectroscopy

Fluorescence intensity measurements were made using aqueous $HClO_4$ solutions containing 3,6-dimethoxy,9-phenyl,xanthen-9-ol at 2×10^{-5} M. The ionic strength was maintained at 0.1 M with $NaClO_4$. Phosphate buffers were used to obtain desired pH from 5.5 to 8.75, and acetic buffer to obtain one point on the graph Fig. III 5 at pH 4.5. The intensities of the ROH and R^+ forms were measured at their uncorrected maxima at 305 and 470 nm respectively, and must be corrected for the overlap between emission spectra of the two species to obtain the true fluorescence intensities of the ROH and R^+ forms (ϕ and ϕ^1) respectively.

The measured and true fluorescence intensities are related as follows:

$$I = \phi + k'\phi'$$

$$I' = \phi' + k\phi$$

Fig. III 5

Relative fluorescence intensities of protonated and unprotonated forms of 3,6-dimethoxy, 9-phenyl,9-xanthen-9-ol as a function of pH.

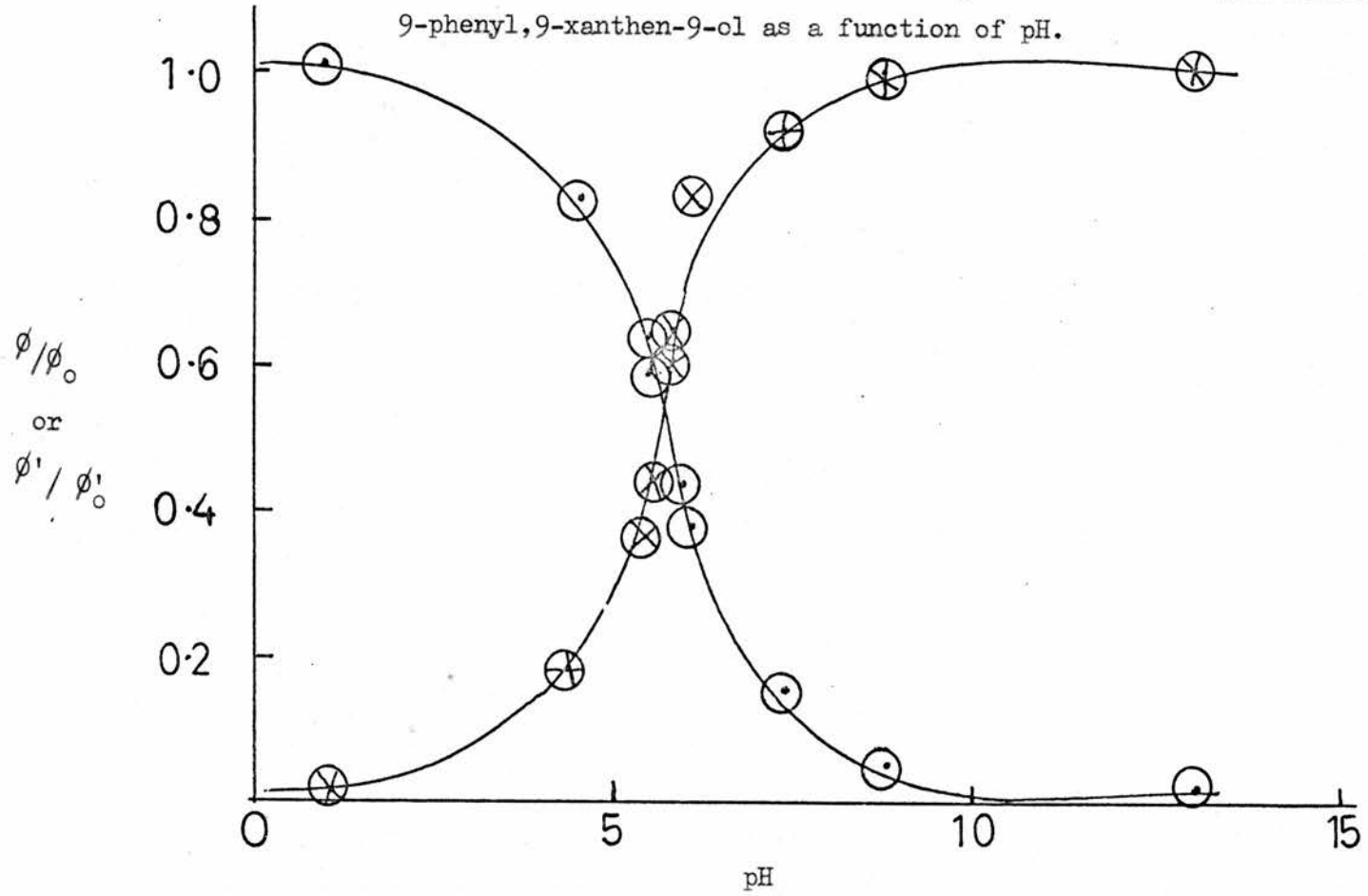

ϕ/ϕ_o at 305 nm, unprotonated form, ⊙

ϕ'/ϕ'_o at 470 nm, protonated form, ⊗

where k and k' are the overlap ratios of the ROH and R^+ forms respectively

and I = measured intensity at 305 nm

and I' = measured intensity at 470 nm.

To obtain the overlap ratios, intensity measurements of solutions which contain only one species in the excited state are made 1 to 2 pH units either side of the $pK(S_1)$ value. The k is obtained in the more alkaline solutions showing only fluorescence of the unprotonated form and is the ratio of the fluorescence intensity of ROH measured at the wavelength where R^+ emission (I') is observed to the intensity at the wavelength where ROH emission (I) is measured.

$$k = \frac{\text{fluorescence intensity at } R^+ \text{ emission wavelength 470 nm}}{\text{fluorescence intensity at ROH emission wavelength 305 nm}} \quad \frac{I'}{I}$$

and similarly

$$k' = \frac{\text{fluorescence intensity at 305 nm}}{\text{fluorescence intensity at 470 nm}} = \frac{I}{I'}$$

So that the true fluorescence intensities (ϕ and ϕ') in terms of I, I', k, and k' are:

$$\phi = \frac{I - k'I'}{1 - kk'} \qquad \text{and} \qquad \phi' = \frac{I' - kI}{1 - kk'}$$

The true fluorescence intensities at various pH values, corrected for the overlap, are given in Table III 3 together with the relative fluorescence intensities ϕ/ϕ_o and ϕ'/ϕ_o of ROH and R^+ forms respectively.

TABLE III 3

True fluorescence intensities of the protonated and unprotonated forms of 3,6-dimethoxy,9-phenyl,xanthen-9-ol as a function of pH.

pH	B* measured at 305 nm				B^*H^+ measured at 470 nm			
	I	kI	$\frac{I-k'I'}{1-kk'}$	ϕ/ϕ_o	I'	k'I'	$\frac{I'-kI}{1-kk'}$	ϕ'/ϕ_o
1.00	0.1	0.1	0	0	370	1.00	370	1.00
4.50	14.4	1.4	13.5	0.15	304	0.91	303	0.82
5.50	31.7	3.1	30.75	0.35	235	0.71	232	0.63
5.75	40.5	3.9	40.00	0.43	225.5	0.67	223.4	0.60
5.80	57.5	5.6	57.30	0.63	157.5	0.47	151.00	0.41
6.00	78.0	7.6	77.80	0.85	136.0	0.41	135.50	0.37
7.33	86.0	8.34	85.8	0.92	55.5	0.17	55.30	0.15
8.75	92.0	8.9	92.00	1.00	22.00	0.07	14.20	0.06
13.00	93	8.7	90.00	0.98	9.00	0.03	8.97	0

$k = \frac{9}{93} = 0.097$ $\quad k' = \frac{0,1}{370} = 0.003$

$\phi_o = 93$ $\quad \phi'_o = 370$

A plot of the relative fluorescence intensity as a function of pH, at room temperature (20.8°C) is shown in Fig. III 5, from which a change-over point is obtained as ≈ 5.5, i.e. very close to the $pK_R+(S_o)$.

The intensities of buffered solutions gave fluorescence intensities proportional to the concentrations of the R^+ and ROH species in the ground state. Obviously, the S_1 state is too short lived for any

shift in the equilibrium to be detected and $pK(S_1)$ cannot therefore be determined in this way for this compound.

(d) Experimental comparison of the quantum yield of fluorescence

The various methods of obtaining luminescence quantum yields have recently been reviewed by Parker[57], Demas and Crosby[68] and took into account problems raised by Fletcher[69], Børresen[70], and Rusakowicz and Testa[71]. The method of Parker[57] for determining only the quantum yields of emission from fluid solution was used in this work, using quinine sulphate (B.D.H. mol.wt 782.97) in 0.5 M H_2SO_4 as a standard. The method for measuring quantum yields was initially verified by comparing the quantum yields of anthracene (B.D.H. mol. wt. 178.22) and quinine sulphate, for which Parker[57] gives values of 0.28 and 0.55 respectively.

A weighed amount of quinine sulphate was dissolved in 0.5 M H_2SO_4 and the solution's optical density at 366 nm was measured. The 3,6-dimethoxy,9-phenyl,xanthen-9-ol was dissolved in aqueous $HClO_4$ and its optical density, also at 366 nm, was measured. Both solutions were diluted suitably to give equal optical densities at 366 nm of 0.02 (to avoid the inner filter effect). The emission of both these solutions excited with 366 nm radiation were recorded and the corrected spectra and area under the curves were obtained from the computer printout. The area under the curve, between 300 and 600 nm was calculated in each case. Blank solutions were treated in a similar way and the area of scattered light was substracted from the emission area. For the quantum yield determination of the ROH form, excitation at 260 nm was used.

Taking a value of 0.55[57] for the quantum yield of quinine sulphate values of 0.32 for ROH form in ethanol and 0.28 for R^+ in aqueous $HClO_4$ were obtained using equation III 2, page 48.

Three determinations for each form gave similar values to within ± 6%. The comparison of quantum yields was also made using the simplest of methods, i.e. weighing of the area under the curve cut out from paper, with similar results reproducible to 5 - 6%

(e) Förster cycle estimates

Förster[75] has shown that excited molecules can undergo acid-base reactions without simultaneous deactivation. Observations in media of varying pH of the fluorescence spectra of molecules with acidic or basic functional groups showed that there are drastic changes in the spectra at a pH which differs considerably from the pH at which the compound undergoes acid/base reactions in the ground state.

This was due to the acid/base reaction of the excited state molecule when either a base picked up a proton from the solvent or an acid lost a proton to the solvent. These reactions are extremely fast, occurring in less than 10^{-8} to 10^{-7}s, since this is the lifetime of the fluorescent state.

An estimate of $\triangle$ pK can be made from a shift in transition energy of a given absorption or fluorescence band in going from acid to the conjugated base or from base to the conjugated acid. Such estimates are based on Förster cycle, illustrated in Fig. III 6 below.

Fig. III 6

Förster relationship of enthalpy changes to electronic transitions

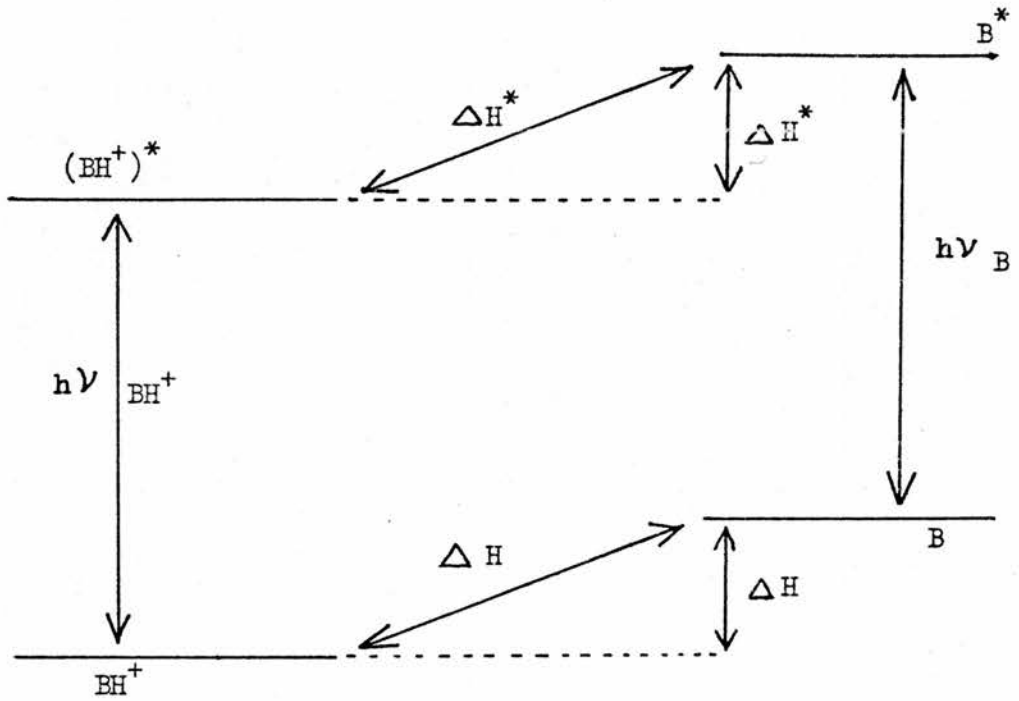

Corresponding transition energies of a base and its conjugated acid, ΔE_B and ΔE_{BH^+}, respectively are related by equation

$$\Delta E_{BH^+} + \Delta H^* = \Delta H + \Delta E_B, \qquad \text{eqn. (III 5)}$$

where ΔH is the enthalpy difference between the prototropic species in the ground state (S_o), and ΔH^* in the excited state (S_1).

If $\tilde{\nu}$ represents frequency of the transition in wave numbers,

h the Planck's constant and

N the Avogadro constant,

pK^* and ΔpK can be evaluated from:

$$\Delta pK = pK^* - pK = \frac{\Delta E_B - \Delta E_{BH^+}}{2.303\ RT} = \frac{(\overline{\nu}_B - \overline{\nu}_{BH^+})\ Nhc}{2.303\ RT} \quad \text{eqn (III 6)}$$

If the temperature is 298°K, insertion of numerical values of constants gives:

$$\Delta pK = 0.00209\ (\overline{\nu}_B - \overline{\nu}_{BH^+})\ /\ cm^{-1} \quad \text{eqn (III 7)}$$

The maximum absorption, fluorescence and phosphorescence wavelengths were converted to wave numbers in TABLE III 4 for the calculation of pK shifts from equation (III 6).

TABLE III 4

Förster cycle Δ pK calculations

	absorption max., $\overline{\nu}$ /cm^{-1}	fluorescence max., $\overline{\nu}$ /cm^{-1}	phosphorescence max., $\overline{\nu}$/cm^{-1}
ROH	36100 (at 277 nm)	32300 (at 310 nm)	24600 (at 407 nm)
R^+	22800 (at 438 nm)	20600 (at 486 nm)	18700 (at 536 nm)
$\Delta\overline{\nu}$/cm^{-1}	13300	11700	5900
Δ pK	$pK(S_1)-pK(S_o)$ = 26.3		$pK(T_1)-pK(S_o)$ = 12.4

The desired $pK(S_1)$ and $pK(T_1)$ of 31.7 and 17.8 respectively show that, in the excited states, ROH is a very much stronger base, with $pK(T_1)$ lying roughly half-way between $pK(S_o)$ and $pK(S_1)$.

Early results[72] indicated that pK (T_1) always lay between pK (S_o) and pK (S_1), but with more evidence accumulating it became evident that pK (T_1) may be nearer to pK (S_1), as in anthroic acid[73], and may even lie outside the pK (S_1) - pK (S_o) range as in xanthone[74].

As stated earlier, the S_1 state of 3,6-dimethoxy,9-phenyl,xanthen-9-ol is too short lived for any shifts in the equilibrium to be detected.

(f) Flash photolysis transient and laser flash photolysis.

These two techniques were used in search for evidence of an increase in R^+ in the triplet state. An attempt to measure the fluorescence life-time of the R^+ form, shows it to be of the same order as the laser flash life-time excited pulse, or even faster, pointing perhaps to a life-time of less than 1 ns. Measurements of the life-time of ROH form fluorescence would have been fruitless, since the only fluorescence emission observed was at higher energy than the exciting laser pulse. We are indebted to Professor Sir G. Porter for the measurement of life-times of our samples by the deconvolusion technique in the Research Laboratory of Davy Faraday, Royal Institution, London. The life-times (τ) were 2.64 $\pm$ 0.3 ns for ROH and 3.51 $\pm$ 0.3 ns for R^+. (There was a 2 months delay between the preparation and measurements of these samples).

From the flash photolysis experiments, two transients were recorded, one in EtOH solution, with the compound in the ROH form in the ground state and the other in dilute $HClO_4$ solutions at pH 2 to 4. The transient in EtOH solution absorbed strongly in the 420 to 450 nm region and had a life-time of 2.5 s. Thus, it was inaccessible for the study

by laser flash photolysis, which uses a pulsed xenon lamp with lifetime in the miliseconds region, as a monitoring source. Its appearance is possibly due to an intermediate formed from the photochemical decomposition reaction.

The transient in $HClO_4$ solutions was weak and was not detectable in pH 5 to 9. This was expected from the triplet form of R^+ if, as with the singlet, there is not enough time for more R^+ to be formed beyond the ground state pK_{R^+} .

Examination of this weak transient by the laser (The Laser Associates "501" ruby laser system) at ≈ 480 nm was not successful. The fluorescence emission overloaded the photomultiplier to such an extent, that the very weak transient possibly present, was completely masked.

(g) Quenching of fluorescence of 3,6-dimethoxy,9-phenyl,xanthen-9-ol

General introduction

Quenching of fluorescence was first reported by Stokes (1852), who noticed that the fluorescence intensity of quinine sulphate solution was reduced by the addition of halide ions. Fluorescence quenching was extensively studied[75] and is generally characterised by the following properties:

a) the decrease in fluorescence intensity is related to concentration of quencher;

b) the absorption spectrum of the fluorescer is unchanged, even at high concentrations of quencher, indicating that quenching is not due to the formation of a complex in the ground state;

c) the lifetime of a molecule in the excited state decreases with the increase of quenching;

d) the rate constant of the quenching process decreases with the

increasing viscosity of the solvent, and it also varies with ionic strength in the same way as the rate constant of a second order ionic reaction.[76]

The a, b, and c properties above indicate that quenching is a result of interaction between the excited molecule and a quencher. Therefore for a molecule M, the quenching process can be represented as follows:

Excitation: $M + h\nu \longrightarrow M^*$ $\quad I_{abs}$ eqn(III 8)

Fluorescence: $M^* \xrightarrow{k_f} M + h\nu$ rate $k_f [M^*]$ eqn(III 9)

Solvent and internal quenching: $M^* \xrightarrow{k_i} M$ rate $k_i [M^*]$ eqn (III 10)

Quenching: $M^* + Q \xrightarrow{k_q} M + Q^*$ $\quad k_q [M^*][Q]$ eqn(III 11)

In equation (III, II) the only quenching process considered is that one which leads to deactivation of M without change in M or in the quencher ion. If the intensity of the excited light is constant, then the rate of formation of excited molecules is also constant. In the absence of quencher, Q :

$$\text{fraction fluorescing, } I / I_{abs} = \frac{k_f (M^*)}{k_i(M^*) + k_f(M^*)} = \frac{k_f}{k_i + k_f} \quad \text{eqn (III 12)}$$

and in the presence of quencher Q :

$$\frac{I_Q}{I_{abs}} = \frac{k_f(M^*)}{k_i(M^*) + k_f(M^*) + k_q(M^*)(Q)} = \frac{k_f}{k_i + k_f + k_q(Q)} \quad \text{eqn(III 13)}$$

$$\therefore \quad \frac{I}{I_Q} = \frac{k_i + k_f + k_q(Q)}{k_i + k_f} = 1 + \frac{k_q(Q)}{k_i + k_f} \quad \text{eqn(III 14)}$$

The $(k_i + k_f)$ is overall rate coefficient for deactivation in absence of quencher and $(k_i + k_f)^{-1} = \tau$, the life-time of the fluorescer in the absence of added quencher. In terms of τ, equation (III 14) can be written as:

$$\frac{I}{I_Q} = 1 + k_q \tau [Q] \quad \text{eqn (III 15)}$$

Equation (III 15) is known as the Stern-Volmer equation and is valid for low quencher concentrations. A plot of $I / I_Q - 1$ against quencher concentration should give a straight line, the slope of which gives k_q, the "quenching constant".

The mechanism of intermolecular quenching of fluorescence has been studied by Förster[77] and Weller[78] for various systems. Different mechanisms have been invoked to explain the experimental results for different systems. Förster[77] concluded that quenching consists of electron transfer from the anion to the excited molecule with the formation of the corresponding radical anion. Other theories suggested were: quenching by heavy atom or paramagnetic molecules due to catalysis of inter-system crossing[79], the so called "heavy atom effect"; quenching proceeding via charge transfer interactions[80]; and quenching due to

the enhanced radiationless decay through an excited complex[81].

The effects of anions upon the fluorescence intensity of R^+

Fluorescence of the R^+ form of 3,6-dimethoxy,9-phenyl,xanthen-9-ol in HCl of 1 mol dm^{-3} or stronger was almost completely quenched, whereas no quenching was observed at all with $HClO_4$ at the same concentrations. To see if the presence of ClO_4^- would protect excited R^+ from Cl^- quenching, as might be expected from R^+ ClO_4^- ion pairs of the type postulated for the trianisylmethylcarbonium ion[28,29], the dependence of fluorescence intensity on concentration of Cl^- was determined at various background concentrations of ClO_4^-, the acid concentration being fixed throughout with a small quantity of $HClO_4$ and the balance being made up with $NaClO_4$. To ensure the absence of complicating photochemical reactions, all solutions were prepared by the addition of: a stock solution of compound (10^{-4} mol dm^{-3}), added anion, acid, and water to a 25 ml volumetric flask, which was blackened on the outside. As a further precaution, fluorescence intensities of each solution were recorded within 5 - 6 min.

Fig. III 7 shows the relative fluorescence intensity of R^+ fluorescence against the concentration of chloride ion at 22°C.

The Stern-Volmer plot, Fig. III 8 shows quenching of fluorescence by NaCl at $\left[H^+\right] = 10^{-3}$ mol dm^{-3} at four different concentrations of ClO_4^- ion. The data for this plot were obtained from Table III 5.

Fig. III 7

Relative fluorescence intensity of the R^+ form of 3,6-dimethoxy,9-phenyl,xanthen-9-ol against added $[Cl^-]$ at 22.0°C.

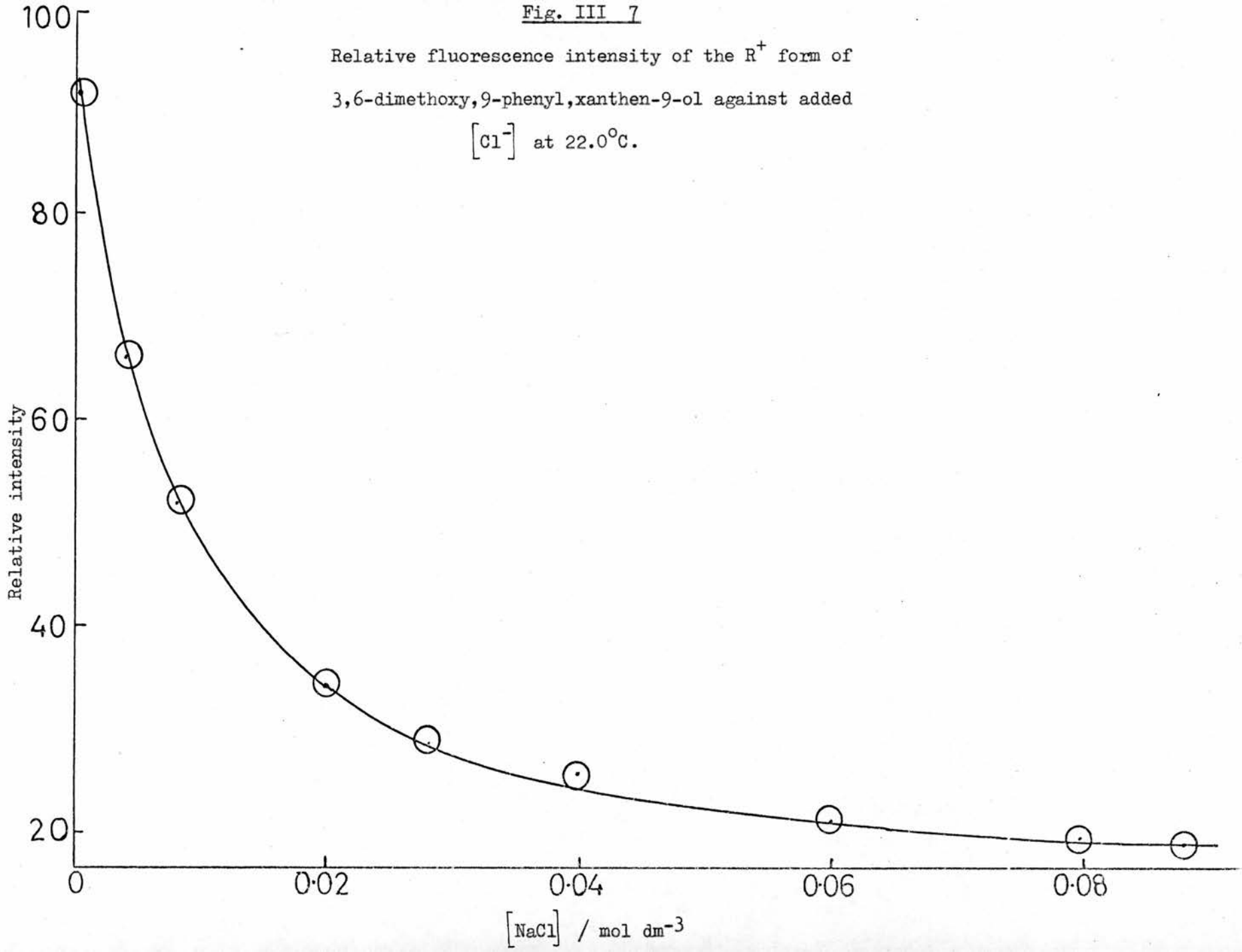

Fig. III 8

Stern-Volmer plots for the quenching of R^+ fluorescence by NaCl in 10^{-3} mol dm^{-3} aq.$HClO_4$ solutions containing additional concentrations of ClO_4^- a 0, b 0.2, c 0.5, d 1.0, e 1.6 mol dm^{-3}

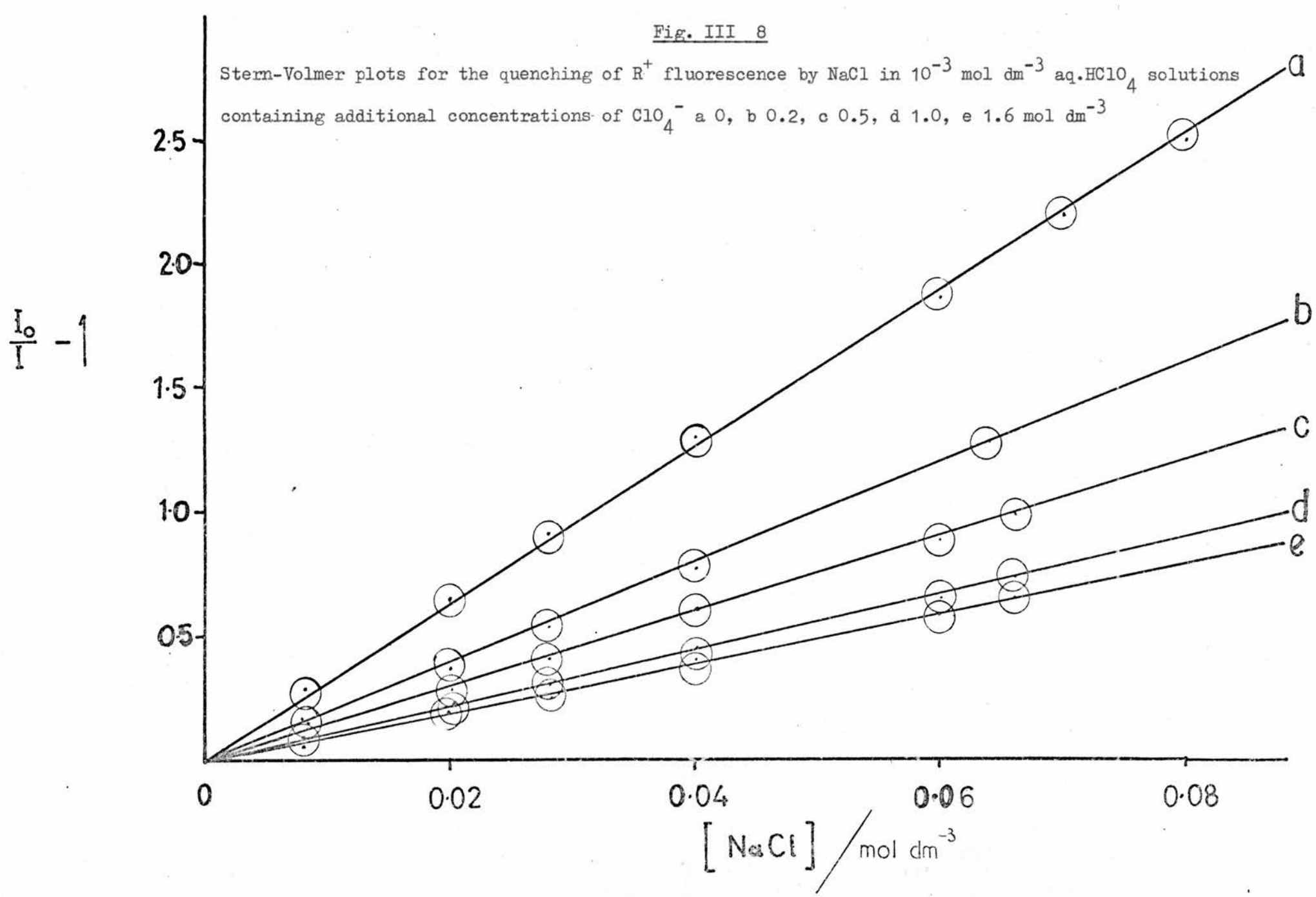

TABLE III 5

Quenching of R^+ fluorescence by the $[ClO_4^-]$ ion at $[H^+] = 10^{-3}$ mol dm^{-3}

I_o represents fluorescence intensity in the absence of a quencher and

I that in its presence

$[NaCl]$	I	$I_o/I - 1$	
0	78.0	0.	$I_o = 78$
0.008	63.2	0.23	
0.020	50.0	0.56	
0.028	43.0	0.81	
0.040	36.0	1.16	$[ClO_4^-] = 0$
0.060	27.4	1.84	
0.080	23.0	2.29	
0.088	22.0	2.55	
0	77.4	0.	$I_o = 77.4$
0.008	66.0	0.17	
0.020	54.8	0.40	
0.028	48.0	0.61	$[ClO_4^-] = 0.2$ mol dm^{-3}
0.040	42.5	0.82	
0.048	38.5	1.01	
0.060	34.2	1.26	
0	80.8	0	$I_o = 80.8$
0.008	71.7	0.12	
0.020	61.0	0.31	
0.028	56.7	0.41	$[ClO_4^-] = 0.5$ mol dm^{-3}
0.040	50.0	0.60	
0.060	42.8	0.87	
0.066	40.0	1.0	

Table III 5 Con.

$[NaCl]$	I	$I_o/I - 1$	
0	79.5	0.	$I_o = 79.5$
0.008	69.5	0.14	
0.020	64.0	0.24	
0.028	60.0	0.32	$[ClO_4^-] = 1.00$ mol dm^{-3}
0.040	55.0	0.45	
0.060	47.0	0.69	
0.066	43.0	0.84	
0	81.0	0.	$I_o = 81$
0.008	76.5	0.06	
0.020	68.0	0.19	
0.028	65.0	0.26	$[ClO_4^-] = 1.6$ mol dm^{-3}
0.040	59.0	0.37	
0.060	54.5	0.49	
0.066	51.0	0.59	

The slopes were identical whether H_2SO_4 or $HClO_4$ was used for the slight acidification.

Very similar slopes were obtained at $\left[H^+\right] = 10^{-1}$ mol dm^{-3} showing that $\left[H^+\right]$ has no effect, providing the pH is sufficiently far from pK_{R^+} .

The presence of ClO_4^- does reduce the quenching efficiency of Cl^- , but very similar results were also obtained with NO_3^- and BF_4^- , (Table III 6)

TABLE III 6

Approximate quenching Constants for ClO_4^- , BF_4^- , and NO_3^- ions.

Concentration of NaCl (mol dm^{-3})	Quenching constants k in mol^{-1}/ dm^3		
	ClO_4^-	BF_4^-	NO_3^-
0	300		
0.1	-	266	-
0.2	226	230	-
0.5	152	143	140
1.0	120	-	116
1.6	87	-	86

Very little quenching effect was produced by ClO_4^- , BF_4^- , and NO_3^- ions and very high concentrations had to be used to produce an observable effect on the emission intensity. It was not therefore possible to determine accurately quenching constants for these ions.

The most probable explanation for those observations is that a direct Brønsted ionic strength effect on the $R^+ + Cl^-$ reaction is involved.

The enhancement of fluorescence by ClO_4^-, although noticeable, is not very large when compared with the marked effects of ClO_4^- at low concentrations (0.1 to 1 mol dm^{-3}) in the case of trianisylmethanol[51]. This might be caused by the greater difficulty of approach of the bulky ClO_4^- ion to the C^+ centre when R^+ has a "semi-planar" configuration due to the oxygen bridge.

The Stern-Volmer plot for higher concentrations of NaCl, Fig. III 9, shows a definite curvature, with a progressively decreasing slope, consistent in magnitude with the ClO_4^- ionic strength effect. Values of fluorescence intensity, I, quencher concentration, $[Q]$ and $(I_o / I) - 1$ are presented in Table III 7.

TABLE III 7

Quenching of 3,6-dimethoxy,9-phenyl,xanthen-9-ol fluorescence by inorganic anions at $[H^+] = 10^{-3}$ mol dm^{-3}

$[Q]$ = concentration of quencher ion in mol dm^{-3}

I = fluorescence intensity in the presence of a quencher

I_o = fluorescence intensity in the absence of a quencher

$[I^-]$	I	$(I_o/I) - 1$	
0	77	0.	$I_o = 77$
0.008	15	4.13	
0.010	25	2.08	
0.020	16	3.81	
0.030	12.3	5.26	
0.040	9.1	7.46	
0.050	7.5	9.26	
0.06	6.27	11.20	

Table III 7 Con.

$[NCS^-]$			
0	77.3	0.	I_o = 77.3
0.02	34	1.28	
0.04	20	2.95	
0.06	14	4.52	
0.08	11	6.05	
0.10	9	7.62	
$[Br^-]$			
0	76.5	0.	I_o = 76.5
0.02	38.5	0.99	
0.04	26.0	1.94	
0.08	16.1	3.75	
0.10	13.3	4.75	
0.14	9.9	6.72	
0.20	7.3	9.47	
$[Cl^-]$			
0	90.7	0.	I_o = 90.7
0.02	5.5	0.64	
0.04	41.0	1.21	
0.10	24.0	2.80	
0.14	18.7	3.85	
0.20	15.0	5.04	
0.24	13.0	5.97	
0.30	11.0	7.24	

The relative intensity measurements for the addition of other quenchers, I^-, Br^-, and NCS^-, to solutions of 3,6-dimethoxy, 9-phenyl,xanthen-9-ol in 10^{-3} mol dm^{-3} $HClO_4$ are also shown on Fig. III 9. For each quencher, a plot of $\{(I_o / I) - 1\}$ against quencher concentration was constructed and from the slopes values of the quenching constants were obtained. In every case a straight line plot was obtained for low quencher concentrations, with no indication that irreversible chemical changes or complex formation in the ground state took place. The initial Stern-Volmer slopes, k_q / k_f were 180, 70, 46, and 32 mol^{-1} dm^3 for I^-, NCS^-, Br^-, and Cl^- respectively.

The fluorescence life-time of the R^+ form as seen on our laser produced a time profile of the same order as the laser excited pulse, showing that $k_f^{-1} \leqslant 5$ ns.

Taking this value for τ in equation III 15, lower limits can be assigned to the quenching constant (k_q) and these are:

6.4×10^9 mol^{-1} dm^3 s^{-1} for Cl^-,
14×10^9 mol^{-1} dm^3 s^{-1} for NCS^-,
9.2×10^9 mol^{-1} dm^3 s^{-1} for Br^-, and
3.6×10^{10} mol^{-1} dm^3 s^{-1} for I^-,

thus closely approaching the encounter rate calculable for R^+ and a halide ion. It seems very likely that the quenching anions remain separated from the C^+ centre by one or more water molecules and that they assist at a stage in the formation of the R-OH bond, probably in some way related to the observed general base catalysis in the water reaction with Malachite green.[35] The mechanism for the quenching of aromatic hydrocarbon emission by inorganic anions discussed by Watkins[82] cannot explain the present results, since in our case quenching by NO_3^-

Fig. III 9

Stern-Volmer plots for the quenching of R^+ fluorescence by KI, NaNCS, KBr and NaCl

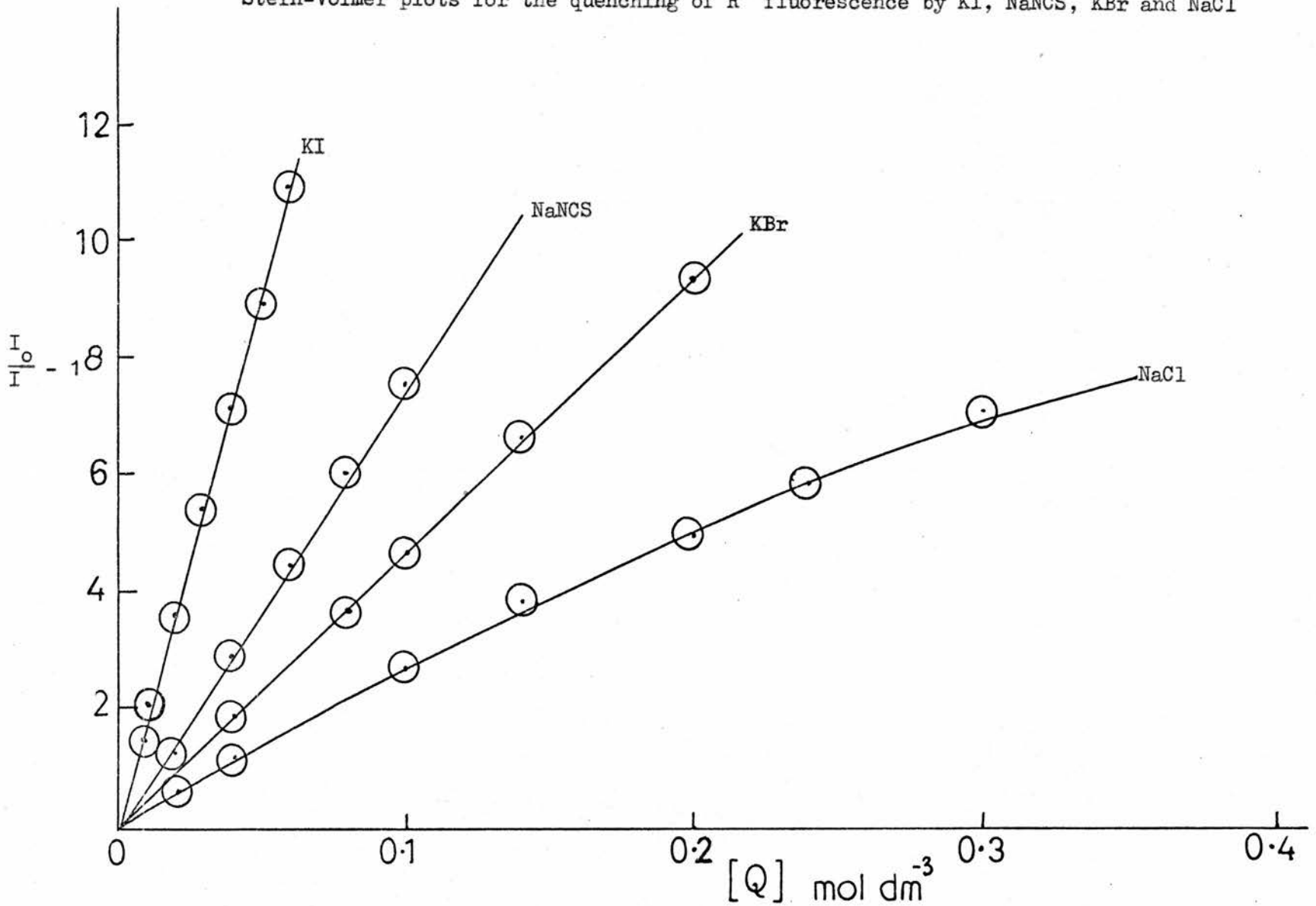

was either absent or extremely small. Our observations agree more with the data of Bartolus[83], (quenching efficiency of fluorescence in the order $Cl^- < Br^- < NCS^- < I^- < SeCN^-$), who ascribes the quenching to interactions by a kind of charge transfer complex formation, and a heavy-atom enhanced inter-system crossing to the triplet state.

5. Salt effects upon the rate of disappearance of 3,6-dimethoxy,9-phenyl xanthen-9-ol

(a) Introduction

Evidence for the association of triphenylmethylcation with ClO_4^- has been reported[28,32,34]. The effect of perchlorates upon the reverse reaction ($R_3C^+ + H_2O \longrightarrow R_3COH + H^+$ was quite marked even at low concentrations and its importance for the interpretation of the H_R acidity function was discussed[28].

Although the cation of 3,6-dimethoxy,9-phenyl,xanthen-9-ol, possessing a structure related to triphenylmethylcation, showed similar ClO_4^- ion effects upon quenching reactions, their magnitude was that expected of a direct primary salt effect between two ions of different charges, leaving no room apparently for a special ion-pairing effect with this cation.

Evidence was therefore sought for possible suppression of ClO_4^- association by the presence of the oxygen bridge, which will alter the "propeller shape" of a molecule of 3,6-dimethoxy,9-phenyl,xanthen-9-ol. If this were the case, a series of indicators based on this compound, but possessing different substituents, could define a new acidity function directly correlated with the water activity for strong acids[20].

These were the underlying reasons for the study of ClO_4^- and other additives upon the rate of disappearance of 3,6-dimethoxy,9-phenyl, xanthen-9-ol by the stopped-flow methods used for the study of parallel reaction of tri-methoxytriphenylcarbinol. The principal object was to discover whether or not perchlorate additions had similar effects on the rates of disappearance of the two carbocations.

(b) Experimental

The reaction $ROH + H^+ \underset{k_b}{\overset{k_f}{\rightleftharpoons}} R^+ + H_2O$,

where ROH is 3,6-dimethoxy,9-phenyl,xanthen-9-ol and k_f and k_b are rate constants of the forward and backwards reaction respectively, was studied on the stopped-flow apparatus described previously in Part II 3(a).

The rate constants of this reaction were calculated from the first order rate equation:

$$kt = \ln \frac{a}{a-x} = 2.303 \log D_o/D_t \quad \text{(page 18)}$$

For the slower reaction rates, the method of Swinbourne[50] was employed to calculate rate constants, (described in detail in Part II 3(c)).

The values of intercept, regression coefficient, and standard error of estimate used to calculate temperature corrections to bring all the rates to 298 K were obtained from the CLBST programme available in the computer laboratory.

(c) <u>The effect of temperature on reaction rates</u>

The variation of the rate constant of a reaction with temperature is expressed by means of an equation:

$$k = Ae^{-E_A/RT} \qquad \text{Eqn. 16}$$

where E_A is the activation energy of the reaction

R is the gas constant

T is Kelvin temperature, and

A is the Arrhenius A factor

On taking logarithms of equation 16, we obtain:

$$\log k = \log A - \frac{E_A}{2.303RT} \qquad \text{Eqn.17}$$

Acidic and basic solutions were mixed in a stopped-flow and the final concentrations of reactants in the mixing chamber were:

the compound, 10^{-5} mol dm^{-3}

perchloric acid, 5×10^{-4} mol dm^{-3}

phosphate buffer, 6.7×10^{-3} mol dm^{-3}

and sodium hydroxide, 5×10^{-4} mol dm^{-3}

Three to four values of rate constant, k for each reaction at temperatures from 11.4°C to 50°C were calculated from the Swinbourne plot, and their average values are tabulated below.

Arrhenius parameters from the variation of rate constant (k_b) for 3,6-dimethoxy,9-phenyl,xanthen-9-ol with temperature.

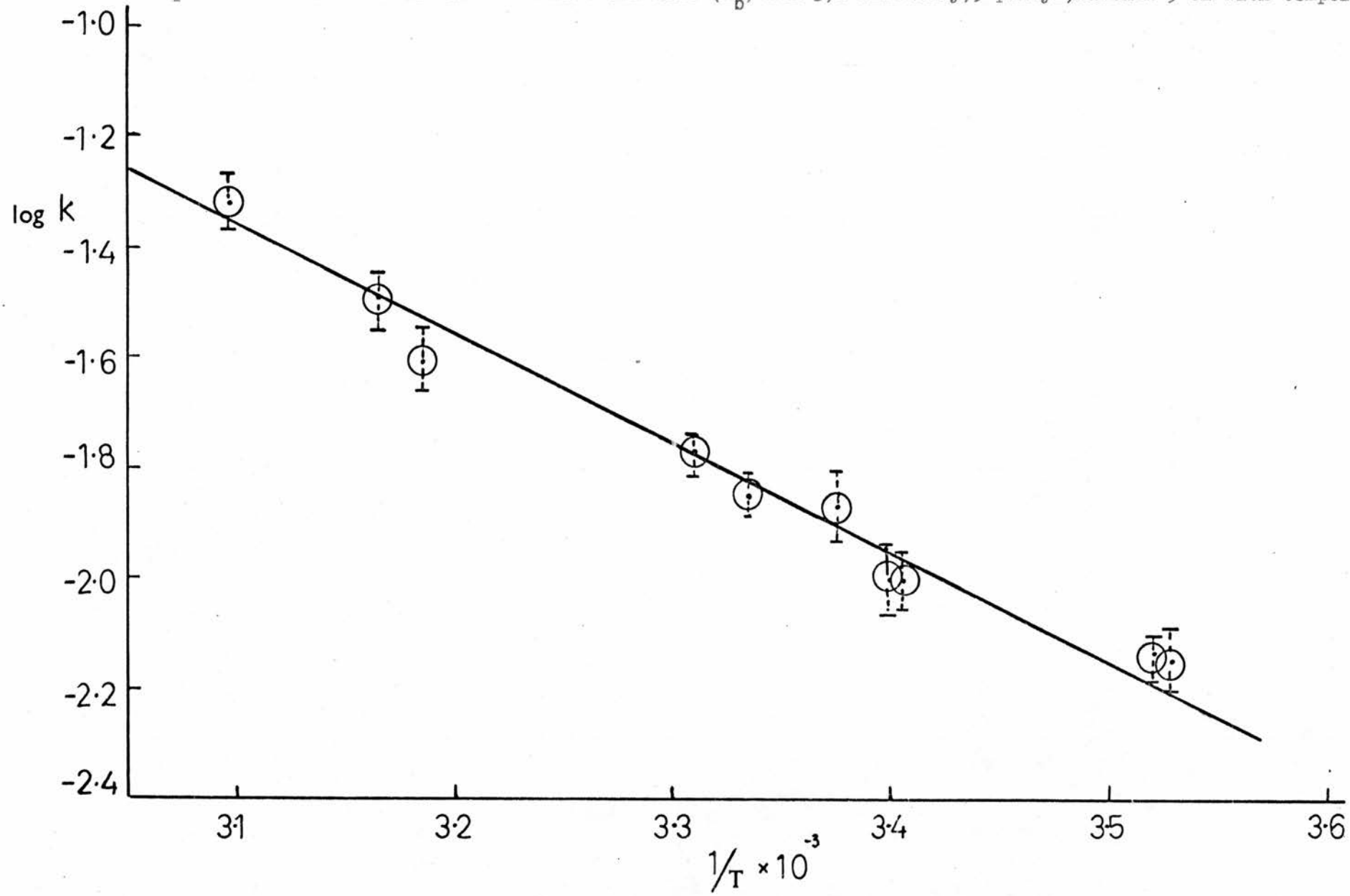

TABLE III 8

Variation of rate constant (k_b) for 3,6-dimethoxy,9-phenyl,xanthen-9-ol with temperature

$t^{\circ}C$	T/Kelvin	$\frac{1}{T} \times 10^{-3}/K^{-1}$	k/s^{-1}	log k
50	323	3.096	4.96×10^{-2}	-1.3045
43	316	3.165	3.31×10^{-2}	-1.4815
41	314	3.185	2.50×10^{-2}	-1.6021
29	302	3.311	1.74×10^{-2}	-1.7602
27.8	300.8	3.334	1.44×10^{-2}	-1.8416
23	296	3.378	1.40×10^{-2}	-1.8539
21.4	294.4	3.397	9.8×10^{-3}	-2.0088
21	294	3.401	1.0×10^{-2}	-2.0000
11.8	284.8	3.531	7.24×10^{-3}	-2.1403
11.4	284.4	3.529	7.35×10^{-3}	-2.1221

A plot of log k versus $\frac{1}{T}$ (Fig. III 10) from these data gave, by eye, a slope from which E_A = 9.37 k cal mol^{-1} (39.19 kJ mol^{-1}). Data from Table III 8 were fed into the computer and, using programme CLBST, polynomial regression analysis gave the slope as - 1846.55 K and intercept 4.3431, from which an approximately determined activation energy of 8.45 k cal mol^{-1} or 35.35 kJ mol^{-1} was obtained.

Approximate corrections for these k values near 298 K bringing all values to a standard temperature to 298 K were made as follows:

from $\log k = \text{slope} \left(\frac{1}{T} \right) + \text{constant}$

$$\log k_{25} = -1846.55 \left(\frac{1}{298}\right) + 4.3431 = -1.8533$$

$$\therefore \log k_{25} = -1.8533 \text{ or } k_{25} = 1.434 \times 10^{-2} \text{ s}^{-1}$$

similarly

$$\log k_{24} = -1.8742 \text{ or } k_{24} = 1.336 \times 10^{-2} \text{ s}^{-1}$$

thus giving a $\Delta \log k / K = 2.09 \times 10^{-2} K^{-1}$

or $\Delta k/K = 0.00066 \text{ s}^{-1} K^{-1}$

$\therefore$ k changes by a factor 1.049 (antilog of $\Delta \log k / K$) or 4.9% per K.

The values of rate constants so corrected are listed (as k_{25}) in the following table.

TABLE III 9

Effect of pH on the rate of reaction at constant buffer concentration.

pH	$k_{obs} \times 10^{-2}/s^{-1}$	temp. °C	$k_{25} \times 10^{-2}/s^{-1}$	
5.90	2.96	24.6	3.01	phosphate buffer, concn. = 6.7×10^{-5} mol dm^{-3}
6.70	1.72	24.0	1.79	
7.00	1.22	22.6	1.37	
7.15	1.22	23.8	1.30	
7.20	1.49	24.5	1.53	
7.67	1.22	24.6	1.24	
7.90	1.47	23.7	1.56	
8.10	1.59	24.5	1.62	borate buffer concn. 6.7×10^{-5} mol dm^{-3}
8.40	1.66	23.7	1.72	
9.21	2.12	24.0	2.27.	

Data from this table is presented in the graph form (Fig. III 11) and indicates moderately stable k values in the pH region 6.70 to 7.90, with variation of k values of less than 0.005 s^{-1}. Effect of buffers on reaction rates at constant pH was studied and results are summarised in tables III 10 and III 11 below.

TABLE III 10

Effect of phosphate buffer concentration on the rate constant k

[buffer]/mol dm^{-3}	$k_{obs}/10^{-2}s^{-1}$	temp°C	$k_{25}/10^{-2}s^{-1}$	effluent pH
$6.7x10^{-4}$	1.48	24.50	1.52	7.46
$26.8x10^{-4}$	1.47	24.40	1.51	7.60
$6.7x10^{-3}$	1.58	24.50	1.62	7.60
$5.0x10^{-2}$	1.53	24.10	1.60	7.51
0.10	1.84	25.70	1.77	7.42
0.20	2.05	26.65	1.88	7.42
0.30	2.41	26.55	2.22	7.38
0.40	2.91	27.00	2.62	7.40

Fig. III 11

Effect of pH on the rate of reaction at constant buffer concentration.

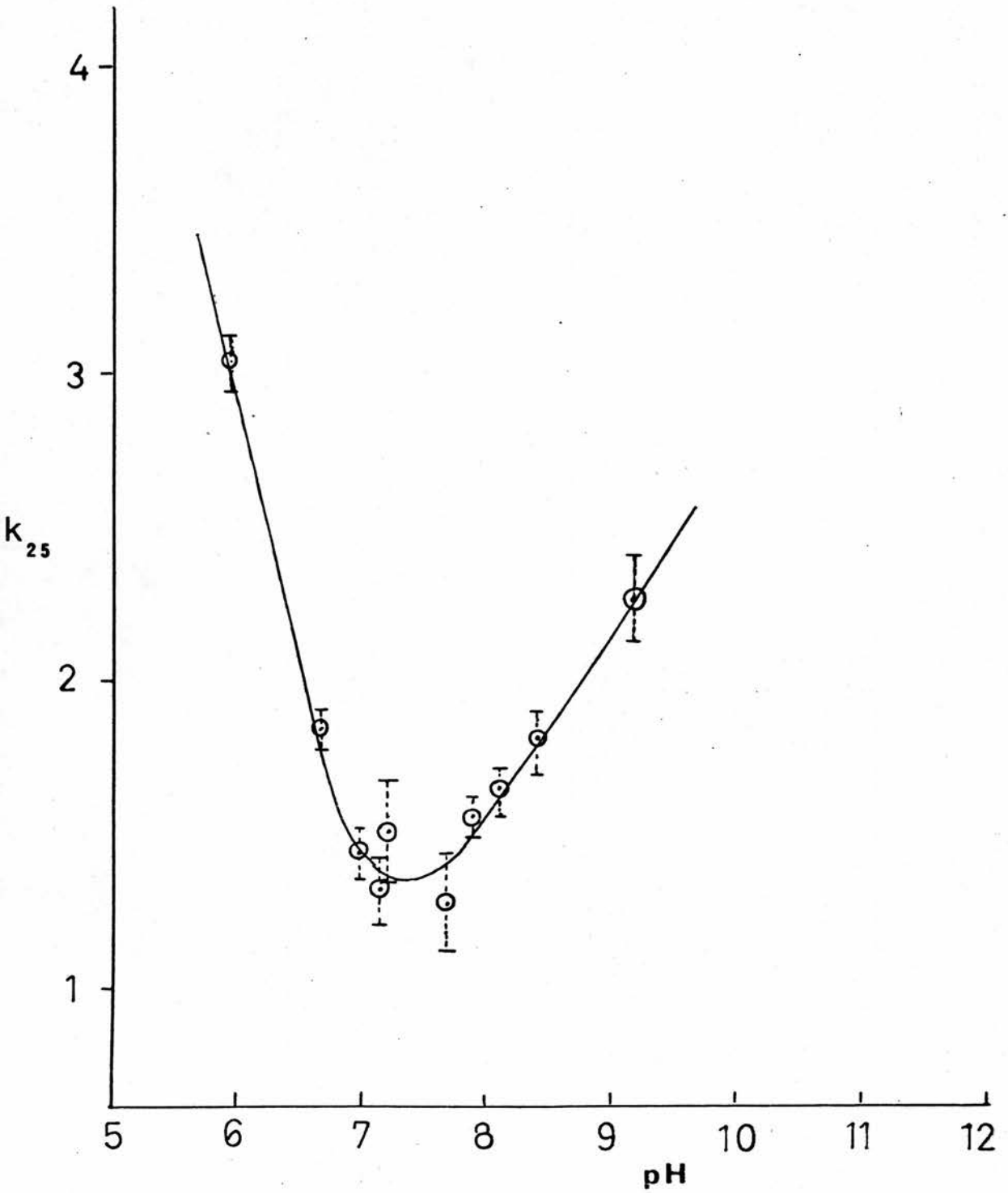

TABLE III 11

Effect of borate buffer concentration on the rate of reaction

[buffer]/mol dm^{-3}	$k_{obs}/10^{-2}s^{-1}$	temp°C	$k_{25}/10^{-2}s^{-1}$	effluent pH
$12.5x10^{-3}$	3.26	26.6	3.00	9.21
$5.0x10^{-3}$	1.93	26.5	1.79	9.30
$0.50x10^{-3}$	1.93	26.7	1.77	9.16
$0.25x10^{-3}$	2.22	26.5	2.06	9.18

The effects of added salts on the rate constants for the reaction

$R^+ + H_2O \longrightarrow ROH + H^+$ (i.e. the disappearance of the 3,6-dimethoxy-9-phenylxanthyliumcation) were studied in the experimental conditions where concentrations of buffer and indicator were kept constant at 6.7×10^{-3} and 10^{-5} mol dm^{-3} and the pH at 7.5 ± 0.1 respectively. Concentrations of added salts varied between 0 and 1.5 mol dm^{-3}, with the exception of sodium sulphate, where due to its low solubility concentrations of 0 to 0.42 mol dm^{-3} were used. The results showing effects of salts on the rate constant, k are presented in Table III 12 and in the graph form, in Fig. III 12.

Fig. III 12

Effects of salts upon the rate constant for the disappearance of the 3,6-dimethoxy-9-phenylxanthylium carbocation in aqueous solution at 298 K

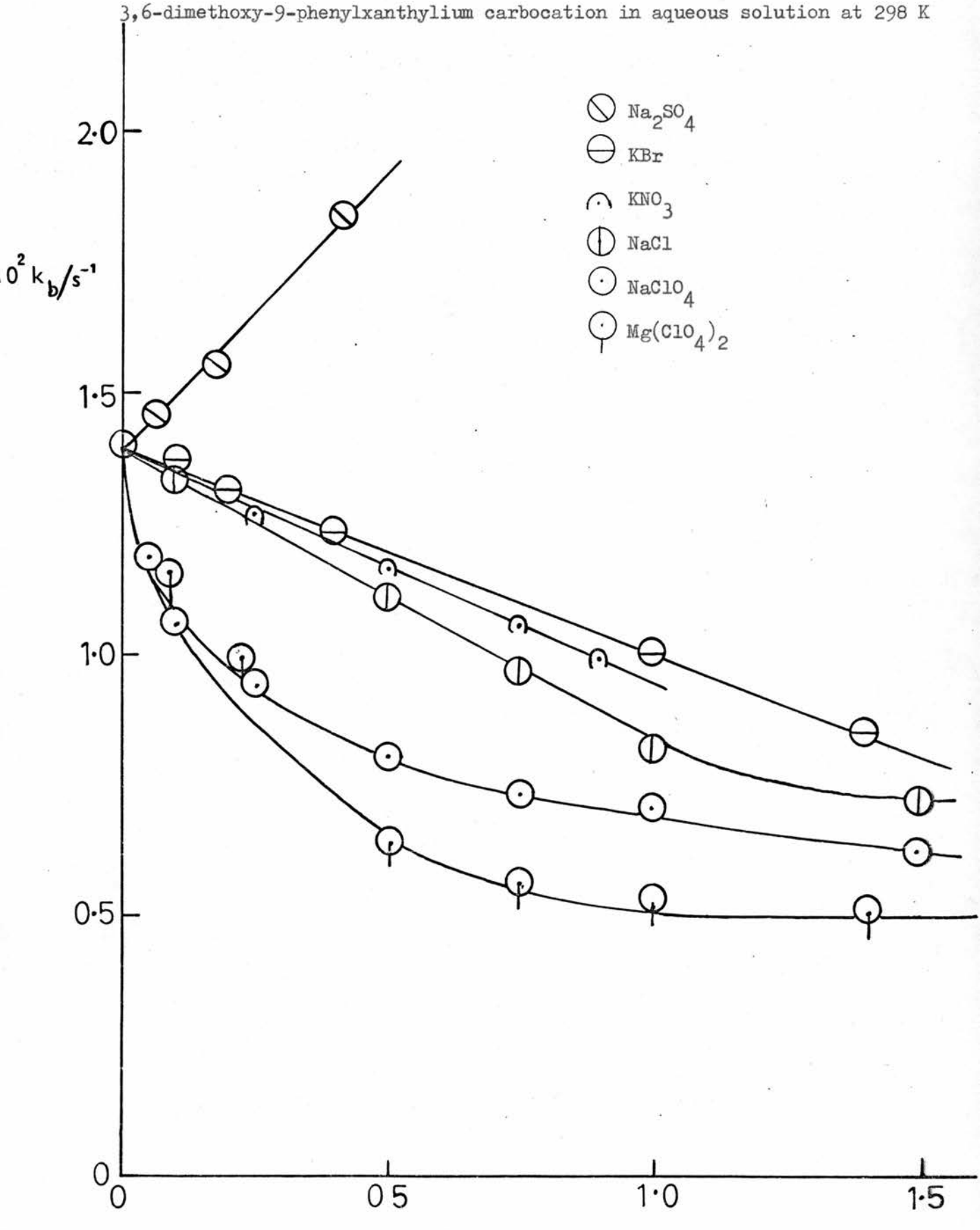

TABLE III 12

The effect of added salts on the backward rate of reaction (k_b) for 3,6-dimethoxy,9-phenyl,xanthene-9-ol.

$[NaCl]$ /mol dm^{-3}	$k_{b(obs)}/10^{-2}s^{-1}$	temp°C	$k_{25}/10^{-2}s^{-1}$
0	1.46	25.1	1.45
0.10	1.43	26.0	1.36
0.25	1.42	26.5	1.32
0.50	1.16	25.6	1.13
0.75	1.05	26.0	1.00
1.00	0.825	25.1	0.82
1.50	0.73	25.2	0.72
$[NaClO_4]$ /mol dm^{-3}			
0.10	1.06	25.0	1.06
0.05	1.24	25.7	1.20
0.25	0.99	25.9	0.95
0.50	0.85	25.9	0.82
0.75	0.74	25.2	0.73
1.00	0.76	26.0	0.72
1.50	0.66	26	0.63
$[Mg(ClO_4)_2]$ /mol dm^{-3}			
0.050	1.16	25.0	1.16

0.125	0.93	24.5	0.95
0.250	0.61	24.5	0.62
0.375	0.54	24.5	0.55
0.500	0.51	24.5	0.52
0.700	0.52	25.5	0.51
$[KBr]$ /mol dm^{-3}			
0.05	1.28	24.0	1.34
0.08	1.35	25.0	1.35
0.10	1.41	25.4	1.38
0.20	1.31	25.0	1.31
0.40	1.21	24.83	1.22
0.75	1.10	25.0	1.10
0.80	1.06	25.0	1.06
1.00	1.00	24.0	1.05
1.40	0.88	24.9	0.88
$[KNO_3]$ /mol dm^{-3}			
0.10	1.32	24.8	1.33
0.25	1.26	25.0	1.26
0.50	1.16	25.0	1.16
0.75	1.01	24.5	1.03
1.00	1.00	25.2	0.99
$[Na_2SO_4]$ /mol dm^{-3}			
0.06	1.46	25.0	1.46
0.18	1.53	24.8	1.54
0.42	1.84	25.0	1.84

(d) Preliminary study of $R_3C^+ + NH_3 \longrightarrow R_3CNH_3^+$ reaction.

With tris-p-methoxyphenylmethanol a sharp increase in the rate of disappearance of R_3C^+ was observed with different bases (e.g. ammonia and diethylamine) at the alkaline end of the scale, at pH 8.3 - 10.23. This was ascribed to direct nucleophilic attack upon the carbonium ion either by the OH^-, to form the same product as the attack by water, or by NH_3 or Et_2NH, to form different products with the resulting loss of a proton. (Table 3 ref. 28). The Et_3N, with no proton to lose, has no effect on the rate of disappearance of R_3C^+ in the pH region 8 - 10.2, where marked effects are observed with low concentrations of NH_3 and Et_2NH (0.01 to 0.07 and 0.01 to 0.4 respectively), despite the fact that it is the strongest base. When increases are observed with Et_3N, Postle and Wyatt concluded that they depend only upon the pH and not on the buffer concentrations, but both Ritchie[35] and Wyatt[31] did observe general base catalysis by the tertiary bases. Results in Table 2 ref. 28, refer therefore to the reaction of R_3C^+ with OH^-.

TABLE III 13

The effect of ammonia buffer concentrations on the rate of reaction

$$R_3C^+ + NH_3 \xrightarrow{k} R_3CNH_2 + H^+$$

$[NH_3]$ /mol dm^{-3}	k_b/s^{-1}	$[k_b-(k_o+k_{OH}[OH^-])]$/s^{-1}	pH
0.5×10^{-2}	0.052	0.032	8.65
1.0×10^{-2}	0.090	0.070	8.95
1.0×10^{-2}	0.100	0.079	9.10

2.0×10^{-2}	0.172	0.152	8.90
4.0×10^{-2}	0.330	0.310	8.80
8.0×10^{-2}	0.630	0.610	8.88
	$k_o = 0.014\ s^{-1}$, $k_{OH}\left[OH^-\right]$ from Fig.III.13		

The slope on the graph, Fig. III 13 is much greater relative to the k_o intercept and is 7.55 $mol^{-1}\ dm^3\ s^{-1}$ relative to $k_o = 0.014\ s^{-1}$ when compared with 260 $mol^{-1}\ dm^3\ s^{-1}$ (ref. 31) relative to $k_{H_2O} = 12\ s^{-1}$ (ref. 32). Probably a very small part of the 7.55 slope is due to the general base catalysis of the same relative magnitude as before.

Whether the general base catalysis is present or not can be possibly determined by further reactions with similar bases, i.e. triethylamine, diethylamine, and 1,4-diazabicyclo $\left[2.2.2\right]$ -octane. Provisionally, we assign this reaction and rate constant, k to the $R_3C^+ + NH_3 \longrightarrow R_3CNH_3^+$. It would be interesting to see whether the effect of additives on this reaction would be similar.

(e) Discussion of results.

The salt effect behaviour of tris-p-methoxyphenylmethanol and 3,6-dimethoxy,9-phenyl,xanthen-9-ol is almost identical. The comparison of data, Fig. III 12 with those of tris-p-methoxyphenylmethanol, (Fig. III ref.[28]) shows once again the remarkable retarding effect of ClO_4^- on the k_b, particularly at low salt concentration, and the SO_4^{2-} effect in the opposite direction. It is possible therefore, that in the fluorescence quenching study of the oxygen-bridged compound, either the Cl^- quenching reaction is not localised at the C^+ of the ion, or a ClO_4^- association effect present is difficult to separate from that

Fig. III 13

Effect of ammonia buffer concentrations on the rate of reaction

$$NH_3 + R_3C^+ \longrightarrow R_3CNH_2 + H^+$$

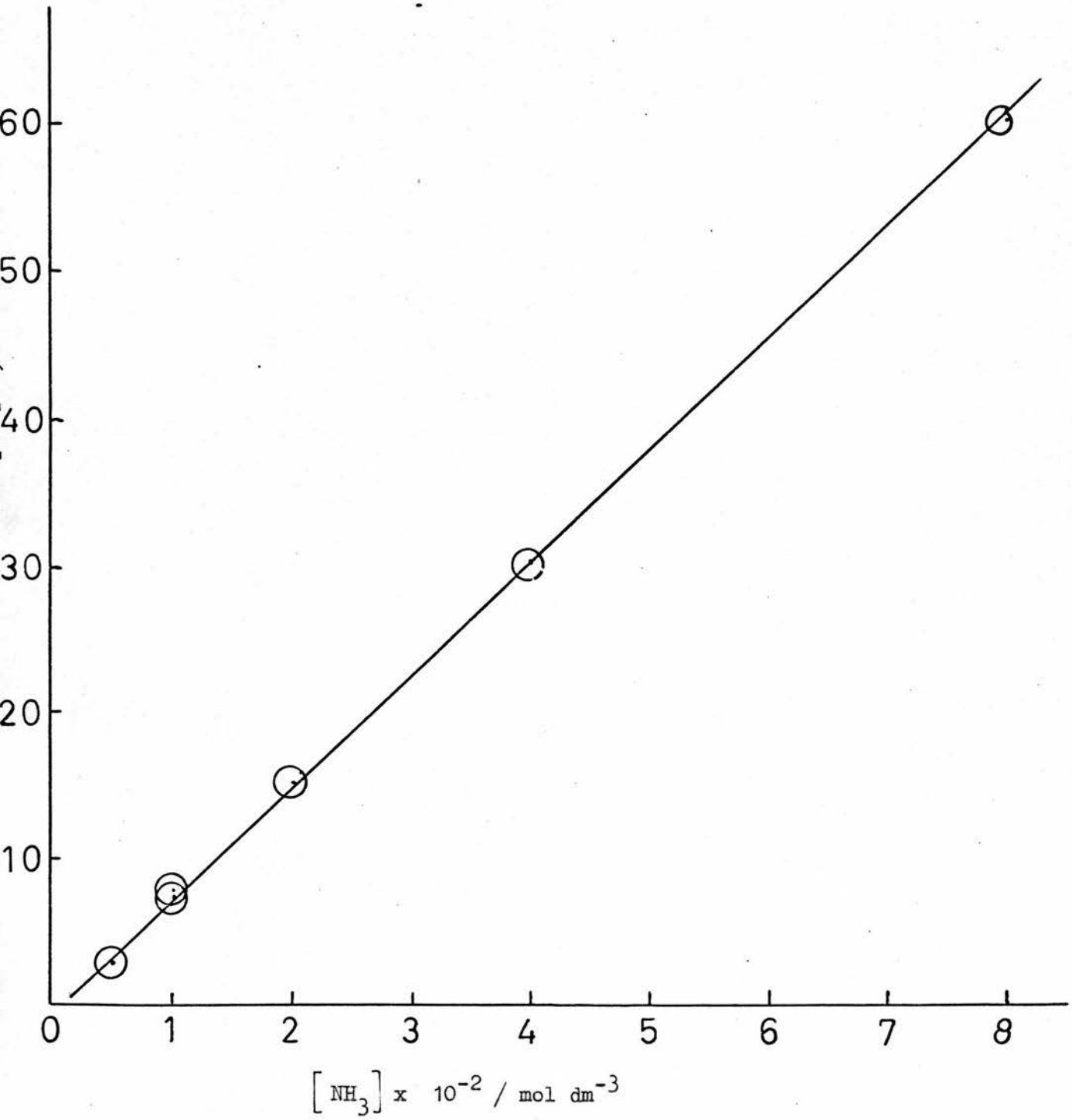

of ionic strength.

The introduction of the oxygen bridge lowered the acidity of the compound (pK_{R^+} = 5.44) compared with that of tris-p-methoxyphenyl (pK_{R^+} = 0.82[65]) and this fact had two effects on the results. The measured rates of reaction were 10,000 times slower and the pH range for observing the reaction of the carbocation with water was much more restricted. The "safe plateau" for measuring the rate constant, $1.46 \times 10^{-2} \pm 0.1\ s^{-1}$ for $R^+ + H_2O$ reaction at 298 K lay between pH 7 and 8, Fig. III 11.

Small temperature corrections, 4.0% / K required to bring all the observed rates to 298 K were calculated from estimated an activation energy of 35.35 kJ mol^{-1}. This was very similar to the value of E_A = 9.7 k cal (40.58 kJ mol^{-1}) for tris-p-methoxyphenyl[28,84] in spite of large difference in rates of reaction.

This might be due to the entropy effects, and it might be useful here to investigate further changes in the equilibrium constant with temperature, or measuring ΔH directly.

PART IV

MISCELLANEOUS PHOTOCHEMICAL DATA FOR RELATED COMPOUNDS

1. 9-Phenylxanthydrol (xanthen-9-ol-9-phenyl)

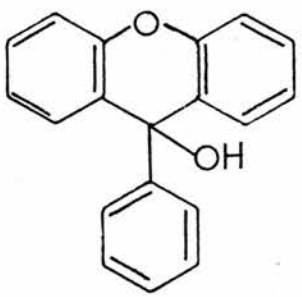

This compound was prepared, as a model, to test the practicability of synthesising tris-p-methoxy-xanthydrol from 3,6-dimethoxyxanthone and p-anisylbromophenol by Grignard coupling. The 9-phenylxanthydrol displayed strong yellow-green fluorescence in concentrated sulphuric acid, which disappeared in alkaline solutions, and a blue phosphorescence in concentrated H_2SO_4 when cooled in liquid nitrogen. Thus, on preliminary examination its photochemical properties were of sufficient interest to warrant further investigation.

Its pK was determined by spectrometry, using the method of Albert and Serjeant[62], described earlier on page 53.

Optical densities of twelve solutions, containing a constant concentration of 9-phenylxanthydrol (4×10^{-5} mol dm^{-3}) and varied amounts of sulphuric acid, were measured at the absorption peak 374 nm. From four separate determinations, the average pK (S_o) was calculated

as 0.21 ± 0.05 at 22°C.

TABLE IV 1

Calculation of pK (S_o) values for 9-phenylxanthydrol from optical density measurements

pH or H_o	Optical density, d at 374 nm	$\log\frac{d - dm}{d_i - d}$	pK_{R^+}
1.50	0.048	-1.276	0.22
1.26	0.084	-1.012	0.25
1.02	0.128	0.812	0.21
0.80	0.184	0.625	0.18
0.63	0.300	0.340	0.29
0.60	0.214	0.337	0.26
0.45	0.360	0.220	0.23
0.44	0.420	0.108	0.33
0.40	0.420	0.108	0.29
0.39	0.560	0.143	-0.26
3.00	0.96, (d_i) optical density of the ion		
13.00	0 , (d_m) optical density of the molecule		
	(d) optical density of the mixture		

The literature values of pK (S_o) previously reported by Conant and Werner[65] were 1.91, at 25°C determined by titration of bases with strong acids in glacial acetic acid solution, and 0.06 at 30°C[85] in aqueous sulphuric acid.

It is interesting to notice that the difference between our value

(0.21) and Conant's (1.91) for the pK_R+ of 9-phenylxanthydrol is 1.70, almost the same, as the difference, 1.74 between their pK_R+ value for tris-p-methoxycarbinol (2.56) in glacial acetic acid and Deno's[67] (0.82) in water.

The possibility of determining the excited state, pK (S_1) was investigated but the fluorescence spectra appeared at all pH values to be those characteristic of the form present in the ground state only.

2. 3,6-Dimethoxyanthone

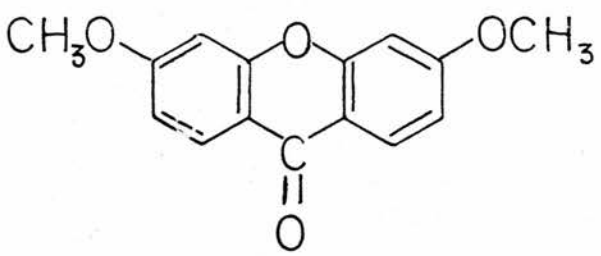

This compound, prepared as an intermediate, for the synthesis of 3,6-dimethoxy,9-phenyl,xanthene-9-ol, displayed some blue fluorescence in sulphuric acid, and was also examined further for excited-state acid-base behaviour.

(a) Absorption spectroscopy, determination of pK (S_o)

The absorption spectra of the B and BH^+ forms of 3,6-dimethoxyanthone were obtained at several different acidities near the pK (S_o) value. The concentration of compound was 4×10^{-5} mol dm^{-3} throughout in aqueous sulphuric acid, and all measurements were performed at the wavelength, λ = 376 nm, at 21°C. The pK (S_o) of

3,6-dimethoxyxanthone, calculated from equation III 4 gave value of -2.74 ± 0.01 from three separate determinations.

The scatter was calculated by taking the antilogarithms of pK values in a set, averaging, and taking the logarithm of the average value.

Since, there is no pK (S_o) value for this compound in the literature, it was intended to double check the obtained value by optical density measurements using the fluorescence technique.

The pK (S_o) is determined by the same method[62], used for optical densities i.e. from the equation

$$pK = H_o + \log \frac{I - I_B}{I_{BH^+} - I} \qquad \text{eqn. IV. 1}$$

where H_o gives the acidity function value of the sample and I is its fluorescence intensity. The I_B and I_{BH^+} are respectively the fluorescence intensities of the base form and the protonated form alone.

It was noticed at this stage that solutions containing H_2SO_4 in concentrations of 4 - 10 mol dm^{-3} became slightly coloured on standing for more than 4 h. To avoid the possibility of sulphonation reactions, although the optical densities of samples in acid were measured within 10-15 min of mixing, subsequent experiments were performed in $HClO_4$. In 9.4 mol dm^{-3} $HClO_4$ our compound was stable for up to 11 h.

Solutions for spectrometric examination were prepared by adding 1 ml of a stock solution of 3,6-dimethoxyxanthone in ethanol (2×10^{-5} mol dm^{-3}) to a 25 ml flask, making the solution 8×10^{-7} mol dm^{-3}. The alcohol was removed in <u>vacuo</u> and weighed amounts of $HClO_4$ were added[63] to give $-H_o$ of final solutions from 1 to 5.08.

(See table IV 2).

TABLE IV 2

Calculation of pK (S_o) values for 3,6-dimethoxyxanthone from fluorescence intensity measurements at 375 nm and t = 22°C

$-H_o$	$\log \frac{I - I_B}{I_{BH^+} - I}$	$-pK\ (S_o)$
1.0	-1.27	2.27
1.34	-1.00	2.34
1.54	-0.85	2.39
1.66	-0.71	2.37
1.87	-0.52	2.39
2.04	-0.34	2.33
2.24	-0.12	2.28
2.51	0.18	2.33
2.67	0.37	2.30
2.80	0.57	2.23
2.96	0.70	2.26
3.08	0.88	2.20
3.24	0.80	2.44

The data from Table IV 2 is presented in the graph form Fig. IV 1 and contains values $I_B = 0$ and $I = 55.0$ obtained in H_2O and 60% $HClO_4$ respectively. The best value obtained from the graph gave pK (S_o) of 3,6-dimethoxyxanthone as 2.34 $\pm$ 0.06 at 22°C. The pK (S_o) of the parent compound, xanthone[74] was measured at 20,40, and 60°C

Fig. IV 1

Calculation of pK (S_o) of 3,6-dimethoxyxanthone from fluorescence intensity measurements, I at 376 nm and temp. of 21°C.

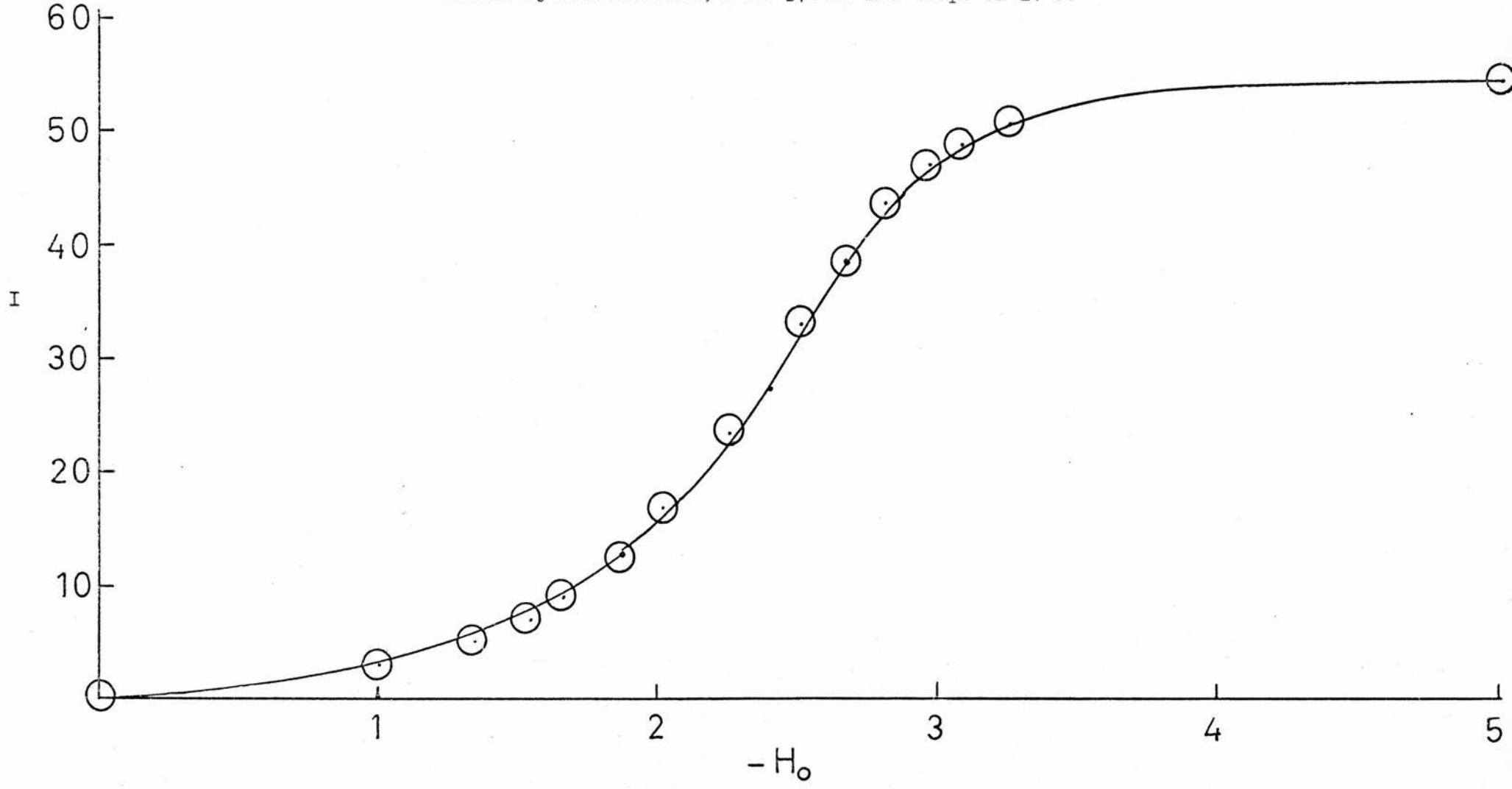

and it was found that temperature has very little effect on the pK.

(b) Fluorescence spectroscopy, determination of pK (S_1)

The change in the fluorescence emission due to a protolytic reaction of 3,6-dimethoxyxanthone in the excited state takes place in solutions of much lower acid concentration than that in the ground state, thus indicating that this compound is a stronger base in the excited state. The neutral and protonated forms have fluorescence maxima at 374 and 430 nm respectively.

To determine pK (S_1), fluorescence measurements were made, using aqueous $HClO_4$ solutions containing 0.96×10^{-6} mol dm^{-3} of the compound. Constant ionic strength was maintained at I = 1 by the addition of 1 mol dm^{-3} $NaClO_4$. Table IV 3 gives the fluorescence intensity measurements of the B and BH^+ forms of 3,6-dimethoxyxanthone as a function of pH at 22.1°C.

These were measured intensities, which must be corrected for overlap between the emission spectra of the two species to obtain the true fluorescence intensities of the B and BH^+ forms (ϕ and ϕ_1) respectively. The correction of overlap and the relation of measured and true intensities were described earlier in III 4 (c). The corrected fluorescence intensities of various pH values are presented in Table IV 3, together with the relative fluorescence intensities ϕ / ϕ_o and ϕ' / ϕ'_o of B and BH^+ forms respectively. A plot of the relative fluorescence intensity as a function of pH is shown in Fig. IV 2, from which a value of 1.20 ± 0.05 for the pK (S_1) is obtained.

Fig. IV. 2

Relative fluorescence intensities of protonated and unprotonated forms of 3,6-dimethoxyxanthone as a function of pH

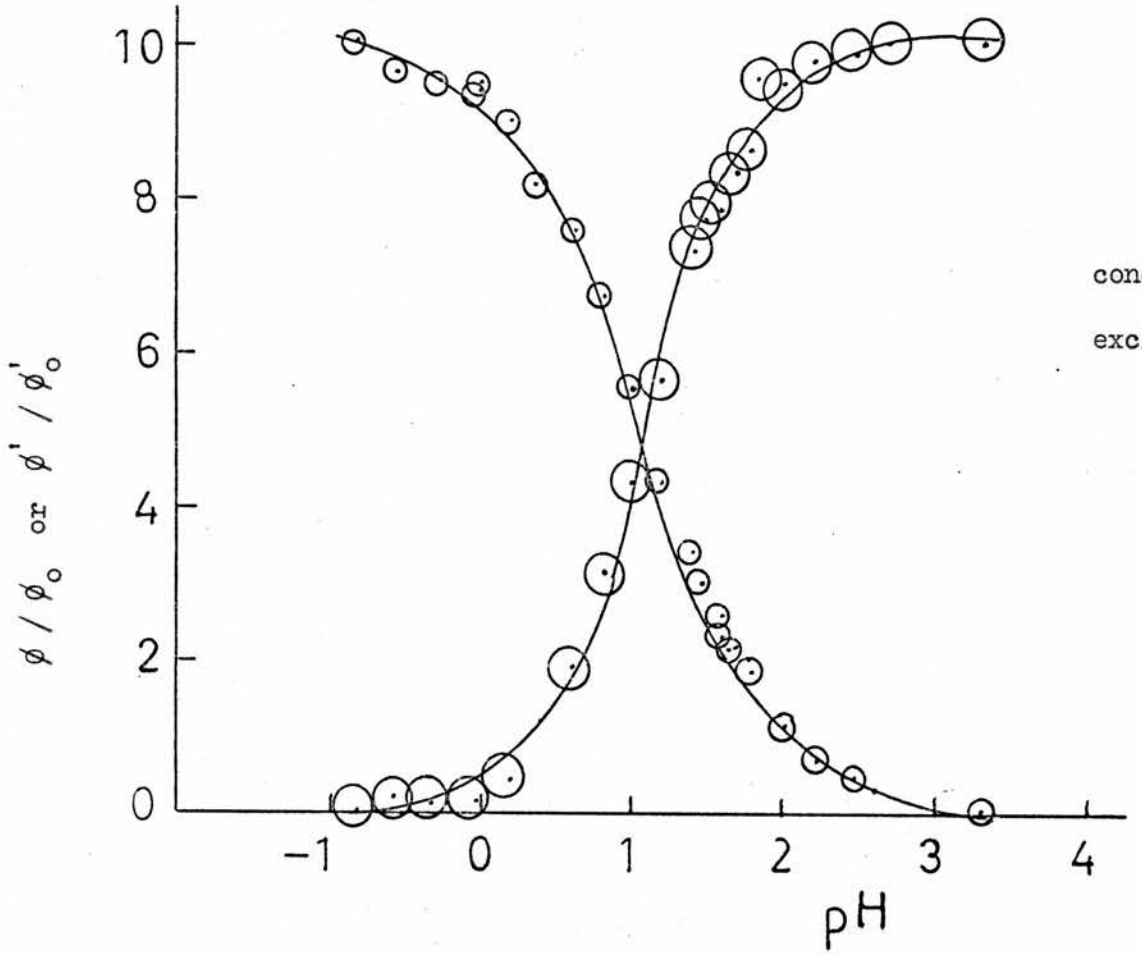

ø' / ø'₀ at 430 nm

ø / ø₀ at 374 nm

concn. of xanthone = 0.96×10^{-6} mol dm^{-3}

excitated at 310 nm

TABLE IV 3

True fluorescence intensities of the protonated and unprotonated forms of 3,6-dimethoxyxanthone as a function of pH. Excitation wavelength = 310nm

pH	$^{*}BH$ measured at 430 nm				$^{*}B$ measured at 374 nm			
	I'	$k'I'$	$\frac{I^{-}-kI}{1-kk'}$	ϕ'/ϕ'_o	I	kI	$\frac{I-k'I'}{1-kk'}$	ϕ/ϕ_o
-0.82	44.0	0.70	43.98	1.00	0.7	0.15	0	0
-0.56	42.3	0.68	42.22	0.96	1.0	0.21	0.32	0.03
-0.26	42.0	0.67	41.98	0.95	0.7	0.15	0.03	0.001
0	41.8	0.67	41.78	0.95	0.7	0.15	0.03	0.001
0.20	39.8	0.64	39.71	0.90	1.1	0.23	0.46	0.04
0.40	36.5	0.58	36.23	0.82	1.8	0.38	1.22	0.12
0.60	33.8	0.54	33.37	0.76	2.5	0.53	1.97	0.19
0.80	30.0	0.48	29.28	0.67	3.8	0.80	3.33	0.31
1.00	25.0	0.40	24.02	0.55	5.0	1.05	4.61	0.43
1.20	20.0	0.32	18.76	0.43	6.2	1.30	5.9	0.56
1.40	16.6	0.27	14.96	0.34	8.0	1.68	7.75	0.73
1.46	15.2	0.24	13.35	0.30	8.2	1.72	7.98	0.78
1.59	13.3	0.21	11.44	0.26	9.0	1.89	8.82	0.83
1.60	11.8	0.19	10.07	0.23	8.4	1.76	8.23	0.78
1.68	11.6	0.18	9.73	0.22	8.3	1.74	8.15	0.77
1.76	10.6	0.17	8.89	0.20	9.0	1.90	8.84	0.83
1.80	10.2	0.16	7.95	0.18	10.8	2.26	10.67	1.00
2.00	7.0	0.11	4.87	0.11	10.2	2.14	10.12	0.95
2.20	5.3	0.08	3.09	0.07	10.8	2.26	10.70	0.97
2.49	3.3	0.05	1.66	0.04	8.88	1.87	8.86	0.84
2.57	3.1	0.05	1.52	0.03	8.65	2.26	10.79	0.98
3.30	2.2	0.04	0	0	11.0	2.31	10.60	1.0

$k' = \frac{0.7}{44} = 0.016$ $\qquad$ $k = \frac{2.2}{11} = 0.200$

$\phi_o = 44$ $\qquad$ $\phi_o = 11$

This assumes that a protolytic equilibrium is established in the lifetime of the excited state. In these solutions, 3,6-dimethoxyxanthone was excited at 310 nm, i.e. as its base form, and the protonation must be complete within the fluorescence lifetime.

No measurements of this lifetime were obtained.

APPENDIX A

General Introduction

Kinetic studies[28,51] of some substituted di- and tri-phenyl methanols, (4-MeOtri-, 4,4',4"-triMe-, 4-Me-, 4,4',4"-trinitro-, 4,4'-diMeO-, and 4-MeO-,triphenyl methanols) in acid solutions showed that the rate of approach to equilibrium for these indicators was too fast to be detected by the stopped-flow technique. Further information on the reaction rates at higher acidities was hindered by the inability of stopped-flow apparatus to cope with reactions of half-lives greater than 5 - 15 ms, and was complicated further by problems caused by the heat of mixing in concentrated acid solutions. Future kinetic studies to elucidate the reaction mechanisms of these compounds with water and of tris-p-methoxyphenylmethanol with water, using the techniques of fast reactions, should be of interest.

The extension of the traditional kinetic methods to shorter half-times reactions has to overcome two main problems, those of mixing and monitoring the reaction. The mixing of two reactants has to be accomplished in a time considerably less than the reaction half-time, and the reaction must be monitored by an analytical technique which requires less time than the reaction half-time.

In the case of relaxation methods, the mixing problem is overcome by initiating a perturbation of a mixture of reactants at equilibrium, by varying some external paramater which affects the equilibrium of the system. While the system approaches a new equilibrium position, the time-lag, "relaxation time" in this approach, is related to the rate constants of the forward and backward reactions[30,86].

The pressure jump technique has been developed[87,88] as a useful tool for the investigation of fast chemical reactions in solutions, and reactions with relaxation times of 5×10^{-5} and 50 s can be studied. Strehlow and Wendt[88] pressure jump method used conductivity measurements to follow the reaction of $VO^{+2} + SO_4^{-2} \rightleftharpoons VOSO_4$, determining the rate constants from relaxation times of the order of 10^{-3}s.

In most pressure jump instruments the perturbation is caused by the bursting of a thin disc, which reduces the pressure on the sample from about 50 atm to 1 atm in approximately 100 μs. The reaction is generally followed by conductimetry, since pressure disturbances set up transient changes in the refractive index of the sample solution, which make spectrophotometric detection difficult[89].

The design of our apparatus was based on the Strehlow and Wendt's[88] design, but the relaxation of the concentrations towards the new equilibrium was nevertheless followed by changes of optical density of the sample solution.

A description of the apparatus and of some tests carried out using $CoCl_2$ solutions in iso-propyl alcohol / water mixtures is given below.

Pressure Jump Apparatus

A fast pressure jump can be achieved in the autoclave, containing two similar conductivity cells[88]. One of the cells contains the solution under investigation, the other one, a non-reacting solution. The concentration of the non-reacting solution is adjusted till both cells have nearly the same resistance. The pressure on the solutions is changed suddenly, and the position of chemical equilibrium existing

in the solution is shifted adiabatically. The relaxation of the concentrations towards the new equilibrium is followed by measuring the conductivity of the solution as a function of time. Here, only conductivity measurements provide sufficient sensitivity to record relaxation signal.

A similar apparatus for pressure jump was constructed for our project to investigate the possibility of following the R^+ disappearance in this way, but the relaxation of the concentrations towards the new equilibrium was followed by changes of optical density of the test solution.

The apparatus consisted of: the SP 500 Unicam monochromator with 6 V tungsten filament light source powered by a 6 V battery; the autoclave, equipped with quartz windows (Fig. A.1.) drilled to permit the flow of water for thermostatting, and containing thermo-couple terminals for the measurement of the temperature inside the autoclave, (Fig. A.2.). The amount of light transmitted through the solution, I_t, fell on the window of an RAC P 28 photomultiplier, powered by a Siemens Ediswan power supply unit, type R 1184, producing 300-1100 V d.c. and 0-2 mA current.

The output of the photomultiplier in μA was fed into a current converter. The voltage was tapped through four ranges. The most sensitive range 4 gave 1 V for 1 μ A current from the photomultiplier, others gave:

range 3 - 4 V for 2 μ A

" 2 - 1 V for 5 μ A

and " 1 - 1 V for 10 μ A

Fig. A.1

Side view of the autoclave

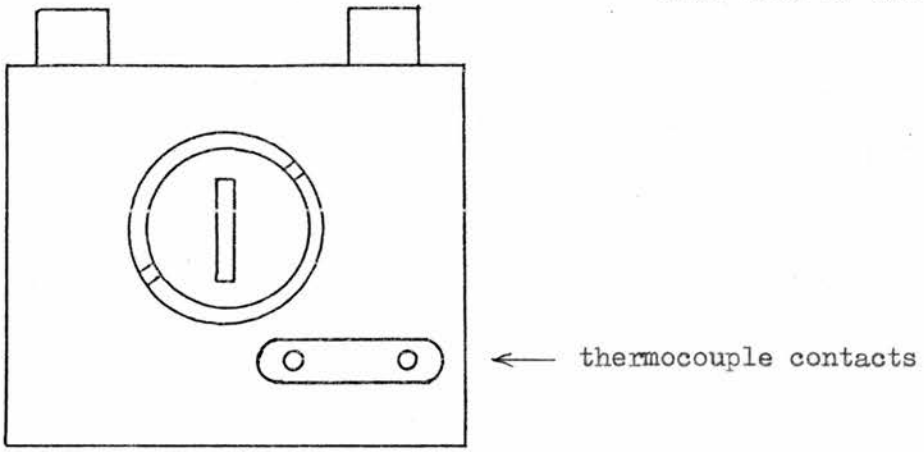

Fig. A.2

Top view of the autoclave

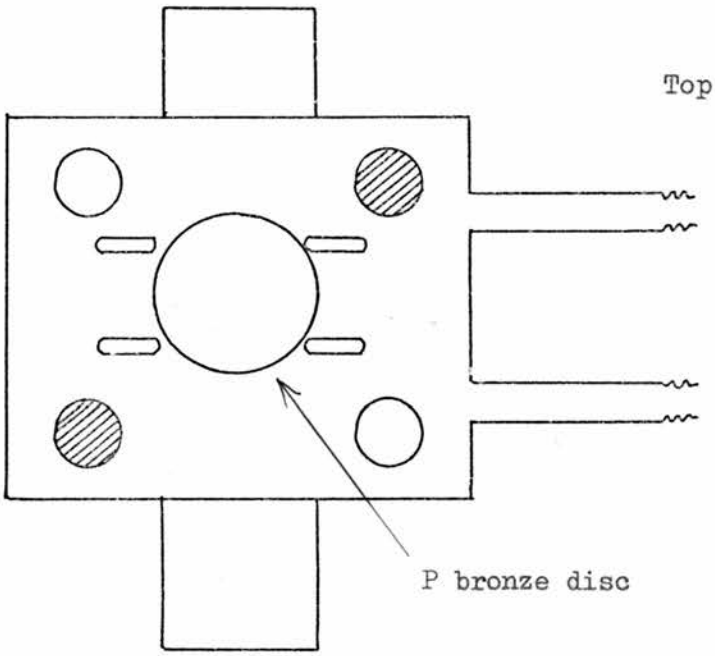

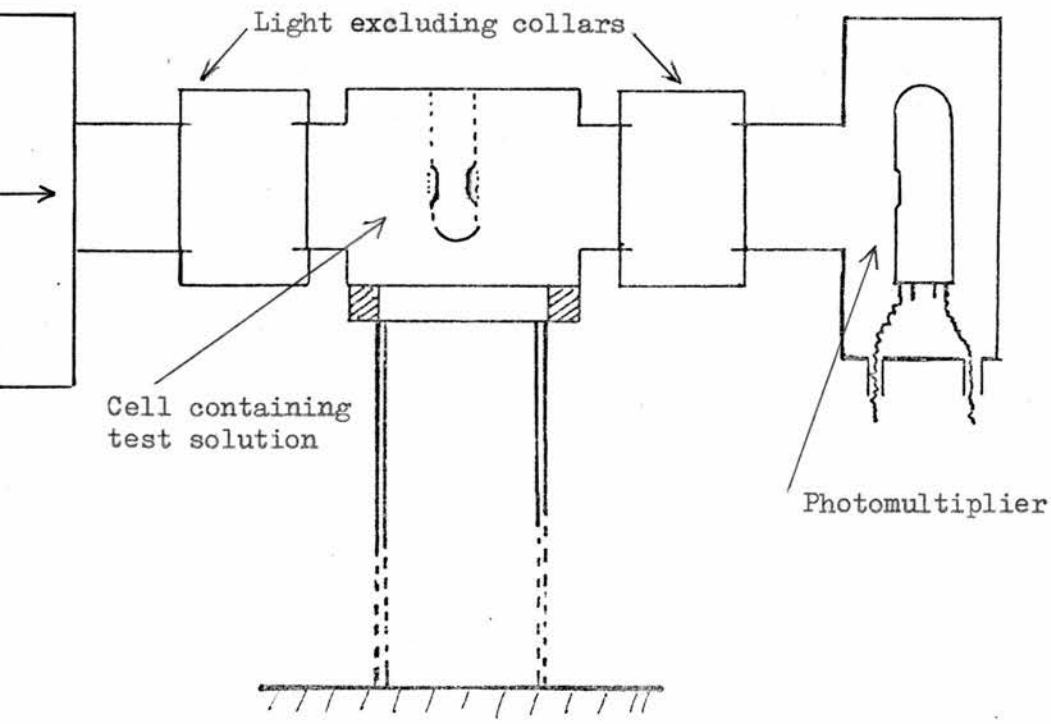

Fig. A.3

Schematic side view of the assembly

The meter gave full deflection for 10 V and the total range available for backing-off was 30 μA. The converter was equipped with two outputs. One from the amplifier section was connected to Heathkit recorder and Roband digital voltmeter simultaneously. The other, to the Southern Instruments d.c. amplifier, M 1266 and Southern Instruments M 1330 A direct recording u.v. oscillograph.

For detection of the kinetic reaction by the oscilloscope, a scope triggering button, also connected to the solenoid trigger for release of steel piercing rod, was provided on the converter.

To minimise vibrations produced during sudden release of pressure, the photomultiplier, in its light-excluding housing, was attached to the monochromator by a rigid (9 mm thick) steel plate, Fig. A 4. The autoclave was suspended in a similarly rigid frame, placed on a 80 mm diameter steel tube fixed to the floor. The autoclave, bolted by two diagonally placed 9 mm bolts was held in the line of light between the monochromator and photomultiplier window, Fig. A 3. The only contact, between the two assemblies was through the light-excluding brass collars, lined with sponge rubber. The autoclave was bolted to 22 mm thick upper steel plate, part of the rigid assembly. The plate was drilled to allow passage of pressurising gas, terminating in a needle valve, and had a 33 mm diameter cavity for placing phosphor-bronze discs of determined thickness. To prevent spillage, the stainless steel cell was closed after rigorous degassing with a polythene disc. Oxygen-free nitrogen was used for pressurising the system at pressures from 0 - 1000 lb /in^2 , corresponding to 0 - 68 otm.

Sheets of phosphor-bronze were of variable thickness and each batch purchased had to be tested to find the exact bursting pressure. Typical variations encountered were: nominal thickness of sheet

Fig. A.4.

Top view of the pressure jump apparatus

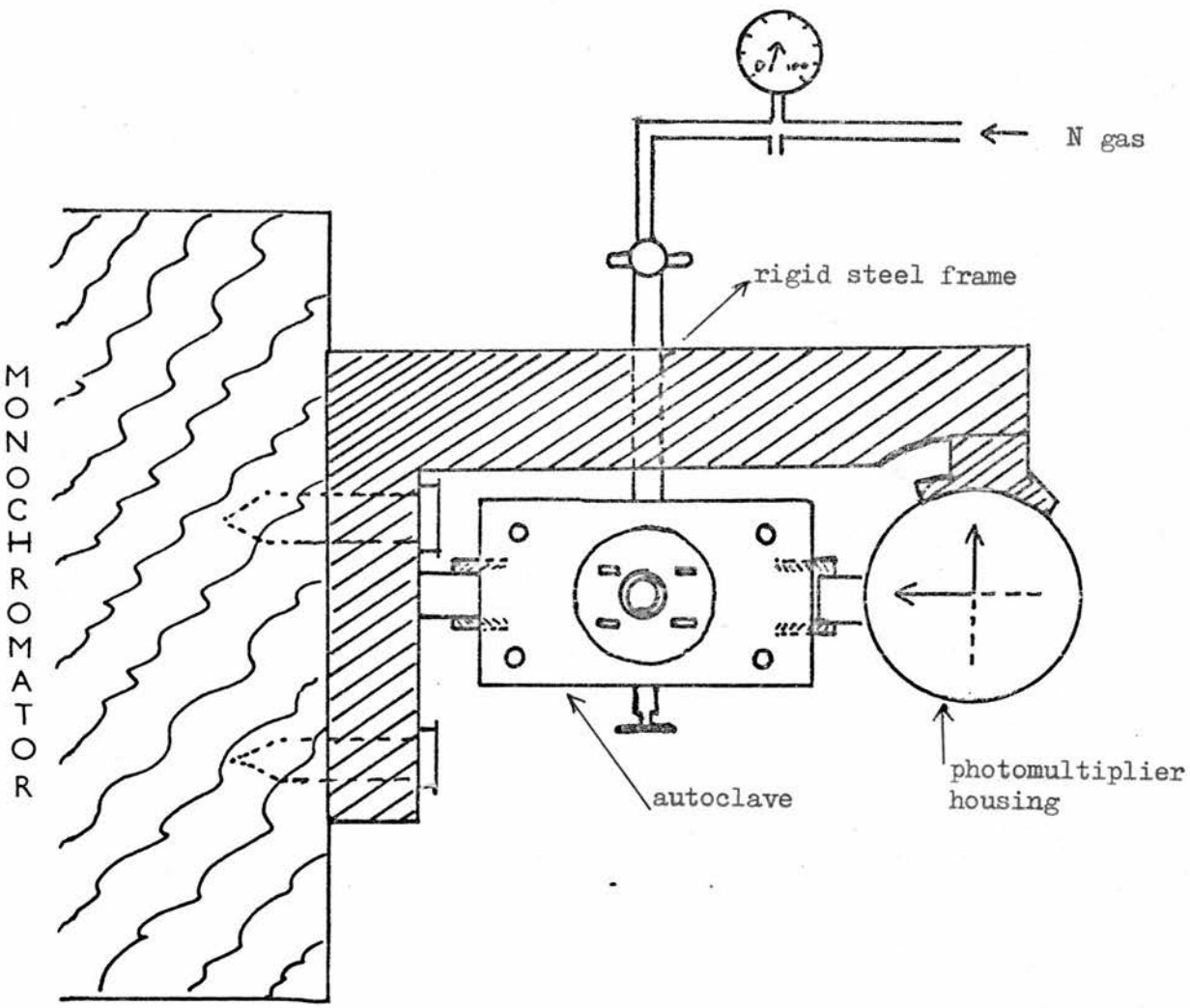

0.005 in, bursting at pressures 610, 620, 640, 700, and 740 lb / in^2. Normal working pressures were about 590 - 600 lb / in^2. Careful exclusion of stray light on the photomultiplier was observed by housing the photomultiplier in light-proof cover and the placing of brass collars at the monochromator / autoclave / photomultiplier junction points. As an extra precaution, the experiments were conducted in a darkroom.

Possible weaknesses of the apparatus are confined to two aspects. Firstly, the liquid cell used (37 mm long, 12 mm diameter) was made from brass. This material was unsuitable for use with acidified solutions, neither was the polythene, due to flexibility under pressure. For these reasons stainless steel cell was used in subsequent experiments. There was also considerable difficulty in fixing quartz windows to metal. The optimum conditions were obtained by glueing 1-2 mm thick quartz windows with Arraldite cement, which was immune to aqueous and acidic solutions, but was slowly attacked by ethanol, and very quickly by iso-propyl alcohol. The possibility of obtaining thick, all quartz cell was investigated . It was assumed that absolutely flat quartz windows are necessary to avoid scatter and distortion of a beam of light. This necessitated construction of the cell from thick wall materials, which afforded a larger surface and better adhesion by the Arraldite cement.

Since the main problem was to obtain a difference between the light intensity of a solution under pressure and one at normal atmospheric pressure, rather than the absolute value of I_t, the imperfections of light beam were of no prime importance. A cell was constructed, which had slightly curved windows and was tested successfully.

The other possible defect, may be the susceptibility of a sensitive

photomultiplier to a considerable shock wave produced during rupture of the bronze disc in a relatively confined space. Each change of pressure in the autoclave produces large displacements of the recorder pen before its return to a new equilibrium. This is possibly due to insufficient separation of the two assemblies to eliminate any effects of a shock wave. Since neither of our available indicators responded to changes of pressure on the pressure jump apparatus in spite of the large hydration changes expected, the experiment of Ewald and Hammann[90], was repeated. They studied the effect of pressure on the ionic equilibria of $CoCl_2$ solutions in aqueous iso-propyl alcohol. Direct measure of this effect was obtained by following colour changes induced by pressure in systems in which the participating ions absorb at characteristic wavelengths. Dilute aqueous solutions of $CoCl_2$ are pink, the concentrated aqueous solutions in organic solvents are blue. The blue colour of the solution, according to Sidgwick[91] is due to the $CoCl_4^{--}$ ion. The absorption of the blue ion is stronger than that of the pink Co^{++} ion and the presence of very little of the blue complexion can completely mask the pink colour of the solution. All the ions are considered to be solvated and it is possible that they are present as ion pairs in solvents of low dialectric constant.

Graph Fig. A. 5, showing the effects of pressure on absorption spectrum of $CoCl_2$ solution is reproduced.

Fig. A 5

Effect of pressure on absorption spectrum of $CoCl_2$ solution at 27°C.

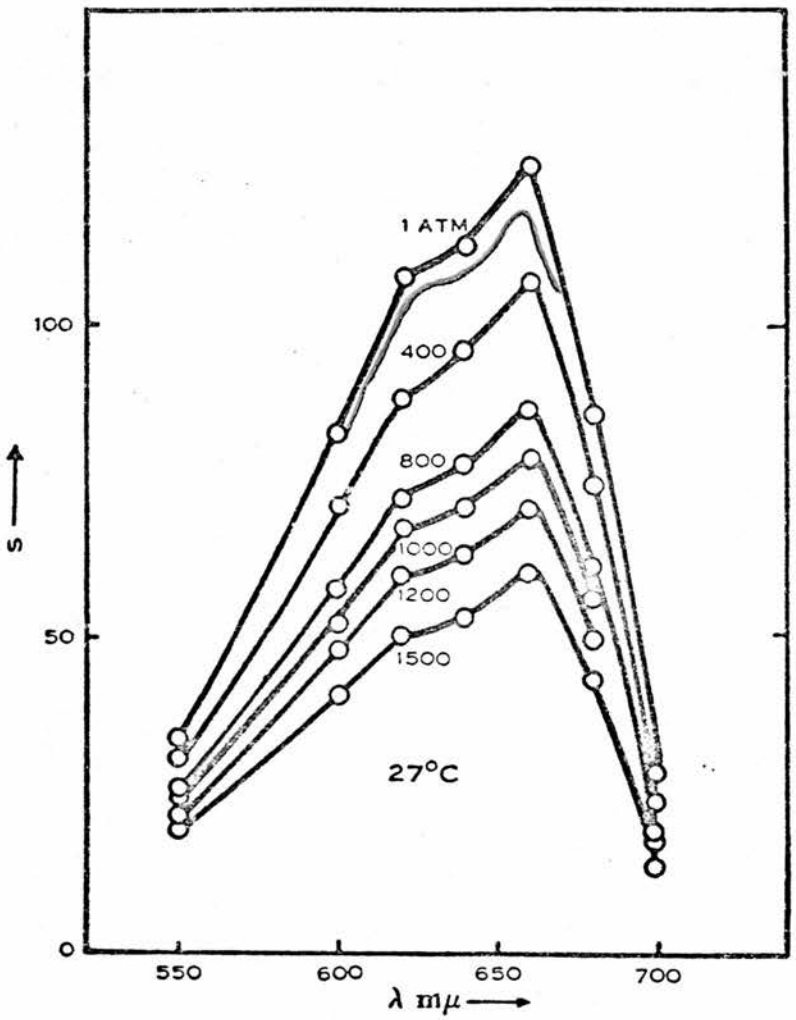

concentration of $CoCl_2$ = 0.00604 mol kg^{-1} in iso-PrOH + 2.91% H_2O

Specific absorption, S of these solutions at various concentrations.

S = D/cl, where D is optical density, c = molar concentration of $CoCl_2$ l = length of absorption cell.

Data obtained on our apparatus are superimposed (in red) and mark the maximum difference of pressure obtained (68 atm), compared with Ewald and Hamann's, 1500 atm.

The reason that T-jump technique has found wider application than

pressure jump (besides being able to follow faster reactions) is that the displacement of a typical reaction produced by a 10° temperature rise is considerably greater than that produced by a 65 atmosphere pressure change[92].

Thus, if $\Delta T = 10^{\circ}$ and $T = 300$ K, then for a ΔH° as small as 1 k cal / mole the ratio of the equilibrium constants at two temperatures is about 1.06, i.e. there is an approximately 6% change in equilibrium constant. The corresponding displacement for a pressure change of 65 atmospheres only comes if ΔV° is about 22 dm^3 / mole. This is a relatively high value and is only found in reactions in which there is a considerable change in the electrostrictive effects of the reactants and products on the solvent, for example, if there is a charge neutralisation. Thus ΔV° is 22 dm^3 / mole for $H^+ + OH^- \rightleftharpoons H_2O$. On the other hand, most reactions have values of ΔH° considerably greater than 1 k cal/mole.

REFERENCES

1. L.P. Hammett and A.J. Deyrup, J. Amer. Chem. Soc., 54, 2721 (1932).
2. M.A. Paul and F.A. Long, Chem. Revs., 56, 1 (1957).
3. E.M. Arnett and G.W. Mach, J. Amer. Chem. Soc., 86, 2671 (1964).
4. K. Yates, J.B. Stevens and A.R. Katritsky, Canad. J. Chem., 42, 1957 (1964).
5. F.A. Long and J. Schulze, J. Amer. Chem. Soc., 83, 3340 (1961).
6. R.L. Hinman and J. Lang, J. Amer. Chem. Soc., 86, 3796 (1964).
7. T.G. Bonner and J. Phillips, J. Chem. Soc., (B), 650 (1966).
8. N.C. Deno, J.J. Jaruzelski and A. Schriesheim, J. Amer. Chem. Soc. 77, 3044 (1955).
9. M.T. Reagan, J. Amer. Chem. Soc., 91, 5506 (1969).
10. J.E.B. Randles and J.M. Tedder, J. Chem. Soc., 1218 (1955).
11. K.N. Bascombe and R.P. Bell, J. Chem. Soc., 1096 (1959).
12. R. Stewart and T. Mathews, Canad. J. Chem., 38, 602 (1960).
13. J.G. Tillett and R.C. Young, J. Chem. Soc., (B), 209 (1968).
14. Ch. Kalides and S.R. Palit, J. Chem. Soc., 3998 (1961).
15. B. Torck, M. Hellin and F. Coussement, Bull. Soc. Chim. France, 1957 (1962).
16. H. Dahn, L. Loewe and G. Rotzler, Ber., 93, 1572 (1960).
17. H. Nicholson and P.A.H. Wyatt, J. Chem. Soc. (B), 198 (1968).
18. M.J. Jorgenson and D.R. Hartter, J. Amer. Chem. Soc., 85, 878 (1963).
19. R.P. Bell and K.N. Bascombe, Disc. Faraday Soc., 24, 158 (1957).
20. P.A.H. Wyatt, Disc. Faraday Soc., 24, 162 (1957).
21. E. Högfeldt, Acta Chim. Scand., 16, 1054 (1962).
22. K. Yates and H. Wai, J. Amer. Chem. Soc., 86, 5408 (1964).
23. K. Yates and J.C. Riordan, Canad. J. Chem., 43, 2328 (1965).

24. R.W. Taft, J. Amer. Chem. Soc., 82, 2965 (1960).

25. J.E. Dixon and T.C. Bruice, J. Amer. Chem. Soc., 93, 3248 (1971).

26. R.H. Boyd, J. Amer. Chem. Soc., 85, 1555 (1963).

27. E.A. Hill and W.J. Mueller, Tetrahedron Lett., 2565 (1968).

28. M.J. Postle and P.A.H. Wyatt, J. Chem. Soc., Perkin II, 474 (1972).

29. C.D. Ritchie, G.A. Skinner and V.G. Badding, J. Amer. Chem. Soc., 89, 2063 (1967).

30. M. Eigen, Disc. Faraday Soc., 17, 194 (1954).

31. J.N. Ride, P.A.H. Wyatt and Z.M. Zochowski, J. Chem. Soc., Perkin II, 1188 (1974).

32. C.A. Bunton and S.K. Huang, J. Amer. Chem. Soc., 94, 3536 (1972).

33. J.N. Ride and P.A.H. Wyatt, J. Chem. Soc., Perkin Trans. 2, 746 (1973).

34. P.A.H. Wyatt and Z.M. Zochowski, Zeitschrift für Phys. Chem. Neue Folge, Bd. 101, S.143 (1976).

35. C.D. Ritchie, J. Amer. Chem. Soc., 94, 3275 (1972).

36. M. Smith, D.H. Rammler, I.H. Goldberg and H.G. Khorana, J. Amer. Chem. Soc., 84, 430 (1962).

37. M. Gomberg and L.H. Cone, Ann., 370, 142, (1909).

38. A. Baeyer and V. Villiger, Ber., 35, 1198 (1902).

39. M.S. Newman and M.C. Deno, J. Amer. Chem. Soc., 73, 3644 (1951).

40. A. Baeyer and V. Villiger, Ber., 35, 3027 (1902).

41. C.S. Marvel, M.S. Mueller, C.N. Himel and J.F. Kaplan, J. Amer. Chem. Soc., 61, 2773, (1939).

42. H. Bünzly and H. Decker, Ber., 37, 2933 (1904).

43. F. Ullman and G. Engi, Ber., 37, 2370 (1904).

44. P.K. Grover, G.D. Shah and R.C. Shah, J. Chem. Soc., 3982 (1955).

45. R. Mayer and A. Conzetti, Ber., 30, 971 (1897).

46. P. Arends and P. Helboe, Dansk. Tids. Skr. Farm. 46, (7), 133-8 (1972).

47. S. Geiger, M. Joannic, M. Pesson, H. Techer, E. Lagrange and M. Aurousseau, Chim. Ther. (1966) (7), 425 - 37.

48. E. Sawicki and Stanley, Talanta, 1965 vol. 12, 605 - 16 Pergamon Press.

49. A.A. Goldberg and A.H. Wragg, J. Chem. Soc., 4227 (1958).

50. O. Hromatka, Ber., 75B, 1302 - 10 (1942).

50a. Q.H. Gibson and L. Milnes, Biochem. J., 91, 161 (1964).

51. M.J. Postle, Ph.D. Thesis, Sheffield University (1969).

52. T.M. Shepherd, Chem. and Ind. 1973 p. 332.

53. F.J. Kezdy and E.S. Swinbourne, J. Chem. Soc., 2371 (1960).

54. J.E. Ablard, D.S. McKinney and J.C. Warner, J. Amer. Chem. Soc., 62, 2181 (1940).

55. D.H. Everett and W.F.K. Wynne-Jones, Proc. Roy. Soc., A 177, 499 (1941).

56. P. Paoletti, J.H. Stern, A. Vacca, J. Phys. Chem., 69, 3759 (1965).

57. C.A. Parker, "Photoluminescence of Solutions", Elsevier, London, New York 1968.

58. C.A. Parker and W.J. Barnes, Analyst 82, 606 (1957).

59. J.D. Winefordner and P.A. St. John, Anal. Chem., 35, 2211 (1963).

60. G. Porter, Techniques of Organic Chemistry, vol. VIII, Part 2, Ed. Weissberger (Interscience, 1963).

61. G. Porter and M.W. Windsor, Disc. Faraday Soc., 17, 178 (1954).

62. A. Albert and E.P. Serjeant, "Ionization constants of acids and bases" (Methuen, 1962).

63. C.H. Rochester, Organic Chemistry 17, Acidity Functions (Academic Press, 1970).

64. R.S. Ryabova, I.M. Medvetskaya, and M.I. Vinnik, Russ. J. Phys. Chem., 40, 182 (1966).

65. J.B. Conant and T.H. Werner, J. Amer. Chem. Soc., 52, 4436 (1930).

66. J.G. Martin and R.G. Smith, J. Amer. Chem. Soc., 86, 2252 (1964).

67. N.C. Deno, H.E. Berkheimer, W.L. Evans and H.J. Patterson, J. Amer. Chem. Soc., 81, 2344 (1959).

68. J.N. Demas and G.A. Crosby, J. Phys. Chem., 75, 991 (1971).

69. A.N. Fletcher, J. Phys. Chem., 72, 2743 (1968).

70. H.C. Børresen, Acta Chem. Scand., 19, 2089 (1965).

71. R. Rusakowicz and A.C. Testa, J. Phys. Chem., 72, 2680 (1968).

72. G. Jackson and G. Porter, Proc. Roy. Soc., A 260, 13 (1961).

73. E. Vander Donckt, Progr. Reaction Kinetics, Ed. G. Porter (Pergamon) 5, 273 (1970).

74. J.F. Ireland and P.A.H. Wyatt, J. Chem. Soc., (Faraday I) 69, 161 (1973).

75. Th. Förster, "Fluoreszenz organischer Verbindungen", (Vanderhoeck and Ruprecht, 1951) p. 85.

76. R.W. Stoughton and G.K. Rollefson, J. Amer. Chem. Soc., 61, 2634 (1959).

77. Th. Förster, Disc. Faraday Soc., 27, 7 (1959).

78. A. Weller, Fast Reactions and Primary Processes in Chemical Kinetics, Ed. S. Claesson (Wiley Interscience, 1967).

79. M. Kasha, J. Chem. Phys., 20, 71, (1952).

80. K.H. Grellman, A.R. Watkins and A. Weller, J. Luminescence, 1, 2, 678 (1970).

81. M.T. McCall, G.S. Hammond, O. Yonemitsu and B. Witkop, J. Amer. Chem. Soc., 92, 6991 (1970).

82. A.R. Watkins, J. Phys. Chem., 78, 2555 (1974).

83. P. Bartolus, G. Bartocci and U. Mazzucato, J. Phys. Chem., 79, (1), 21 (1975).

84. R.A. Diffenbach, K. Sano and R.W. Taft, J. Amer. Chem. Soc., 88, 4447 (1966).

85. E.M. Arnett and R.D. Bushick, J. Amer. Chem. Soc., 86, 1564 (1964).

86. M. Eigen, Disc. Faraday Soc., 24, 25 (1957).

87. H. Strehlow and M. Becker, Z. Electrochem., 63, 457 (1959).

88. H. Strehlow and H. Wendt, Inorg. Chem., 2, 6 (1963).

89. A. Jost, Ber. Busenges Phys. Chem., 70 (9-10), 1057 (1966).

90. A.H. Ewald and S.D. Hamann, Aust. J. Chem., 9, 55 (1956).

91. N.V. Sidgwick, "The Chemical Elements and their Compounds" vol. 2, 1930, (Oxford University Press).

92. D.N. Hague, "Fast Reactions", Wiley-Interscience 1971, page 41.